12-2003

Comparison of Microbial Cell Densities and Treatment Performance in Nitrifying Activated Sludge Reactors

Janalyn Rae Brown
University of Tennessee - Knoxville

To the Graduate Council:

I am submitting herewith a thesis written by Janalyn Rae Brown entitled "Comparison of Microbial Cell Densities and Treatment Performance in Nitrifying Activated Sludge Reactors." I have examined the final electronic copy of this thesis for form and content and recommend that it be accepted in partial fulfillment of the requirements for the degree of Master of Science, with a major in Environmental Engineering.

Kevin Robinson, Major Professor

We have read this thesis and recommend its acceptance:

Kung-Hui Chu, Alice Layton

Accepted for the Council:
Carolyn R. Hodges

Vice Provost and Dean of the Graduate School

(Original signatures are on file with official student records.)

To the Graduate Council:

I am submitting herewith a thesis written by Janalyn Rae Brown entitled "Comparison of Microbial Cell Densities and Treatment Performance in Nitrifying Activated Sludge Reactors." I have examined the final electronic copy of this thesis for form and content and recommend that it be accepted in partial fulfillment of the requirements for the degree of Master of Science, with a major in Environmental Engineering.

Kevin Robinson
Major Professor

We have read this thesis and
recommend its acceptance:

Kung-Hui Chu

Alice Layton

Acceptance for the Council:

Anne Mayhew
Vice Provost and Dean of
Graduate Studies

(Original signatures on file with official student records.)

Comparison of Microbial Cell Densities and Treatment Performance in Nitrifying Activated Sludge Reactors

A Thesis
Presented for the
Master of Science
Degree
The University of Tennessee, Knoxville

Janalyn Rae Brown
December 2003

Abstract

A thorough understanding of microbial dynamics in activated sludge treatment is currently unrealized due, in part, to quantitative techniques that rely on culture-dependent methods. The bias inherent with cultivation techniques may result in isolates that do not necessarily represent those dominant in the system evaluated. *In situ* analysis of microorganisms functioning in wastewater reactors will provide a greater understanding of how particular groups of organisms, such as nitrifiers, are impacted by system fluctuations. This information is vital for improved process design and control. The overall goal of this research was to investigate the use of the real-time polymerase chain reaction (PCR) technique as a tool for quantifying nitrifying bacteria in activated sludge. To facilitate evaluation of the real-time PCR assays over a range of nitrification performance efficiencies, operational parameters were manipulated to induce stress on the nitrifiers. The specific objective of this study was to assess the impact of operational and environmental changes on traditional measures of process performance and microbial cell densities of targeted microorganisms.

Bench-scale activated sludge treatment units, consisting of four continuous-stirred tank reactors (CSTRs) operating in parallel, each with an external secondary clarifier, were operated to treat municipal wastewater collected from a full-scale wastewater treatment plant. The activated sludge reactors were operated at three constant temperature levels (20°C, 15°C, and 10°C) and three dissolved oxygen (DO) levels [high (≥ 2.0 mg/L), intermediate (1.0-1.5 mg/L) and low (≤0.5 mg/L) over a 21-month period. The reactors were operated at solids retention times (SRTs) of 20-, 10-, 5-, and 2-days. Treatment performance was determined by traditional physical/chemical parameters of chemical oxygen demand (COD) removal efficiency, mixed liquor volatile suspended solids (MLVSS) concentrations, and ammonia and nitrite oxidation rates. Real-time PCR assays were used to determine cell concentrations of total bacterial 16S rDNA, a gross measure of biomass content, the *amo*A gene of *N. oligotropha*-type bacteria, a measure of ammonia-oxidizing bacteria (AOB), and the *Nitrospira* 16S rDNA gene, a measure of nitrite-oxidizing bacteria (NOB).

Efficient COD removal occurred throughout all phases of the study and carbon, however, carbon treatment performance was found to increase with increasing SRT. In contrast, DO concentration and temperature were not found to impact COD removal efficiency. SRT was found to be the prime determinant of both MLVSS and total eubacterial concentration and, as expected, the two parameters were positively correlated. Temperature and DO were not found to have a clear impact on either measure of total biomass.

Consistent with the literature, the findings of this study indicated SRT was the single most important factor in determining whether or not nitrification will occur in a treatment system. Efficient nitrification occurred at low temperatures and low DO levels for the higher SRT reactors, but the 5-day and 2-day SRT reactors were dramatically affected by changes in these parameters. The contribution of *N. oligotropha*-type AOB to the total eubacteria population (<0.5%) determined by real-time PCR was much lower than expected based on theoretical calculations (2-17%) suggesting that *N. oligotropha* was not the dominant AOB species in the bench-scale reactors. The concentration of *N. oligotropha*-type AOB and ammonia oxidation rate did not closely follow the same trends with respect to changes in SRT, temperature, and DO and were not highly correlated. The percentages of *Nitrospira*, with respect to total eubacteria measured using real-time PCR, ranged from 0.2 to 5.6% when nitrification was occurring and corresponded very well with the predicted values of 0.4 to 4.0%. A strong logarithmic relationship existed between *Nitrospira* cell density and nitrite oxidation rate under all experimental conditions, with a Pearson correlation coefficient of 0.78 between the two measures. A similar relationship was found between the concentration of *Nitrospira* and ammonia oxidation, suggesting that it may not be necessary to monitor only NOB. This would eliminate the complicated task of characterization of the AOB population and reduce the labor and cost associated with monitoring nitrifying organisms in a treatment system.

Table of Contents

Page

Chapter 1.0 Introduction 1
1.1 Background 1
1.2 Research Objectives 2
Chapter 2.0 Literature Review 4
2.1 Introduction to the Activated Sludge Process 4
2.2 Fundamentals of Nitrification 6
2.2.1 Nitrification Stoichiometry 7
2.2.2 Nitrifying Bacteria 8
2.3 Effects of SRT on Activated Sludge Treatment Performance 11
2.3.1 Impacts of SRT on Carbon Oxidation 14
2.3.2 Impacts of SRT on Nitrification 15
2.4 Effects of DO on Activated Sludge Treatment Performance 17
2.4.1 Impacts of DO on Carbon Oxidation 18
2.4.2 Impacts of DO on Nitrification 20
2.5 Effects of Temperature on Activated Sludge Treatment Performance 21
2.5.1 Impacts of Temperature on Carbon Oxidation 24
2.5.2 Impacts of Temperature on Nitrification 25
2.6 Introduction to Molecular Methods 27
2.6.1 Oligonucleotide Probe Hybridization 29
2.6.2 Polymerase Chain Reaction (PCR) 31
2.6.3 Fundamentals of Real-time PCR 33
2.7 Applications of Molecular Methods in the Quantification of Nitrifiers 35
2.7.1 Fluorescence *in situ* Hybridization (FISH) 36
2.7.2 Competitive PCR 37
2.7.3 Real-time PCR 39
2.8 Attempts to Correlate Nitrifier Cell Densities With Process Performance 40
Chapter 3.0 Materials and Methods 43
3.1 Experimental Treatment System 43
3.1.1 Equipment Design and Configuration 43
3.1.2 Collection and Storage of Influent Wastewater 48
3.1.3 DO Delivery and Control System 49
3.2 Operating Procedures 52
3.2.1 Selection of Reactor SRTs 52
3.2.2 Sampling and Reactor Maintenance Procedures 52
3.2.3 Sample Analysis Procedures 55
3.3 Real-time PCR 58
3.3.1 DNA Extraction 58
3.3.2 Real-Time PCR Assays 59
3.3.3 Data Acquisition and Analysis 62
3.3.4 Application of Real-time PCR to Mixed Liquor Samples 63
3.4 Computation of Process Performance Parameters 64

3.4.1 Carbon Treatment Performance 64
3.4.2 Nitrification Performance 64
3.5 Statistical Analyses 66
Chapter 4.0 Results and Discussion 69
4.1 Selection of Samples for Real-time PCR Analysis 69
4.2 Carbon Treatment Performance 73
4.2.1 20°C Operation 73
4.2.2 15°C Operation 75
4.2.3 10°C Operation 75
4.2.4 Overall Carbon Treatment Performance 78
4.3 Measures of Total Biomass 80
4.3.1 MLVSS 80
4.3.2 Total Eubacterial Concentration 89
4.4 Nitrification Performance 101
4.4.1 Ammonia Oxidation 101
4.4.2 *Nitrosomonas oligotropha*-type AOB Concentration 115
4.4.3 Comparison of Ammonia Oxidation and AOB Concentration 124
4.4.4 Nitrite Oxidation 132
4.4.5 *Nitrospira* spp. NOB Concentration 141
4.4.6 Comparison of Nitrite Oxidation and NOB Concentration 149
Chapter 5.0 Summary and Conclusions 156
5.1 Evaluation of Carbon Treatment Performance and Total Biomass 156
5.1.1 COD Removal Efficiency 156
5.1.2 MLVSS and Total Eubacterial Concentrations 156
5.2 Evaluation of Nitrification Performance 157
5.2.2 Ammonia Oxidation Rate and *N. oligotropha*-type AOB Concentration 157
5.2.3 Nitrite Oxidation Rate and *Nitrospira*-type NOB Concentration 157
5.3 General Conclusions 159
List of References 161
Appendices 173
Appendix A Sample Calculation for Conversion of Real-Time PCR Data into Units of Cells/L 174
Appendix B Sample Calculation for Theoretical Values of %AOB and %NOB 175
Vita 178

List of Tables

Page

Table 2-1. Effect of DO Concentration on MLSS and COD Removal Efficiency for a Pure Continuous Culture of *Citrobacter sp*. (Adapted from Lau et al. 1984) 19
Table 3-1. Primers and Probes Used in This Study....60
Table 3-2. PCR Mix for the Quantification of Total Eubacteria....61
Table 3-3. PCR Mix for the Quantification of *Nitrosomonas oligotropha*-type AOB 62
Table 3-4. PCR Mix for the Quantification of *Nitrospira*....63
Table 4-1. DO Levels and Operational Dates for 20°C Study 70
Table 4-2. DO Levels and Operational Dates for 15°C Study 70
Table 4-3. DO Levels and Operational Dates for 10°C Study 70
Table 4-4. Real-time PCR Sampling Dates for the 20° C Study....71
Table 4-5. Real-time PCR Sampling Dates for the 15°C Study....72
Table 4-6. Real-time PCR Sampling Dates for the 10°C Study....72
Table 4-7. Average COD Treatment Performance During Operation at 20°C 74
Table 4-8. Average COD Treatment Performance During Operation at 15°C 76
Table 4-9. Average COD Treatment Performance During Operation at 10°C 77
Table 4-10. Average MLVSS Concentrations (mg/L) During Operation at 20°C....82
Table 4-11. Average MLVSS Concentrations (mg/L) During Operation at 15°C....85
Table 4-12. Average MLVSS Concentrations (mg/L) During Operation at 10°C....86
Table 4-13. Average Total Eubacterial Concentrations (cells/L) During Operation at 20°C 90
Table 4-14. Average Total Eubacterial Concentrations (cells/L) During Operation at 15°C 92
Table 4-15. Average Total Eubacterial Concentrations (cells/L) During Operation at 10°C 95
Table 4-16. Summary of Linear Regression Analyses for MLVSS and Total Eubacterial Concentrations 100
Table 4-17. Average Ammonia Oxidation During Operation at 20°C 106
Table 4-18. Average Ammonia Oxidation During Operation at 15°C 110
Table 4-19. Average Ammonia Oxidation During Operation at 10°C 113
Table 4-20. Average *N. oligotropha*-type AOB Concentrations (cells/L) During Operation at 20°C 116
Table 4-21. Average *N. oligotropha*-type AOB Concentrations (cells/L) During Operation at 15°C 119
Table 4-22. Average *N. oligotropha*-type AOB Concentrations (cells/L) During Operation at 10°C 121
Table 4-23. Summary of Linear Regression Analyses for Ammonia Oxidation Rate and *N. oligotropha*-type AOB Concentrations 123
Table 4-24. Average Steady-state Influent Parameters During High DO

Operation....126
Table 4-25. Average Steady-state Effluent Parameters During High DO Operation....127
Table 4-26. Typical Kinetic Parameters for Heterotrophs (Adapted from Rittmann and McCarty, 2001) 127
Table 4-27. Typical Kinetic Parameters for Ammonia-Oxidizers (Adapted from Rittmann and McCarty, 2001) 128
Table 4-28. Comparison of %AOB Determined From Theoretical Calculations and Real-time PCR 128
Table 4-29. Pearson Correlation Coefficients Between *N. oligotropha*-type AOB Concentrations and Ammonia Oxidation Rates....130
Table 4-30. Average Nitrite Concentrations and Nitrite Oxidation Rates During Operation at 20°C 133
Table 4-31. Average Nitrite Concentrations and Nitrite Oxidation Rates During Operation at 15°C 136
Table 4-32. Average Nitrite Concentrations and Nitrite Oxidation Rates During Operation at 10°C 139
Table 4-33. Average *Nitrospira* Concentrations (cells/L) During Operation at 20°C 141
Table 4-34. Average *Nitrospira* Concentrations (cells/L) During Operation at 15°C 144
Table 4-35. Average *Nitrospira* Concentrations (cells/L) During Operation at 10°C 147
Table 4-36. Summary of Linear Regression Analyses for Nitrite Oxidation Rate and *Nitrospira* Concentrations....149
Table 4-37. Typical Kinetic Parameters for Nitrite-Oxidizers (Adapted from Rittmann and McCarty, 2001) 150
Table 4-38. Comparison of %NOB Determined From Theoretical Calculations and Real-Time PCR 150
Table 4-39. Correlation Coefficients Between *Nitrospira* Concentrations and Nitrite Oxidation Rates 152
Table 4-40. Correlation Coefficients Between *Nitrospira* Concentrations and Ammonia Oxidation Rates....155

List of Figures

Page

Figure 2-1. Typical Activated Sludge Process (Adapted from Grady et al., 1999).....5
Figure 3-1. Experimental Treatment System Containing Four Parallel Treatment Units (reproduced from Parker, 2001).....44
Figure 3-2. Diagram of One of the Treatment Units, which Consisted of a Continuous-Stirred Tank Reactor and an External Secondary Clarifier....45
Figure 3-3. Schematic Diagram of Experimental Treatment System.....47
Figure 3-4. Influent Feed Tank and DO Control System (reproduced from Wood, in preparation).....50
Figure 4-1. Effect of DO Concentration on COD Treatment Performance During 20°C Operation.....74
Figure 4-2. Effect of DO Concentration on COD Treatment Performance During 15°C Operation.....76
Figure 4-3. Effect of DO Concentration on COD Treatment Performance During 10°C Operation.....77
Figure 4-4. Fluctuations in MLVSS Concentration Due to Changing DO and Influent COD Concentrations Throughout the 20°C Study.....82
Figure 4-5. Fluctuations in MLVSS Concentration Due to Changing DO and Influent COD Concentrations Throughout the 15°C Study.....84
Figure 4-6. Fluctuations in MLVSS Concentration Due to Changing DO and Influent COD Concentrations Throughout the 10°C Study.....86
Figure 4-7. Comparison of Trends in MLVSS Concentration and Total Eubacterial Concentration at Varying SRT and DO Levels at 20°C.....91
Figure 4-8. Comparison of Trends in MLVSS Concentration and Total Eubacterial Concentration at Varying SRT and DO Levels at 15°C.....93
Figure 4-9. Comparison of Trends in MLVSS Concentration and Total Eubacterial Concentration at Varying SRT and DO Levels at 10°C.....96
Figure 4-10. Steady-state Concentration of Total Eubacteria as a Function of SRT (A) 20°C, (B) 15°C, (C) 10°C.....98
Figure 4-11. Steady-state Concentration of MLVSS as a Function of SRT (A) 20°C, (B) 15°C, (C) 10°C.....99
Figure 4-12. 20-day SRT Reactor Nitrogen Results (A) 20°C, (B) 15°C, (C) 10°C....102
Figure 4-13. 10-day SRT Reactor Nitrogen Results (A) 20°C, (B) 15°C, (C) 10°C....103
Figure 4-14. 5-day SRT Reactor Nitrogen Results (A) 20°C, (B) 15°C, (C) 10°C.....104
Figure 4-15. 2-day SRT Reactor Nitrogen Results (A) 20°C, (B) 15°C, (C) 10°C.....105
Figure 4-16. Comparison of Trends in Ammonia Oxidation Rate and *N. oligotropha*-type AOB Concentration at Varying SRT and DO Levels at 20°C.....118
Figure 4-17. Comparison of Trends in Ammonia Oxidation Rate and *N. oligotropha*-type AOB Concentration at Varying SRT and DO Levels at 15°C.....120

Figure 4-18. Comparison of Trends in Ammonia Oxidation Rate and *N. oligotropha*-type AOB Concentration at Varying SRT and DO Levels at 10°C 122
Figure 4-19. Correlation between Ammonia Oxidation Rate and *N. oligotropha*-type AOB Concentration (Includes Data From All Operational Conditions) 130
Figure 4-20. Steady-state Specific Ammonia Oxidation Rates as a Function of Effluent Ammonia Concentration (A) High DO, (B) Intermediate DO (C) Low DO 131
Figure 4-21. Comparison of Trends at 20°C in Nitrite Oxidation Rate and *Nitrospira* Concentration at Varying SRT and DO Levels 143
Figure 4-22. Comparison of Trends at 15°C in Nitrite Oxidation Rate and Nitrospira Concentration at Varying SRT and DO Levels 146
Figure 4-23. Comparison of Trends at 10°C in Nitrite Oxidation Rate and *Nitrospira* Concentration at Varying SRT and DO Levels 148
Figure 4-24. Correlation of Nitrite Oxidation Rate and *Nitrospira* Concentration (Includes Data From All Conditions Studied) 152
Figure 4-25. Steady-state Specific Nitrite Oxidation Rates as a Function of Effluent Nitrite Concentration (A) High DO, (B) Intermediate DO (C) Low DO 154
Figure 4-26. Correlation between Ammonia Oxidation Rate and *Nitrospira* (Includes Data from All Conditions Studied) 155

Nomenclature

b	endogenous decay coefficient
C	Celsius
COD^0	influent chemical oxygen demand
COD^e	effluent chemical oxygen demand
cm	centimeter
K	half-saturation constant
k_1	unknown value of any parameter at temperature T
k_2	known value of any parameter at a reference temperature
kg	kilogram
kPa	kilopascal
K_{SO2}	oxygen half-saturation constant
kW	kilowatt
L	liter
m	meter
m^3	cubic meter
mg	milligram
min	minute
mL	milliliter
mm	millimiter
mM	millimole
ng	nanogram
nm	nanometer
pg	picogram
psi	pounds per square inch
Q	volumetric flow rate
q_{max}	maximum specific rate of substrate utilization
R_n^-	fluorescence emission of the baseline
R_n^+	fluorescence emission of product at each time point
ΔR_n	change in fluorescence emission
S	substrate concentration
S^0	influent substrate concentration
S_{O2}	oxygen concentration in the reactor
SS	suspended solids concentration
T	temperature
V	volume
W_F	final filter weight
W_{FV}	final filter weight after MLSS analysis
W_I	initial filter weight
X	biomass concentration
X_T	total active biomass
Y	true yield
µg	microgram

μm	micrometer
μM	micromole
μ_{max}	maximum specific growth rate
μ_{obs}	observed specific growth rate
θ	hydraulic retention time
θ	temperature coefficient
θ_x	solids retention time
θ_x^{min}	minimum solids retention time

Abbreviations

A	adenine
AMO	ammonia monooxygenase enzyme
amo	ammonia monooxygenase gene
amoA	ammonia monooxygenase gene subunit A
AOB	ammonia-oxidizing bacteria
AODC	acridine orange direct counts
APHA	American Public Health Association
BNR	biological nutrient removal
BOD	biochemical oxygen demand
BOD_5	five-day BOD
C	cytosine
COD	chemical oxygen demand
COD_s	soluble COD
COD_t	total COD
cPCR	competitive PCR
CSTR	continuous-stirred tank reactor
DDE	dynamic data exchange
DGGE	denaturing-gradient gel electrophoresis
DNA	deoxyribonucleic acid
dNTP	deoxynucleotide triphosphates
DO	dissolved oxygen
EPA	Environmental Protection Agency
ESS	effluent suspended solids
FAM	6-carboxy-fluorescein
FISH	fluorescence in situ hybridization
G	guanine
HAO	hydroxylamine oxidoreductase enzyme
hao	hydroxylamine oxidoreductase gene
HART	Highway Addressable Remote Transducer
HPLC	high pressure liquid chromatography
HRT	hydraulic retention time
IAWPRC	International Association on Water Pollution Research and Control
IC	ion chromatograph

KHP	potassium hydrogen phthalate
KUB	Knoxville Utilities Board
MLSS	mixed liquor volatile suspended solids concentration
MLVSS	mixed liquor volatile suspended solids
MPN	most probable number
N	nitrogen
NOB	nitrite-oxidizing bacteria
NOR	nitrite oxidoreductase enzyme
PC	personal computer
PCR	polymerase chain reaction
rDNA	ribosomal DNA
RNA	ribonucleic acid
rRNA	ribosomal RNA
SBR	sequencing batch reactor
SRT	solids retention time
T	thymine
TAMRA	6-carboxy-tetramethyl rhodamine
TBE	Tris borate
TDPH	Tennessee Department of Public Health
TKN	total kjeldahl nitrogen
UDG	uracil DNA glycosylase
VSS	volatile suspended solids
WWTP	wastewater treatment plant

Chapter 1.0
Introduction

1.1 Background

Nitrification, the bacterially catalyzed oxidation of ammonia to nitrate, is an integral process in the global cycling of nitrogen and a vital component of most modern activated sludge wastewater treatment plants (WWTPs) (Juretschko et al., 1998). In such plants, nitrification plays a key role in reducing the oxygen demand of ammonia and organic nitrogen and is the preliminary step to the complete removal of nitrogen compounds by denitrification (Hall and Murphy, 1980). The reduction of the ammonia content of sewage is necessary because ammonia is toxic to aquatic life and can cause local oxygen depletion and eutrophication of receiving waters (Purkhold et al., 2000).

While the nitrification process has been the subject of intense research during the past several decades and its biochemistry is well known, it is still recognized as being sensitive to upsets and consequently difficult to maintain in engineered systems. The bacteria responsible for nitrification are characterized by slow growth rates and sensitivity to toxic shocks and changes in operational and environmental conditions (Marisili-Libelli and Giovannini, 1997). The extent and rate of nitrification are controlled by the process conditions prevailing in the reactor and environmental factors including the solids retention time (SRT), hydraulic retention time (HRT), substrate concentration, pH, temperature, and dissolved oxygen (DO) concentration (Wilderer et al., 2002). It is widely accepted that an SRT of greater than 3 to 4 days should be employed to achieve complete nitrification in activated sludge for municipal wastewater treatment, and that if nitrification is to be prevented, the SRT should be smaller (Grady et al., 1999). It is also recognized that the SRT required for complete nitrification increases with decreasing temperature and dissolved oxygen concentration (e.g. Wild et al., 1971; McClintock et al., 1993; Ydestbo et al., 2000).

A number of steady-state design and kinetic simulation models have been developed to describe nitrification in single-stage activated sludge systems (Bitton, 1999). Even so, the biological fundamentals behind most treatment technologies are often treated as "black boxes" with presumably known inputs and outputs (Keller et al., 2002). In spite of the fact that the efficiency and robustness of a nitrifying WWTP depends primarily on the composition and activity of its microbial community, monitoring relies on chemical and physical parameters rather than microbiological data. This is largely due to the lack of suitable techniques to monitor and control the content of nitrifying bacteria in the biomass of a microbial community (Wagner et al., 2002). Nitrifiers are difficult to cultivate and traditional culture-based enumeration techniques undoubtedly result in an underestimation of both number (Phillips et al., 2000; Erlich et al., 1995) and diversity (Juretschko et al., 1998). Due to the problems associated with quantification of nitrifying bacteria by cultivation techniques, culture independent molecular detection methods have been pursued, resulting in new tools that yield unprecedented opportunities for insight into the community structure of activated sludge. These tools are based on the detection and quantification of target molecules that are unique to specific microbial populations. Together with traditional physical and chemical analyses, these techniques offer an opportunity to better define treatment performance and to improve process design and control. A reliable and reproducible method for quantifying nitrifiers would be valuable for evaluating correlations between microbial population numbers, the effects of different operational parameters on cell density, and population changes in time and space, which might lead to more effective models for nitrification in wastewater treatment plants.

1.2 Research Objectives

The overall goal of this research was to investigate the use of the real-time polymerase chain reaction (PCR) technique as a tool for quantifying nitrifying bacteria in activated sludge. Operational parameters were manipulated to induce stress on the nitrifiers, facilitating evaluation of the real-time PCR assays over a range of nitrification performance efficiencies. The specific objective of this study was to assess and compare

the impacts of changes in operational and environmental parameters (SRT, DO, and temperature) on:

- traditional measures of process performance
    - chemical oxygen demand (COD) removal efficiency,
    - mixed liquor volatile suspended solids (MLVSS) concentration, and
    - ammonia and nitrite oxidation rates, and
- the cell densities of specific microbial populations using real-time PCR assays targeting
    - the eubacterial 16S ribosomal deoxyribonucleic acid (rDNA) gene (a measure of the total bacteria present),
    - the *Nitrosomonas oligotropha*-type ammonia monooxygenase subunit A (amoA) gene (a measure of the ammonia-oxidizers present), and
    - the 16S rDNA gene from *Nitrospira* (a measure of nitrite-oxidizers present).

Chapter 2.0
Literature Review

2.1 Introduction to the Activated Sludge Process

The activated sludge process utilizes a fluidized, mixed growth of microorganisms under aerobic conditions to consume the soluble and colloidal organic materials in wastewater as substrates, thus converting them to new biomass, carbon dioxide and water by microbial respiration and synthesis (Reynolds and Richards, 1996). The carbon dioxide produced is evolved as a gas and the biomass is removed by gravity sedimentation, leaving the wastewater free of the original organic matter. While the primary treatment objective in most activated sludge systems is the removal of soluble organic matter and oxidation of the carbon contained in it, nitrification is also desired in many cases (Grady et al., 1999). In nitrifying activated sludge systems, the ammonia-nitrogen (ammonia-N) is converted to nitrate-nitrogen (nitrate- N), which is then released in the effluent, or subjected to a denitrification step if complete nitrogen removal is desired (Davis and Cornwell, 1998).

While there are many variations of the activated sludge process, a common characteristic of all of them is the use of a flocculent suspended-growth culture of microorganisms in an aerobic bioreactor and the employment of some means of biomass recycle (Grady et al., 1999). The main units of the conventional activated sludge system, as shown in Figure 2-1, are a biological reactor with its oxygen supply (the aeration tank), a solid-liquid separator (the secondary clarifier), solids recycle from the clarifier to the aeration tank, and a sludge wasting line. In practice, wastewater flows continuously into an aeration tank, where the microorganisms consume and oxidize input organic electron donors (biochemical oxygen demand (BOD)) (Rittmann and McCarty, 2001). As the microorganisms grow and are mixed together by the agitation caused by aeration, individual organisms floc together and form an active mass of microbes called activated sludge (Davis and Cornwell, 1998). The activated sludge-wastewater mixture is termed the mixed liquor. When mixed liquor flows from the aeration tank to the secondary

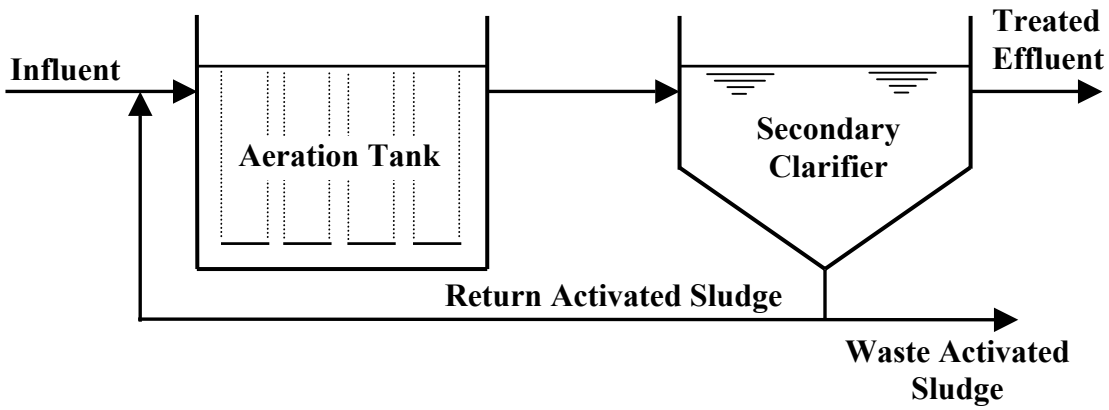

Figure 2-1. Typical Activated Sludge Process (Adapted from Grady et al., 1999)

clarifier, the flocs are removed from the treated wastewater via settling (Rittmann and McCarty, 2001). The clear effluent is discharged to the environment or sent for further treatment and most of the settled sludge is returned to the aeration tank to maintain a population of microbes that permits rapid breakdown of the organics. Because more activated sludge is produced than is desirable in the process, some of the return sludge is diverted to the sludge handling system for treatment and disposal (Davis and Cornwell, 1998).

Activated sludge is a heterogeneous microbial culture composed mostly of bacteria, protozoa, rotifers, and fungi, however the primary consumers of organic and inorganic wastes are the bacteria (Rittmann and McCarty, 2001). Like all organisms, bacteria derive energy and reducing power from oxidation reactions, which involve the removal of electrons. Two important sources of the electrons in activated sludge are organic and inorganic compounds that are present in the wastewater or released during treatment. Since the removal and stabilization of organic matter are the primary use of the activated sludge process, heterotrophic bacteria, which are bacteria that use organic compounds as their electron donor and their source of carbon for cell synthesis, predominate in these systems (Grady et al., 1999). Although heterotrophic bacteria are quite diverse in activated sludge, they have certain common characteristics that are important for design and analysis. In general, heterotrophic bacteria in activated sludge are reasonably fast growers and can drive the substrate concentrations quite low (Rittmann and McCarty, 2001). Bacteria that use inorganic compounds as their electron donor and carbon dioxide as their source of carbon (chemoautotrophic bacteria) are responsible for nitrification in activated sludge when ammonia-N and nitrite-N are used as electron donors (Rittmann and McCarty, 2001).

2.2 Fundamentals of Nitrification

Nitrification is the bacterially catalyzed oxidation of ammonia to nitrate, and is a vital component of most modern WWTPs where large amounts of ammonia are produced through decomposition of organic material (Juretschko et al., 1998). Nitrification plays a

key role in reducing the oxygen demand of ammonia and organic nitrogen and is the preliminary step to the complete removal of nitrogen compounds by denitrification (Hall and Murphy, 1980). Lowering sewage ammonia levels is necessary since this nitrogenous compound is toxic to aquatic life, can cause local oxygen depletion and eutrophication of receiving waters, and can affect chlorine disinfection efficiency (Chermisinoff, 1996).

2.2.1 Nitrification Stoichiometry

The microbial oxidation of ammonia and ammonium ions to nitrate is a two-step process that occurs primarily through the coordination of two distinct chemoautotrophic groups of bacteria: ammonia-oxidizing bacteria (AOB) and nitrite-oxidizing bacteria (NOB) (Prosser, 1989). The chemoautotrophs utilize ammonia or nitrite as an electron donor, oxygen as the terminal electron acceptor, ammonia as the nitrogen source, and carbon dioxide as a carbon source (Rittmann and McCarty, 2001). In the first step of nitrification, the AOB convert ammonium (NH_4^+) to nitrite (NO_2^-) via a two-step enzymatic process encoded by the ammonia monooxygenase (*amo*) and hydroxylamine oxidoreductase (*hao*) genes (Bothe et al., 2000). The AMO enzyme catalyzes the oxygenation of ammonium to hydroxylamine:

$$NH_4^+ + O_2 + H^+ + 2e^- \rightarrow NH_2OH + H_2O \qquad (2\text{-}1)$$

The two electrons required in this process are derived from the oxidation of hydroxylamine to nitrite by HAO:

$$NH_2OH + H_2O \rightarrow NO_2^- + 5H^+ + 4e^- \ . \qquad (2\text{-}2)$$

Following this step, the NOB oxidize NO_2^- to nitrate (NO_3^-) in a single step catalyzed by the enzyme nitrite oxidoreductase (NOR) according to the following reaction (Gray, 1989).

$$NO_2^- + 0.5O_2 \rightarrow NO_3^- \qquad (2\text{-}3)$$

The overall rate of reaction may be represented by Equations 2-4 (EPA, 1975).

$$NH_4^+ + 2O_2 \rightarrow NO_3^- + 2H^+ + H_2O \qquad (2\text{-}4)$$

The overall nitrification reaction shows that the oxidation of NH_4^+ to NO_3^- requires a high input of oxygen (about 4.5 kg for each kg of ammonia-N oxidized) (Grady et al., 1999).

Assimilative reactions are also occurring during nitrification according to Equation 2-5, in which $C_5H_7NO_2$ is the empirical formula of a bacterial cell (Cheremisinoff, 1996).

$$NH_4^+ + 4CO_2 + HCO_3^- + H_2O \rightarrow C_5H_7NO_2 + 5O_2 \quad (2\text{-}5)$$

By combining Equations 2-4 and 2-5, the overall oxidation and assimilation reaction for NH_4^+ is:

$$22NH_4^+ + 37O_2 + 4CO_2 + HCO_3^- + H_2O \rightarrow C_5H_7NO_2 + 21NO_3^- + 20H_2O + 42H^+ \quad (2\text{-}6)$$

Equation 2-6 shows that alkalinity is destroyed during the nitrification process. The theoretical amount of alkalinity destroyed per mg ammonia-N oxidized is 7.14 mg/L as $CaCO_3$ (EPA, 1975). However, theoretical alkalinity destruction is rarely observed in data obtained from laboratory, pilot plant, or full-scale studies. In most cases, the actual alkalinity destroyed is less than the theoretical value because mineralization of organic nitrogen to ammonia-N occurs in the activated sludge process and imparts alkalinity to the wastewater. The theoretical value is only valid for wastes in which no ammonia-N is obtained from mineralization of organic nitrogen, i.e., the total kjeldahl nitrogen (TKN): ammonia-N ratio is one (Cheremisinoff, 1996).

2.2.2 Nitrifying Bacteria

According to many older textbooks, the model organism for ammonia oxidation is *Nitrosomonas europaea*. However, recent analyses of nitrifying activated sludge and biofilms showed that other ammonia-oxidizers are also important (Wagner et al., 2002). Based on ultrastructural properties, AOB had been divided into five genera, *Nitrosomonas*, *Nitrosococcus*, *Nitrosospira*, *Nitrosovibrio*, and *Nitrosolobus* (Madigan et al., 1997), but 16S rRNA analysis has caused the number of genera of the characterized

bacteria to be reduced to three (Schramm et al., 1998;Wagner et al., 1998). *Nitrosococcus mobilis* has now been moved into *Nitrosomonas,* while *Nitrosospira*, *Nitrosovibrio*, and *Nitrosolobus* have all been reclassified as *Nitrosospira*, all of which fall within the beta subclass of the *Proteobacteria* (Schramm et al., 1998). The remaining members of the genus *Nitrosococcus*, which are all marine organisms, constitute a coherent group within the gamma subclass of the *Proteobacteria* (Wagner *et al.*, 1998). Almost all recognized lineages of betaproteobacterial ammonia-oxidizers can be found in wastewater treatment plants (Wagner et al., 2002). While some nitrifying WWTPs are dominated by a single ammonia-oxidizing species (Juretschko 1998), other plants harbor at least five different co-existing ammonia-oxidizing populations that are present in significant numbers (Daims 2001a).

The NOB belong to several phylogenetic groups including *Nitrobacter* (alpha subclass *Proteobacteria*), *Nitrococcus* (gamma subclass *Proteobacteria*), *Nitrospina* (delta subclass *Proteobacteria*) and *Nitrospira*, which constitutes an independent phylum in the domain *Bacteria* (Belser, 1979; Juretschko *et al.*,1998). Known members of the genera *Nitrococcus* and *Nitrospina* are marine organisms, whereas both freshwater and marine organisms are found within *Nitrobacter* and *Nitrospira* (Madigan et al., 1997). Until the late 1990s, it was generally assumed that *Nitrobacter* were the key NOB in wastewater treatment (Bitton, 1999; Mobarry et al., 1996). However, several recent molecular studies demonstrated that *Nitrospira* occurred more frequently and at higher concentrations than *Nitrobacter* in nitrifying reactors (Burrell et al., 1998; Hovanec et al., 1998; Okabe et al., 1999; Schramm et al., 1998, 1999), suggesting that *Nitrospira* plays a larger role in nitrite oxidation than *Nitrobacter* in wastewater treatment systems. It has been postulated that the predominance of *Nitrospir*a-like bacteria over *Nitrobacter* in most WWTPs is a reflection of their different survival strategies. While *Nitrospira*-like nitrite-oxidizers are, according to data extracted from microelectrode-fluorescence *in situ* hybridization (FISH) analyses, K-strategists and thus well adapted to low nitrite and oxygen concentrations, *Nitrobacter* are postulated to be relatively fast-growing r-strategists with low affinities to nitrite and oxygen (Schramm 1999). K-strategists are characterized by high affinities for substrate, which corresponds to small half-saturation

constants in terms of Monod kinetics. Therefore, K strategists are better adapted to crowded and resource-limited environments. In contrast, r-strategists are characterized by high growth rates and lower substrate affinities, which enable them to succeed particularly well in uncrowded and resource-abundant environments (Andrews and Harris, 1986). Since nitrite-N concentrations in most WWTP reactors are low, *Nitrospira* may out compete *Nitrobacter* in these systems (Wagner et al., 2002).

Nitrifying bacteria have several unique growth characteristics that are important to their impact on and survival in biochemical operations. The first is that the maximum specific growth rates for both AOB and NOB are low for pure and mixed-culture systems in comparison to those of heterotrophs (Prosser, 1989). This is due to the low energy yield, which is linked to the oxidation of ammonia-N to nitrate-N (Henze et al., 1995). Consequently, if suspended growth reactors are operated in a manner that requires the bacteria to grow rapidly, the nitrifying bacteria will be lost from the system and nitrification will cease even though organic substrate removal continues. Second, the amount of biomass formed per nitrogen utilized is small. As a result, nitrifying bacteria may make a negligible contribution to the mixed liquor suspended solids (MLSS) concentration even when they have a significant effect on process performance (Grady et al., 1999).

Under steady-state conditions, experimental evidence has shown that nitrite accumulation is insignificant (EPA, 1975; Wong-Chong and Loer, 1975, Charley et al., 1980), suggesting that ammonia oxidation is the rate-limiting step in nitrification. The lack of nitrite build-up can be attributed to the fact that the maximum growth rate of nitrite-oxidizers is considerably larger than the maximum growth rate of ammonia-oxidizers and that both organisms have half saturation constant values that are typically less than 1 mg/L (EPA, 1975). Nitrification is, therefore, modeled on the specific growth rate of ammonia-oxidizers.

2.3 Effects of SRT on Activated Sludge Treatment Performance

The SRT is commonly used in activated sludge systems to control efficiency of wastewater treatment as well as the physical and biological characteristics of the sludge (Rittmann and McCarty, 2001). SRT, symbolized by θ_x, is defined as the average length of time a unit of biomass remains in the treatment system, or

$$\theta_x \equiv \frac{X_T}{\left(\frac{\Delta X_T}{\Delta t}\right)} \qquad (2\text{-}7)$$

where: X_T = total active biomass in treatment system (kg)

$\left(\frac{\Delta X_T}{\Delta t}\right)$ = total quantity of active biomass withdrawn from the system daily (kg/day)

As shown in the following rearrangement of Equation 2-7, the appropriate value of SRT can be maintained by a controlled solids wasting policy in which a fraction equal to the total system biomass over the SRT is removed each day (Lawrence and Brown, 1976),

$$\left(\frac{\Delta X_T}{\Delta t}\right) = \frac{X_T}{\theta_x} \qquad (2\text{-}8)$$

In practice, the total active biomass is generally computed to be the product of the reactor volume and the MLVSS concentration.

The SRT is used as a fundamental variable because it is functionally related to the steady-state specific growth rate of the biomass in a complete-mix reactor. Since at steady state, the mass of organisms wasted must equal the net mass formed; that is, the new growth minus the loss due to lysis, death, and decay, it follows that the SRT is inversely proportional to the net average specific growth rate of the entire system (Benefield and Randall, 1980). Consequently, the SRT controls the concentration of the growth-limiting substrate in the reactor and determines important system characteristics, such as the electron acceptor requirement and the excess biomass production rate (Grady et al., 1999).

Garret and Sawyer (1951) were the first to directly apply the idea of SRT as a measure of activated sludge performance, however, the systematic use of this basic concept for the design of suspended growth biological treatment systems was not described until almost 20 years later by Lawrence and McCarty (1970). By incorporating the equations describing microbial growth into mass balance equations for biomass and substrate in the treatment system, Lawrence and McCarty were able to develop Equation 2-9, which clearly shows the relationship between SRT and treatment performance. Detailed derivations for this equation and others described below can be found in the classic paper by Lawrence and McCarty (1970) and numerous textbooks, (e.g. Benefield and Randall, 1980; Grady et al., 1999; Rittmann and McCarty, 2001).

$$S = K\frac{1 + b\theta_x}{\theta_x\left(Yq_{max} - b\right) - 1} \tag{2-9}$$

where: S = concentration of the rate-limiting substrate (mg/L)
K = half-saturation constant (mg/L)
b = endogenous decay coefficient (day^{-1})
θ_x = solids retention time (days)
Y = true yield (mg/mg)
q_{max}= maximum specific rate of substrate utilization (mg/ mg-d)

Equation 2-9 is also often written in terms of the maximum specific growth rate of the microorganisms, μ_{max}, which is defined by the following equation.

$$\mu_{max} = Yq_{max} \tag{2-10}$$

Substitution of Equation 2-10 into 2-9 yields:

$$S = K\frac{1 + b\theta_x}{\theta_x\left(\mu_{max} - b\right) - 1}. \tag{2-11}$$

Lawrence and McCarty (1970) also described a minimum SRT value (θ_x^{min}) which represents the SRT below which complete failure of the biological process will

occur. Below θ_x^{min}, the organisms are removed at a rate greater than their maximum synthesis rate, so that eventually no organisms will remain in the system. θ_x^{min} is computed by setting S in Equation 2-11 to the influent substrate concentration and solving for θ_x^{min}:

$$\theta_x^{min} = \frac{K + S^0}{S^0(\mu_{max} - b) - bK} \quad (2\text{-}12)$$

where: S^0 = influent concentration of the rate-limiting substrate (mg/L)

A relationship between the SRT and the steady-state mixed liquor microbial mass concentration was also developed by Lawrence and McCarty (1970) and is shown below in Equation 2-13.

$$X = \frac{\theta_x}{\theta} \frac{Y(S^0 - S)}{1 + b\theta_x} \quad (2\text{-}13)$$

where: X = concentration of biomass in the reactor (mg/L)
θ = hydraulic retention time (days)

Once the SRT for a system has been selected, the steady state biomass level can be determined. Although the range in MLSS concentration typically used in activated sludge systems is between 500 and 5000 mg/L, practical designs generally limit the MLSS concentration between 2,000 and 5,000 mg/L (Grady et al., 1999).

The equations described in this section can be applied to both the heterotrophic bacteria responsible for carbon oxidation and the autotrophic bacteria that carry out nitrification when the respective kinetic parameters and growth-limiting substrates for each population are considered. In the case of heterotrophic bacteria, the growth-limiting substrate is the BOD, for the ammonia-oxidizers, it is ammonia-N, and for the nitrite-oxidizers, it is nitrite-N.

2.3.1 Impacts of SRT on Carbon Oxidation

The maximum specific growth rate, μ_{max}, is the kinetic parameter that exerts the most pronounced effect on SRT (Grady et al., 1999). Heterotrophic bacteria in activated sludge are characterized by relatively large maximum specific growth rates, resulting in low values of minimum SRT. A typical limiting value for the minimum SRT is 0.11 days for an activated sludge system operating at 20°C (Rittmann and McCarty, 2001). The range of SRTs necessary for efficient removal of soluble organic matter from municipal wastewater is generally between 0.5-1.5 days (Grady et al., 1999). In practice, a safety factor is employed to guard against upsets in treatment performance and account for uncertainty in the kinetic parameters and influent characteristics, as well as natural variability in the microbial community. The SRT values typically used in full-scale WWTPs are in the range of 4-10 days for carbon oxidation (Metcalf and Eddy, 1991). These values represent conservative designs where high reliability in performance is required and have evolved from empirical practice over the years, rather than directly from treatment process theory (Rittmann and McCarty, 2001).

As discussed in the previous section, once the system SRT has been selected, the biomass concentration can be determined. The total biomass in the system is a function of the reactor volume and the biomass concentration in the reactor. Thus for a fixed reactor volume, selection of the SRT determines the MLSS concentration in the system. In general, a higher SRT results in a greater amount of biomass in the system and therefore a higher MLSS concentration. Several studies have demonstrated that for a given waste stream and reactor configuration, MLSS concentration increases with SRT. Stover and Kincannon (1976) conducted a series of experiments on bench-scale activated sludge systems treating synthetic wastewater operated at 20°C and SRTs ranging from 2 days to 12 days. The resulting MLSS concentrations for an influent COD of 500 mg/L ranged from approximately 500 mg/L in the 2-day SRT reactor to 4000 mg/L in the 12-day SRT reactor. McClintock et al. (1993) obtained similar results when operating a pilot-scale activated sludge system treating domestic wastewater operating at 20°C and SRTs of 1.2, 2.7, 5, and 15 days. The resulting MLVSS concentrations for influent COD values

ranging from 257 to 344 mg/L were 424, 658, 1284, and 1348 mg/L for the 1.2-, 2.7-, 5-, and 15-day SRT operation periods, respectively.

2.3.2 Impacts of SRT on Nitrification

The single most important factor that determines whether or not a WWTP will support nitrification is the SRT (Chermisinoff, 1996). As discussed previously, for a complete-mix activated sludge process operating at steady state, the specific growth rate is equal to the inverse of the SRT. This implies that if a nitrifying culture is to be established, the reciprocal of the operating SRT must be less than the maximum specific growth rate (μ_{max}) of the ammonia-oxidizer. If this requirement is not met, the rate of organism wasting from the system will be greater than the rate of production, so that washout of the nitrifying culture will occur (Benefield and Randall, 1980). Since the μ_{max} value for autotrophic nitrifying bacteria is very low, the corresponding minimum SRT may be quite high (See Equation 2-12). Typical μ_{max} values for autotrophs are almost an order of magnitude lower than those of heterotrophs, suggesting a minimum SRT for nitrifying bacteria almost an order of magnitude larger (Grady et al, 1999). As a consequence, autotrophic organisms can be lost from bioreactors under conditions that allow heterotrophic bacteria to grow freely (Cheremisinoff, 1996). Therefore special consideration must be given to the choice of the SRT in systems containing autotrophic bacteria and it cannot be assumed that the conditions suitable for the removal of soluble organic matter are suitable for the conversion of ammonia-N to nitrate-N. The minimum SRT values reported for nitrification range from 2 to 20 days with the variations in reported values being largely due to differences in temperature, pH, DO and system type (Cheremisinoff, 1996). Grady and coauthors (1999) suggest that a minimum safety factor of 1.5 be applied to the minimum SRT for the most slowly growing organisms required in the bioreactor to ensure that their washout does not occur, although larger safety factors may be required in some circumstances.

In addition to low μ_{max} values, nitrifying bacteria are also characterized by very low half-saturation constants. Consequently, complete-mix activated sludge systems containing autotrophic bacteria will have low ammonia-N concentrations whenever the SRT is large enough to ensure stable growth. It also means that the ammonia-N concentration will rise rapidly as the SRT is decreased to the point of washout. (Grady et al, 1999). It is for this reason that nitrification has gained the reputation of being an all or none phenomenon, i.e. the extent of nitrification approaches 100% whenever the SRT is long enough to give stable growth and rapidly falls to zero as washout occurs.

Several studies have been conducted to determine the necessary SRT for effective nitrification. Stover and Kincannon (1976) compared one-versus two-stage nitrification in reactors operated under complete mix conditions at 20°C treating a synthetic wastewater with an influent COD: ammonia-N ratio of 500:50 mg/L. The results of the study for the one-stage system showed that greater than 40% ammonia removal was achieved at an SRT of 2 days and that the extent of ammonia removal increased with SRT up to about 10 days then leveled off at 99%. Hanaki et al. (1990) obtained similar results when operating a laboratory-scale mixed flow reactor treating a synthetic substrate containing 80 mg/L of ammonia-N as part of a study on nitrification at low DO levels. During operation at 25°C and sufficient DO, complete nitrification was observed when the SRT was greater than or equal to 3.8 days, while operation at an SRT of 1.5 days resulted in only 60% ammonia oxidation and 40% nitrite oxidation. However, this system did nitrify more than 30 mg/L of influent ammonia at an SRT of only 1.5 days. In a study comparing nitrification rates and efficiencies for a biological nutrient removal (BNR) process and a conventional activated sludge process, McClintock et al. (1993) also noted that efficient nitrification could be achieved in reactors operating at low SRTs. In their experiment, a pilot-scale activated sludge system, treating domestic wastewater with influent ammonia-N levels ranging from 16-30 mg/L, was operated at SRTs of 15, 5, 2.7, and 1.5 at 20°C. The researchers found that complete nitrification occurred at SRTs greater than or equal to 2.7 days, while operation at an SRT of 1.5 days resulted in 79% nitrification.

2.4 Effects of DO on Activated Sludge Treatment Performance

Dissolved oxygen is required as an electron acceptor in the energy metabolism of aerobic organisms indigenous to the activated sludge process (Benefield and Randall, 1980). In general, the growth rate of an aerobe increases with the concentration of oxygen until a critical DO is reached. At this point, the maximum growth rate occurs under prevailing conditions and no further increase is possible (Gray, 1989). The oxygen dependency for aerobic processes can be described mathematically by a Monod expression, as shown in Equation 2-14 (Henze et al., 1995).

$$\mu_{obs} = \mu_{max} \frac{S_{O_2}}{S_{O_2} + K_{S,O2}} \tag{2-14}$$

where: μ_{obs} = observed specific growth rate
S_{O2} = oxygen concentration in the reactor,
$K_{S,O2}$ = half saturation constant for oxygen (Henze et. al., 1995)

The dual effects of substrate and oxygen limitation can be modeled using the following double Monod expression (Grady et al., 1999).

$$\mu_{obs} = \mu_{max} \frac{S}{S + K} \bullet \frac{S_{O_2}}{S_{O_2} + K_{S,O2}} \tag{2-15}$$

where: S = substrate concentration in the reactor
K = half saturation constant for substrate

The saturation constant $K_{S,O2}$ is defined as the oxygen concentration where the rate of substrate utilization is one-half of the maximum rate, and indicates a microorganism's affinity for oxygen. For example, a low value of $K_{S,O2}$ corresponds to a high affinity for oxygen and the ability of a microorganism to effectively utilize substrate even at low DO concentrations. The $K_{S,O2}$ value depends on floc size and on temperature as it reflects diffusional limitations for oxygen into flocs and differs greatly for heterotrophs and autotrophs making it an especially important parameter in combined carbon removal/ nitrification activated sludge systems (Henze et al, 1995).

2.4.1 Impacts of DO on Carbon Oxidation

Estimation of the oxygen half-saturation constant for heterotrophic bacteria in mixed microbial cultures is difficult because population shifts in the community often occur in response to changes in the DO concentration (Grady et al., 1999). However, a limited body of research performed on pure cultures indicates that $K_{S,O2}$ is quite low for heterotrophs. Lau et al. (1984) conducted a series of experiments in order to compare the growth kinetics of filamentous and floc-forming bacteria isolated from activated sludge. In this study, the $K_{S,O2}$ value of the filamentous bacterium *Sphaerotilus natans* was determined to be 0.01 mg/L when grown on a glucose-mineral salts medium in pure continuous culture. Under the same conditions, the floc-forming bacterium, *Citrobacter sp*. was found to have a $K_{S,O2}$ value of 0.15 mg/L. Sinclair and Ryder (1975) observed a $K_{S,O2}$ value in the middle of this range for the yeast *Candida utilis*. The oxygen half-saturation constant for this organism was found to be 0.08 mg/L when grown on a glycerol medium in a chemostat. A conservative value of 0.2 mg O_2/ L has been selected as the default parameter for the heterotrophic oxygen half-saturation constant in the International Association for Water Pollution Research and Control (IAWPRC) Activated Sludge Model No. 1 (Henze et al., 1987).

The low reported heterotrophic $K_{S,O2}$ values indicate that very low DO concentrations would be necessary to significantly impact the growth of heterotrophic organisms and the associated carbon treatment efficiency. This has been supported by the results of several studies. Chuang et al. (1997) investigated the effects of DO and SRT on nutrient removal in a combined activated sludge-biofilm process and found that at SRTs of 5, 10, and 15 days, carbon treatment performance was not impacted by changes in DO concentrations between 0.1 and 2.0 mg/L. When the system, treating a synthetic feed with an influent COD concentration of 300 mg/L, was operated at a 10-day SRT, COD removal efficiencies of 96.7%, 96.3%, and 96.3% were achieved at DO concentrations of 2.0, 0.5, and 0.1 mg/L DO, respectively. Similar results were obtained for carbon treatment performance during 5- and 15-day SRT operation. Chuang et al. (1997) also observed that MLSS levels were not affected by DO concentration. For example, when

operated at a 5-day SRT, average MLSS concentrations in the system were 920, 1010, and 1030 mg/L, at DO levels of 2.0, 0.5, and 0.1 mg/L, respectively.

Similar findings were reported by Lau et al. (1984), who found that effective carbon removal could be achieved at DO concentrations as low as 0.088 mg/L. In their study comparing filamentous and floc-forming bacteria, *S. natans* and *Citrobacter sp*. were grown in pure and dual cultures and fed a glucose-mineral salts medium with a theoretical influent COD of 1067 mg/L. Continuous culture studies were conducted in a chemostat and the DO and SRT were varied. When operated at an SRT of 0.308 days and DO concentrations of 6.16, 0.352, and 0.088 mg/L, the pure culture *S. natans* achieved 98.0%, 96.3%, and 97.2% COD removal, respectively, with MLSS concentrations of 502, 525, and 490 mg/L. This data indicates that the carbon treatment performance was not affected by the change in DO concentration nor was the heterotrophic biomass content, since heterotrophic bacteria comprise the majority of the MLSS in activated sludge systems (Grady et al., 1999). Similar results were obtained for the dual culture study. At an SRT of 0.33 days and DO levels of 7.04 and 0.44 mg/L, COD removal efficiencies of 97.9% and 98.5% were observed, with MLSS concentrations of 519 mg/L and 491 mg/L. In a series of experiments conducted on the floc-forming bacteria *Citrobacter sp*., the SRT was maintained at 0.125 days. The results of this study are shown in Table 2-1 and indicate that at the lowest DO level of 0.44 mg/L, a decrease in biomass content and treatment performance occurs. This suggests that under these conditions, the interaction between DO and SRT becomes important.

Table 2-1. Effect of DO Concentration on MLSS and COD Removal Efficiency for a Pure Continuous Culture of *Citrobacter sp*. (Adapted from Lau et al. 1984)

DO (mg/L)	MLSS (mg/L)	COD Removal (%)
8.80	523	94.3
6.60	543	94.0
6.16	534	93.9
4.40	531	91.4
3.96	531	92.3
1.76	542	94.6
0.88	493	88.7
0.44	337	57.7

2.4.2 Impacts of DO on Nitrification

Nitrifying bacteria are more sensitive to DO conditions than the majority of heterotrophs found in activate sludge (Cheremisinoff, 1996). The oxygen half-saturation constants are higher than those for heterotrophs and as a result, nitrifiers are likely to be poor competitors for oxygen at low DO concentrations (Prosser, 1989). Reported values of $K_{S,O2}$ are in the range of 0.1 to 2.0 mg/L for nitrification in the activated sludge process with values of 0.2 to 0.4 mg/L being quoted most commonly (Benefield and Randall, 1980).

In general terms, nitrification is inhibited at low DO concentrations. Although there is disagreement in the literature as to the minimum DO level required for nitrification to proceed in the activated sludge process, it is generally accepted that nitrification does not occur below 0.2-0.5 mg/L (Gray, 1989). Examples of WWTPs can be found with completely nitrified effluents operating at DO levels of 0.5 mg/L (EPA 1975), and while this type of evidence indicates that nitrification occurs at low DO, it does not mean that rates are unaffected (Cheremisinoff, 1996). The rates at which nitrification proceeds at low DO will be significantly lower than those observed at higher DO concentrations, and as a result, the aeration tank retention time must be increased to permit complete nitrification at lower DO concentrations (EPA, 1975). It is generally agreed that DO concentrations of at least 1.5 to 2.0 mg/L are necessary for optimum nitrification rates (Benefield and Randall, 1980).

The DO level necessary for effective treatment has also been found to vary with SRT and organic loading for a given system. Stenstrom and Poduska (1980) found that in many WWTPs, nitrification occurs at DO concentrations in the range of 0.5 to 1.0 mg/L when operated at higher SRT values, and when operated at lower SRT values, much higher DO concentrations were required. Hanaki et al. (1990) studied nitrification at low DO levels and examined the effect of organic loading on nitrification in a laboratory-scale mixed flow reactor. They found that for a combined carbon removal/ nitrification system treating a basal substrate containing 80 mg/L of ammonia-N and glucose in concentrations of 160, 500, and 1000 mg/L COD, effluent ammonia increased with

increasing influent COD. The results of their experiments showed that at an influent COD of 160 mg/L, the effect of DO on nitrification was not significant, however, low DO dramatically decreased nitrification efficiency when the organic loading to the reactor was increased. The researchers concluded that the inhibitory effect on nitrification was strengthened by low DO under these conditions.

There is some evidence in the literature to suggest that nitrite-oxidizers are more sensitive to low DO concentrations than ammonia-oxidizers. In the study performed by Hanakai et al. (1990) discussed previously, low DO was found to strongly inhibit nitrite oxidation, even at the lowest organic loading. Dancong et al. (2000) also found the inhibitory effects of low DO to be greater for nitrite-oxidizers than ammonia-oxidizers during a nitrification study using a sequencing batch reactor (SBR) and two different oxygen supply methods. In the controlled oxygen supply method, the DO was maintained between 2 and 3 mg/L, while in the uncontrolled oxygen supply method, the DO level changed ambiently with the oxygen use rate. When the reactor DO level was maintained at 2 to 3 mg/L, ammonia and nitrite oxidation occurred simultaneously, however, when the oxygen supply was not controlled, nitrite oxidation was completely inhibited at the low DO, but recovered during high DO operation. Ammonia oxidation proceeded throughout the low DO period of the reactor cycle. Dancong et al. (2000) reported that ammonia-oxidizers developed an ability to endure the fluctuation of DO, but nitrite-oxidizers did not. Nitrite-oxidizers are thought to be more sensitive to low DO environments than ammonia-oxidizers since their specific affinity for oxygen is lower than that of the ammonia oxidizers (Laanbroek et al., 1994). For this reason, nitrite oxidizers have difficulty competing for the available oxygen and adapting to the environment.

2.5 Effects of Temperature on Activated Sludge Treatment Performance

Temperature is an important consideration in the design of an activated sludge process because of the effect it has on the activity of wastewater microbial populations and the rate of biological reactions (Benefield and Randall, 1980). The biochemical

reactions employed in microbial metabolism for substrate utilization and endogenous degradation are enzyme-catalyzed, and reactions catalyzed by enzymes are temperature dependent (Reynolds and Richards, 1996). It is well known that bacterial growth is optimal at a certain temperature (Antoniou et al., 1990). The majority of biological treatment systems operate in the mesophilic temperature range, which is 10-45°C (Gray, 1989). For mesophilic bacteria, the optimal temperature for bacterial growth occurs at approximately 35°C (Tortora et al., 1993). Below this temperature, the rate of enzymatically catalyzed biological reactions increases with temperature in a linear fashion. Above 35°C, the rate of activity will decline as enzyme denaturation occurs and will eventually reach zero at a temperature around 45°C (Benefield and Randall, 1980). Activated sludge systems operate at the temperature of the wastewater, which is generally between 12°C and 25°C, and thus below the optimum temperature for biological activity (Gray, 1989). Therefore, in activated sludge systems, removal efficiency tends to increase with increasing temperature.

From the preceding discussion, it is evident that the physiological state of bacteria can be directly affected by temperature changes in their environment. Therefore it is necessary to account for changes in the operating temperature of an activated sludge process and determine the effect such changes will have on the values of the biokinetic coefficients used in process design (Benefield and Randall, 1980). The modified Arrhenius equation, represented in Equation 2-16, is the most commonly used temperature adjustment technique for the kinetic and stoichiometric parameters characterizing activated sludge (Sayigh and Malina, 1978).

$$k_1 = k_2\theta^{T-20} \qquad (2\text{-}16)$$

where: T = temperature (°C)
k_1 = the unknown value of any parameter at temperature T
k_2 = the known value of any parameter at a reference temperature, usually 20°C
θ = temperature coefficient

The two parameters required to characterize biomass growth are μ_{max} and K. The maximum specific growth rate is dependent upon the prevailing temperature and is assumed to vary according to the Arrhenius relationship over the range of normal

operating temperatures (Antoniou et al., 1990). The half-saturation constant describes how substrate concentration influences the specific growth rate, and thus the impact of temperature on this parameter is less clear, increasing under some circumstances and decreasing under others (Grady et al., 1999). Consequently there is no consensus about the relationship of K to temperature, and each situation must be experimentally determined.

As noted in Equation 2-10, biomass growth and substrate utilization are proportional to each other with the yield (Y) being the proportionality coefficient. Research indicates that the yield will not substantially vary according to the modified Arrhenius relationship (Benefield and Randall, 1980). Furthermore, there is some disagreement as to what a particular response will be to variations in temperature. Muck and Grady (1974) found that yield increased from 10 to 20°C but then decreased as the temperature was increased above 20°C. However, Benefield et al. (1975) and Sayigh and Malina (1976) found that the yield value was basically independent of temperature within the range of 4-20°C. Due to the uncertainty associated with the impact of temperature on the yield coefficient, most engineers assume that this parameter is independent of temperature, thereby allowing the same temperature coefficient to be used for both growth and substrate utilization (Grady et al., 1999).

Because the factors contributing to decay of bacteria are the same as those contributing to growth, it is logical to expect temperature to have similar effects on the microbial decay coefficient (b) and μ_{max}. Benefield et al. (1975) found that b varied according to the Arrhenius relationship between 15 and 25°C, but deviated appreciably at 32°C. However, as 32°C is outside the operating range of most activated sludge plants, it is reasonable to assume that variations in b with temperature can be estimated by Equation 2-16.

2.5.1 Impacts of Temperature on Carbon Oxidation

Several studies have been conducted to assess the impact of temperature on the aerobic growth of heterotrophs. Characklis and Gujer (1979) have reported an average value of 1.09 for the μ_{max} temperature coefficient (θ) for heterotrophs, while Eckenfelder (1989) reported that this value ranges from 1.03 to 1.09. Grady et al. (1999) suggest using a θ value of 1.08. The variation in reported values is due to the difference between various activated sludge systems, and this is dependent upon the specific wastewater of interest (Reynolds and Richards, 1996). Benefield et al. (1975) found that b varied according to the Arrhenius relationship between 15 and 25°C, and that θ varies between 1.02 and 1.06. Reynolds and Richards (1996) report a slightly higher range of 1.065 to 1.085 for θ. Grady et al. (1999) suggest an average value of 1.04 for use in equation (2-16) for the microbial decay coefficient for heterotrophs. Due to the relatively few studies available that report the effects of temperature on the parameters K and Y, and the lack of consensus among them as to whether the values increased or decreased with increasing temperature, a θ value of 1 is generally used for these parameters (Grady et al., 1999). Although the Arrhenius relationship can be used to approximate the variation in reaction rates with temperature, it is recommended that, when possible, all biokinetic constants be evaluated at the aeration tank temperature expected under both critical summer and winter conditions (Grady et al., 1999).

Experimental evidence indicates the process of carbon oxidation by heterotrophic bacteria is fairly insensitive to temperature because of the high solids levels maintained in activated sludge systems (Benefield and Randall, 1980). In a set of bench-scale activated sludge experiments, Sayligh and Malina (1978) found that at SRTs lower than 2 days, the efficiency of soluble BOD removal deteriorated appreciably as the temperature decreased from 31° to 4°C. However, at SRTs of 3 days or more, effluent soluble BOD concentrations were less than 10 mg/L over the entire temperature range studied, suggesting that BOD removal efficiency was relatively independent of temperature variations between 4°C and 31°C. McClintock et al. (1993) reported similar results with a

pilot-scale activated sludge system treating domestic wastewater with an average influent COD concentration of 110-344 mg/L. When operated at and SRT of 15 days, the system achieved COD removals of 88%, 91% and 87% at 20°C, 15°C, and 10°C, respectively, while at an SRT of 5 days, 93%, 96%, and 86% COD removal was observed at temperatures of 20°C, 15°C, and 10°C, respectively. This data suggests that variations in temperature had no significant effect on carbon treatment over the range of normal operating temperatures for activated sludge systems.

2.5.2 Impacts of Temperature on Nitrification

While nitrification has been found to occur over a wide range of temperatures, the overall rate of nitrification has been shown to decrease with decreasing temperature (Poduska and Andrews, 1975). Temperature effects on nitrification are primarily related to the slow growth rate of nitrifying bacteria, which is exacerbated at low temperatures (Ydstebo et al., 2000). As discussed previously, nitrifying bacteria have much lower μ_{max} values than heterotrophs at optimum conditions, and the literature suggests that nitrifiers are also more sensitive to changes in temperature than heterotrophs. This statement is evidenced by the larger temperature coefficients reported for nitrifiers than heterotrophs. For example, Characklis and Gujer (1979) reported an average θ of 1.11 for μ_{max} for nitrification, as opposed to 1.09 for heterotrophs. As with heterotrophic bacteria, the yield coefficient is generally assumed to be independent of temperature due to the uncertainty associated with the impact of temperature on Y. However, unlike heterotrophs, for which temperature appears to have variable effects on K, increases in temperature cause the half-saturation coefficient for nitrifiers to increase. The most widely cited data is that of Knowles et al. (1965) for which θ =1.13 for *Nitrosomonas* and 1.16 for *Nitrobacter*. In spite of the importance of temperature to nitrification, few studies have systematically studied the effects of temperature on the decay coefficient for nitrifying bacteria (Grady et al., 1999).

Nitrosomonas and *Nitrobacter* seem to be influenced similarly by temperature; however, there are conflicting reports about the relative effects of temperature on the maximum specific growth rates of the two major genera of nitrifiers (Shammas, 1986). Characklis and Gujer (1979) reported average θ values of 1.12 and 1.07 for μ_{max} for *Nitrosomonas* and *Nitrobacter*, respectively. In contrast, Hall and Murphy (1985) reported θ values of 1.10 and 1.11 for *Nitrosomonas* and *Nitrobacter*, respectively. Randall and Buth (1984) also found *Nitrobacter* to have a larger temperature coefficient than *Nitrosomonas* over the temperature range of 5° to 30°C. The results of their study indicated that although the maximum possible rate of nitrate formation may be substantially greater than the maximum rate of nitrite formation at 20°C, there exists a lower critical temperature below which the rate of nitrite formation will exceed that of nitrate, resulting in a build-up of nitrite. In their experiments, the critical temperatures for a laboratory-scale and a full-scale reactor were 14° and 12°C, respectively. Below the critical temperature, the rate of nitrate formation controls the overall nitrification rate.

Several studies have been conducted to assess the impact of temperature on the efficiency of nitrification. Wild et al. (1971) conducted temperature studies over the range 5° to 30°C, and found that nitrification occurred at all temperatures investigated. Their results indicated that an approximate straight-line relationship existed between the nitrification rate and temperature. They found that the rate at 27°C was 90% of that at 30°C, and at 17°C was 50% of that at 30°C. Wild et al. (1971) concluded that it may be necessary to increase the SRT by a factor of five to insure complete nitrification in colder seasons. In another study, McClintock et al. (1993) measured complete nitrification in a pilot-scale activated sludge system treating domestic wastewater at an SRT of 15 days and temperatures of 10°, 15°, and 20°C, and at a 5-day SRT at 15°, and 20°C. Partial nitrification was noted with a 5-day SRT during operation at 10°C, with 65% conversion of ammonia-N to nitrate-N. Their results showed that an SRT of between 5 and 8 days was needed to maintain complete nitrification at 10°C. Ydstebo et al. (2000) also demonstrated nitrification at low temperatures in their study on nutrient removal in a Norwegian BNR treatment facility. Results of the study demonstrate effective

nitrification at temperatures as low as 6°C can be accomplished by operating at higher SRTs to support nitrifier growth. Low temperature impacts were minimized by increasing the SRT from 4 days at 15°C to 14 days at 6°C (Ydstebo et al., 2000). Thus, the literature suggests that while the rate of nitrification decreases with decreasing temperature, negative effects can be overcome (to a considerable degree) by increasing the SRT in the activated sludge system.

2.6 Introduction to Molecular Methods

The accumulation and diversity of a nitrifying microbial community in activated sludge play a crucial role in the performance of a wastewater treatment system (Kim and Ivanov, 2000). Until recently, suitable techniques to monitor and control the content of nitrifying bacteria in the biomass of a microbial community have been limited (Rittmann, 2002). Much of our knowledge about the physiology of nitrifying bacteria and requirements for their growth has come from pure culture studies (Grady and Filipe, 2000). However, it is known that only a small proportion of bacteria found in natural and engineered environments can be cultivated under standard laboratory conditions (Hermansson and Lindgren, 2001). Due to the low maximum growth rates and low biomass yields of nitrifiers, pure culture isolation is extremely difficult, resulting in an underestimation of both the number and diversity of organisms (Prosser, 1989). Estimation of nitrifier kinetic parameters in mixed cultures of heterotrophs and autotrophs is difficult because nitrifying bacteria are morphologically indistinct from heterotrophs (Hall and Murphy, 1980). Without a method of estimating the fraction of microorganisms that are autotrophic in a mixed culture sample, it is impossible to estimate parameters such as specific growth rate or specific substrate removal rate. Routine bacteriological enumeration by spread-plate or most-probable-number (MPN) count are not suitable for determining the mass of nitrifying organisms within samples of activated sludge because of the difficulty in obtaining nitrifier isolates (Mendum et al., 1999). Thus, ecological studies of nitrifiers have been severely limited by the lack of

reliable and convenient techniques for estimating cell or biomass concentrations (Phillips et al., 2000).

Only recently have tools become available that make the quantification of individual microbial populations possible. These tools fall within the broad range of molecular signature techniques and are based on the detection and quantification of target molecules that are unique for specific microbial populations (Oerther et al., 1999). A common target is the 16S rRNA gene, which codes for the ribosomal RNA (rRNA) molecules needed for protein synthesis (Wilderer et al., 2002). The 16S rRNA molecule has approximately 1500 bases that can be sequenced and contains both highly variable and conserved regions (Rittmann and McCarty, 2001). Analysis of the variable regions of the 16S rRNA can identify stretches of 15-20 bases that are unique to a given organism or set of similar organisms. These regions can be used as targets for the identification and quantification of different microorganisms present in complex microbial communities such as those found in activated sludge (Rittmann, 2002). Another target molecule is a gene that codes for catabolic enzymes restricted to a strain or related group of strains. For nitrifying bacteria, the gene that encodes the ammonia-monooxygenase (AMO) enzyme, which catalyzes the critical first step of ammonia oxidation to hydroxylamine, is a good target for assessing a community's potential to perform nitrification (Rittmann, 2002).

Before nitrifying bacterial concentrations in a particular treatment facility can be measured, key microbes in that plant must first be identified. This is accomplished by obtaining an inventory of the microorganisms present and establishing a 16S rRNA gene clone library (Wagner et al., 2002). The first step in the identification process is to extract DNA from the bacterial cells and construct a data bank consisting of specific genes, which can be used to identify bacterial cells independent of cultivation. Extracted 16S rRNA genes are amplified enzymatically using the PCR, which will be described in detail in section 2.6.1. Following amplification, the 16S rRNA gene are then cloned and maintained in *Escherichia coli*, which serves as a host and further multiplies the DNA copies as part of its growth cycle. These *E. coli* cells effectively act as a gene library, an inventory of rRNA genes of the original microbial population (Wilderer et al., 2002). The DNA fragments can be sequenced to reveal the identity of the corresponding bacteria by

comparative analysis with 16S rRNA sequences of other bacteria (Rittmann and McCarty, 2001). Currently more than 17,000 16S rRNA sequences are maintained in public databases (Klappenbach et al., 2001).

A 16S rRNA gene library for an environmental sample provides information about the composition of the microbial community, but does not provide a quantitative estimate of microbial abundance (Wilderer et al., 2002). In order to determine the relative abundance of the respective bacterial populations, the information gained from the gene library must be incorporated into quantitative molecular techniques such as nucleic acid hybridization with oligonucleotide probing, fluorescence *in situ* hybridization (FISH), or real-time PCR.

2.6.1 Oligonucleotide Probe Hybridization

Nucleic acid hybridization is based on the ability of two complementary single-stranded DNA molecules or single-stranded DNA and RNA molecules to form a hydrogen bonded duplex structure. Oligonucleotide probing exploits the unique sequences in the rRNA that were identified from the 16S rRNA gene clone library, by creating small DNA molecules approximately 15-25 bases (the probes) that have nucleotide sequences perfectly complementary to a region in the target cell's DNA or RNA (Rittmann, 2002). The specificity of the probes is freely adjustable and the targets may be as specific as a single organism or as broad as all prokaryotes (Biesterfeld and Figueroa, 2002). Under strictly controlled assay conditions, the single-stranded oligonucleotide probe forms base pair hydrogen bonds only with those sequences that are homologous to the complementary base sequences of the target nucleic acid (Atlas et. al., 1992). If the complementary sequence is not present, hybridization does not occur and the probe is washed away from the target site (Biesterfield et al., 2001). By attaching a reporter molecule to the oligonucleotide probe, hybridization can be monitored making it possible to detect the presence and quantity of target nucleic acid using radioactivity (phosphorous-32) or fluorescence (Wilderer et al., 2002).

Oligonucleotide probe hybridization can occur *ex situ* to isolated nucleic acid or *in situ* to whole cells. Examples of *ex situ* hybridization include DNA hybridizations with catabolic DNA probes and dot blot hybridization using 16S rRNA targeted oligonucleotide probes. DNA hybridization with catabolic probes consists of applying appropriate amounts of total DNA extracted from activated sludge to a nylon membrane, together with a set of DNA standards that allows the generation of a standard curve to quantify the target DNA. The DNA is hybridized on the membrane with an appropriate gene probe, followed by detection and quantification (Applegate et al., 1995). The quantitative dot blot hybridization method using 16S rRNA targeted oligonucleotide probes can be used to determine the relative rRNA abundance of a specific bacterial group relative to total rRNA, as long as it is above the detection limit. In this method, RNA extracted from a sample is immobilized on nylon membranes and hybridized with labeled universal and specific oligonucleotide probes. A limitation of *ex situ* rRNA-targeted hybridization is that the relative abundance of RNA cannot be directly translated into cell numbers (Wilderer et al., 2002).

In contrast, FISH targets the 16S ribosomal subunit of whole cells allowing cell numbers to be obtained directly by manual counting in an epifluorescence microscope. During whole cell *in situ* hybridization the morphology of the cells in the sample is stabilized in order to maintain morphological integrity of the cells and the cell walls and membranes are permeabilized with fixatives to allow free penetration of the fluorescent oligonucleotides to the intracellular rRNA (Theron and Cloete, 2000). The cells are either attached to gelatin-coated microscope slides or hybridized in suspension and immersed in hybridized solution containing fluorescently labeled oligonucleotides. Following incubation at the hybridization temperature for one to several hours, to allow the probe to bind to complementary rRNA sequences, washing steps are used to remove unbound or part of the nonspecifically bound fluorescent probe and the sample is then viewed by epifluorescence microscopy (Theron and Cloete, 2000). Usually the relative abundance of a probe target population is determined by comparison of the obtained numbers with counts of all bacterial cells detectable by FISH via simultaneous hybridization with a bacterial probe or with counts of all organisms containing DNA by simultaneous

application of nucleic acid staining dyes (Daims et al., 2001c). Because the cells are not destroyed, FISH is able to provide information on the spatial relationships among different types of cells (Rittmann and McCarty, 2001).

While FISH provides good qualitative data, it is difficult to use for high throughput quantification of nitrifying bacteria in activated sludge. FISH suffers from tediousness and limited accuracy for samples containing densely aggregated cells like activated sludge flocs. Even when combined with such technology as confocal laser scanning microscopy, it is not feasible to manually count a sufficient number of cells in each hybridization experiment in a reasonable time period to obtain statistically reliable results (Daims et al., 2001c). Another disadvantage is that in hybridization experiments the measured target cannot be verified, whereas in amplification techniques the PCR product can be cloned and sequenced to verify that the measured target is correct.

2.6.2 Polymerase Chain Reaction (PCR)

PCR is a relatively simple but elegant technique by which a DNA template is amplified many thousand or million-fold quickly and reliably (Saiki et al., 1998). The PCR process generates sufficient material for subsequent experimental analyses.

PCR is closely patterned after the natural principle of DNA replication. When any cell divides, polymerase enzymes make a copy of the DNA in each chromosome (Tortora et al., 1995). The first step in this process is to "unzip" the two DNA chains of the double helix. As the two strands separate, DNA polymerase makes a copy using each strand as a template (Saiki et al., 1988). In addition to the DNA polymerase, two other components are required for DNA replication: a supply of the four nucleotide bases and a primer. The four nucleotide bases, adenine (A), cytosine (C), guanine (G), and thymine (T) are the building blocks of DNA. The A on one DNA strand always pairs with the T on the other strand, whereas C always pairs with G. Thus, the two strands are said to be complementary to each other. DNA polymerases cannot copy a chain of DNA without a short sequence of nucleotides to "prime" the process (Tortora et al., 1995). Therefore, the cell has another enzyme (primase) that actually makes the first few nucleotides of the

copy. This stretch of DNA is referred to as the primer, and once it has been made, the polymerase can continue to develop the new chain (Saiki et al., 1985).

A typical polymerase chain reaction includes all the necessary components for DNA duplication: the sample of target DNA, large quantities of the four nucleotides in the form of deoxynucleotide triphosphates (dNTPs), large quantities of two oligonucleotide primers, a thermostable DNA polymerase, reaction buffer, magnesium and optional additives (Erlich et al., 1991). In PCR, the goal is not to replicate the entire strand of DNA but to replicate a target sequence of approximately 100-600 base pairs that is unique to the organism. The oligonucleotide primers mark the ends of the target sequence. These primers are short, synthetic sequences of single-stranded DNA typically consisting of 20-30 bases that are specific for the target region of the organism (Saiki et al., 1985). Two primers are included in the PCR, one for each of the complementary single DNA strands. The components of the reaction are mixed and the reaction is placed in a thermal cycler, which is an automated instrument that takes the reaction through a series of different temperatures for varying amounts of time. This series of temperature and time adjustments is referred to as one cycle of amplification (Erlich et al., 1991).

The initial step in a cycle denatures the target DNA by heating it to 95°C or higher for 15 seconds to 2 minutes (Erlich et al., 1991). In the denaturation process, the two intertwined strands of DNA separate from one another, producing the necessary single-stranded DNA template for the thermostable polymerase (Holland et al., 1991). Since the hydrogen bonds linking the bases to one another are weak, they break at high temperatures, whereas the bonds between deoxyribose and phosphates, which are stronger covalent bonds, remain intact (Erlich et al., 1991).

The primers cannot bind to the DNA strands at such a high temperature, so for the second step of the PCR cycle the vial is cooled to approximately 40-60°C (Erlich et al., 1991). At this temperature, the oligonucleotide primers can form stable associations (anneal) with the separated target DNA strands and serve as primers for DNA synthesis by the *Taq* polymerase. This step lasts approximately 30-60 seconds.

The final step of the reaction is to make a complete copy of the templates. The synthesis of new DNA begins when the reaction temperature is raised to the optimum for

the thermostable DNA polymerase, which is approximately 74°C. *Taq* DNA polymerase is a recombinant thermostable DNA polymerase from the organism *Thermus aquaticus* and, unlike normal polymerase enzymes, is active at high temperatures (Saiki et al., 1988). *Taq* DNA polymerase begins the synthesis process at the region marked by the primers. It synthesizes new double stranded DNA molecules, both identical to the original double stranded target DNA region, by facilitating the binding and joining of the complementary nucleotides that are free in solution (dNTPs) (Holland et al., 1985). The length of the products generated during PCR is equal to the sum of the lengths of the two primers plus the distance in the target DNA between the primers (Erlich et al., 1991).

The three steps in the polymerase chain reaction (the separation of the strands, annealing the primer to the template, and the synthesis of new strands) take less than two minutes. Each is carried out in the same vial. At the end of a cycle, each piece of DNA in the vial has been duplicated, and the cycle can be repeated 30 or more times (Wilderer et al.2002). Each newly synthesized DNA piece can act as a new template, so after 30 cycles, 1 million copies of a single piece of DNA can be produced. Taking into account the time it takes to change the temperature of the reaction vial, 1 million copies can be made in about 3 hours (Saiki et al., 1998).

2.6.3 Fundamentals of Real-time PCR

The one weakness of the original PCR method is that it is not quantitative. To overcome this shortcoming, variations of PCR, such as limiting-dilution PCR, kinetic PCR, competitive PCR and real-time PCR, have been developed to allow quantification of specific targets present in a complex sample (Hermansson and Lindgren, 2001). Real-time PCR requires the addition of dual-labeled fluorogenic probes (Lee et. al., 1993; Bassler et al. 1995; Livak et al., 1995a,b) that anneal to a target sequence located between the two primer binding sites during the polymerase chain reaction. Several different fluorescent probes can be used in real-time PCR including TaqMan (Livak et al., 1995a). The TaqMan probe is a linear oligonucleotide complementary to a target nucleic acid sequence, with a reporter fluorophore attached to the 5’ end and a quencher fluorophore

attached to the 3' end (Heid et al., 1996). Modification of the probe with a 3'-blocking phosphate prevents extension of the annealed probe during amplification, i.e. because the 3' end is blocked, it cannot act as a primer (Lie and Petropoulos, 1998). When the probe is intact, fluorescent energy transfer occurs and the fluorescent emission from the reporter dye, 6-carboxy-fluorescein (FAM) is absorbed by the quenching dye 6-carboxy-tetramethyl-rhodamine (TAMRA) (Heid et al., 1996). During the extension phase of the PCR cycle, the TaqMan probe that is annealed to the target sequence is cleaved by the 5'-3' exonuclease activity of the extending Taq polymerase, resulting in the separation of the reporter dye from the quencher dye (Lie and Petropoulos, 1998). When this occurs, the reporter dye emission is no longer transferred efficiently to the quenching dye, resulting in an increase of the reporter dye fluorescent emission spectra (Heid et al., 1996). This process occurs in every cycle and does not interfere with the exponential accumulation of PCR product (Gulietti et al., 2001).

The increase in fluorescence emission can be read by a fluorescence detector in "real-time," during the course of the reaction, and is a direct consequence of target amplification during PCR (Gulietti et al., 2001). A computer software program calculates the change in fluorescence emission according to the following equation (Heid et al. 1996).

$$\Delta R_n = R_n^+ - R_n^- \qquad (2\text{-}16)$$

where: R_n^+ = the fluorescence emission of the product at each time point
R_n^- = the fluorescence emission of the baseline

Thus, ΔR_n expresses the probe degradation during the PCR process (Gulietti et al., 2001). The computer software constructs amplification plots using the fluorescence emission data that are collected during PCR amplification, in which the ΔR_n values are plotted versus cycle number. Typically an amplification plot has a sigmoidal shape (Lie and Petropoulos, 1998). Within the initial flat part of the curve, the amount of reporter that has been cleaved is not large enough to elevate the emission intensity above the baseline (Gulietti et al., 2001). After a certain number of amplification cycles, enough probe cleavage has occurred so that the ΔR_n values exceed the baseline. The subsequent

exponential phase in the curve represents a logarithmic amplification of PCR product. Finally, a plateau phase is reached and no significant further product accumulation takes place (Lie and Petropoulos, 1998). To delineate the beginning of the exponential phase, an arbitrary threshold is chosen, based on the variability of the baseline. Usually this is determined as 10 times the standard deviation of the baseline, set from cycles 3 to 15, although this can be manually changed for each individual experiment if necessary (Gulietti et al., 2001). The cycle at which the emission intensity of the sample rises above baseline is referred to as the threshold cycle, or C_T and is inversely proportional to the target sequence concentration (Heid et al., 1996). The higher the target concentration, the lower number of amplification cycles required to detect the rise in reporter emission above the baseline (Lie and Petropoulos, 1998). Therefore, this can be used as a quantitative measurement of the input target. The C_T of each sample is then compared to a standard curve and the result is a numerical value of the number of target sequences in the sample (Hall et al., 2002).

Real-time PCR has several advantages over other quantitative PCR methods that rely on end-point analysis. Because the determination of the target input copy number is performed during the exponential phase of the reaction, a more accurate estimation of sample concentration is obtained (Heid et al., 1996). In addition, the large dynamic range (5-9 logs) of real-time PCR assays permits the simultaneous analysis of samples with varying input concentrations without the worry that high copy number samples reach plateau while lower copy number samples continue to amplify exponentially (Lie and Petropoulos, 1998). Finally, real-time PCR is performed in a closed tube system and requires no post-PCR manipulation of samples, which reduces the risk of cross-contamination in the laboratory and also increases sample throughput (Heid et al., 1996).

2.7 Applications of Molecular Methods in the Quantification of Nitrifiers

Quantification of nitrifying bacteria has been attempted using several different methods including quantitative blot hybridization (Hovanec and Delong, 1996; Mobarry et al., 1996; Rittmann et al., 1999), fluorescence in situ hybridization (FISH) (Wagner et

al.1995, 1996; Mobarry et al. 1996; Schramm et al., 1999), competitive PCR (Kowalchuck et al., 1999; Phillips et al., 2000; Stephen et al., 1999; Bjerrum et al., 2002, Dionisi et al. 2002a,b), and most recently real-time PCR (Hermansson and Lindgren, 2001; Hall et al., 2002; Harms et al., 2003).

2.7.1 Fluorescence *in situ* Hybridization (FISH)

FISH has been used to successfully characterize nitrifying bacteria in wastewater treatment systems (Juretschko et al., 1998; Okabe et al., 1999; Schramm et al., 1996; Wagner et al., 1993 and 1995). Results to date have yielded qualitative information about community structure; for example, which organisms are present and where they are located with respect to other populations (Biesterfeld et al., 2001). The variability of microscopic images obtained for one sample and the presence of bacterial aggregates and non-transparent particles in the environmental samples, complicate the enumeration of cells by whole-cell FISH when analyzed by fluorescent microscopy and image analysis (Kim and Ivanov, 2000). This can be particularly problematic for the nitrifying bacteria in the activated sludge, which grow in the form of microcolonies embedded in a flock of heterotrophic microorganisms (Wagner et al., 1998), making the heterogeneity of microscopic images high. Even so, FISH has been successfully applied for the quantification of nitrifiers in activated sludge in several studies (Wagner et al., 1996; Juretschko et al., 1998; Daims et al., 2001). Wagner et al. (1996) and Juretschko et al. (1998) both performed studies on an intermittently aerated nitrification-denitrification basin of an industrial WWTP receiving sewage from an animal waste processing facility. This particular wastewater treatment plant receives sewage with exceptionally high ammonia concentrations (up to 5000 mg/L), resulting in high numbers of ammonia oxidizers compared to domestic sewage treatment plants. Wagner et al. (1996) reported ammonia-oxidizer cell densities of 6.6 ($\pm$ 1.3) x 10^8 cells (13% of total cell counts) per mL of activated sludge based on FISH measurements in this industrial plant. The researchers used this value to estimate a specific activity per *in situ* detected ammonia oxidizing cell of 0.00022 $\pm$ 0.000045 pmol/cell per hour. In a related study performed by

Juretschko et al. (1998), FISH demonstrated *Nitrospira*-like bacteria comprised 9% of the total bacterial counts and ammonia oxidizers represented 10 to 20% of total number of cells in this industrial treatment plant. Daims et al. (2001a) reported similar ammonia-oxidizer cell densities for a separate stage nitrifying municipal WWTP. In this study 9.8 ($\pm$ 1.9) x 10^7 ammonia-oxidizer cells/ mL were found in the activated sludge, representing approximately 8.4% of total population measured by FISH. Based on the measured cell density, the average *in situ* activity was calculated to be 0.0023 pmol of ammonia converted to nitrite per ammonia-oxidizer per hour.

2.7.2 Competitive PCR

Competitive PCR (cPCR) has previously been used to quantify AOB in environmental samples and has been demonstrated both with 16S rDNA template (Mendum et al., 1999; Phillips et al., 2000; Bjerrum et al., 2002) and with the *amo*A gene (Kowalchuk et al., 1999; Mendum et al., 1999; Stephen et al., 1999; Daims et al., 2001b; Bjerrum et al., 2002; Dionisi et al., 2002a,b). However, the use of cPCR with this group of bacteria in activated sludge has been limited (Kowalchuk et al., 1999; Daims et al., 2001, Bjerrum et al., 2002, Dionisi et al., 2002a,b). To date, the only studies of cPCR applications for NOB in activated sludge have been performed by Dionisi et al. (2002a,b).

Ammonia Oxidizing Bacteria

Several researchers have suggested that the *amo*A gene, encoding the ammonia monooxygenase enzyme active site, may be a more reliable tool than 16S rDNA-based approaches for enumeration of AOB in environmental samples, since it reduces the number of non-target organisms detected (Åakra et al., 2001; Mendum et al., 1999; Bjerrum et al., 2002; Norton et al., 2002). The 16S rDNA approach for ecological investigations of AOB often yields an overestimation of both number and diversity of AOB, while *amo*A gives a better estimate of the actual number and activity of AOB, but might give less information concerning the distribution of the phylogenetic groups of

AOB (Åakra et al., 2001). While it is likely that the *amo*A primers only amplify *amo*A genes from a subset of AOB present in the sample, this may be preferable to 16S rRNA primer based assays where non-AOB may contribute to the obtained population estimates (Bjerrum et al., 2002).

Kowalchuck et al. (1999) studied the distribution and community composition of beta subgroup proteobacterial AOB in different types of compost and composting materials with cPCR targeted at the *amo*A gene. In their experiments, a calf slurry-fed activated sludge sample was used as a positive control and was found to contain 1.7 (± 1.1) x 10^{12} cells/g of *Nitrosospira* cluster 3 AOB. Daims et al. (2001b) also measured the concentration of AOB by cPCR of an *amo*A sequence fragment and used their results to calculate ammonia turnover rates in a nitrifying biofilm, two separate stage nitrifying activated sludge wastewater treatment plants, as well as a denitrifying biofilm as a negative control. Results were reported in average ammonia turnover rates per cell, assuming that 80% of the influent ammonia was oxidized to nitrite and 20% was assimilated by the bacteria. Cell numbers were not provided. The ammonia turnover rates were 0.048 pmol ammonia per cell per hour for the nitrifying biofilm and 0.016 and 0.043 pmol ammonia per cell per hour for the two nitrifying activated sludge systems. The denitrifying biofilm had a much lower ammonia turnover rate of 0.003 pmol ammonia per cell per hour. The researchers found that these results were similar to those obtained in pure culture studies, with turnover rates of 0.0018-0.023 pmol ammonia per cell per hour as reported by Belser (1979). In another study, Bjerrum et al. (2002) used cPCR assays to estimate cell densities of AOB in many different environmental samples, such as intertidal mud flats, rice paddy soil, and activated sludge. Competitive PCR estimates of *amo*A gene copy number in activated sludge from Marselisborg Municipal WWTP aerobic activated sludge basin (Aarhus, Denmark) revealed an AOB density of approximately 10^8 cells/g wet weight. This cell concentration was in agreement with results from other sewage treatment plants (using FISH) including Wagner et al. (1996) who reported 6.6 (± 1.3) x 10^8 AOB cells per mL of activated sludge. Dionisi et al. (2002a) utilized cPCR (based on *amo*A gene fragments) to detect ammonia-oxidizers in a single sludge full-scale municipal treatment plant, and reported values of 4.3 (± 0.6) x 10^4

to 4.1 (± 0.3) x 10^5 *Nitrosomonas oligotropha*-type cells/mL activated sludge mixed liquor. While there appears to be a large discrepancy between these values and those obtained by other researchers, the difference can be attributed to the type of treatment process studied. Dionisi et al. (2002a) studied a single stage activated sludge process treating low nitrogen levels, whereas the other studies assessed separate-stage nitrification processes and/or systems with high influent nitrogen loading. It has been established that the fraction of biomass that is composed of nitrifiers is considerably larger in separate-stage nitrification when compared to that in the single-stage process (Benefield and Randall, 1980). It is also likely that the *amo*A gene fragment used in the study performed by Dionisi et al. (2002a) did not account for all of the AOB present in the activated sludge.

Nitrite Oxidizing Bacteria

Thus far, the only studies of cPCR applications for NOB in activated sludge have been performed by Dionisi et al. (2002a,b). In their analyses of a full-scale municipal activated sludge treatment process, a PCR assay targeted toward *Nitrospira* 16S rDNA resulted in NOB concentrations ranging from 5.8 (± 0.98) x 10^6 to 5.5 (± 0.2) x 10^7 *Nitrospira* cells/mL activated sludge mixed liquor.

2.7.3 Real-time PCR

While real-time PCR has been used extensively in medical research, its application to environmental research has only recently been established (Suzuki et al., 2000; Bowers et al., 2000; Gruntzig et al., 2001; Hermansson and Lindgren, 2001; Becker et al., 2002; Yuan and Blackall, 2001; Hall et al., 2002; Harms et al., 2003).

Ammonia Oxidizing Bacteria

Hermansson and Lindgren (2001) used real-time PCR with primers and probes targeting a 16S rDNA region of AOB to quantify populations of AOB samples of arable soil. Cell numbers in both fertilized and unfertilized soil were studied to determine the effect of fertilization on soil AOB density. A two- to three-fold increase in AOB was

found in the fertilized soil suggesting that an increase in ammonia yields an increase in the number of AOB present. Harms et al. (2003) utilized real-time PCR for quantification of *N. oligotropha*-like AOB using an *amo*A assay in a municipal WWTP. Samples were collected an analyzed monthly for a period of one year and were found to contain an average *N. oligotropha*-like AOB cell concentration of 7.5×10^6 cells/ mL of mixed liquor.

Nitrite Oxidizing Bacteria

Yuan and Blackall (2002) used a real-time PCR assay targeting *Nitrospira* 16S rDNA to quantify NOB in lab-scale reactors treating municipal wastewater and found *Nitrospira* concentrations of approximately 3×10^6 *Nitrospira* cells/mL activated sludge mixed liquor. Hall et al. (2002) applied the same real-time PCR *Nitrospira* assay to samples from five full-scale municipal WWTPs. *Nitrospira* cell densities of 2.9×10^3, 4.1×10^7, 1.8×10^9, 1.2×10^4, and 2.3×10^{10} cells/mL mixed liquor were reported for the WWTPs achieving 48.1%, 98.8%, 99.3%, 99.7%, and 99.8% nitrification, respectively. Ammonia in the influent for all plants ranged from 21-42 mg/L. Hall et al. (2002) reported that, on the surface, nitrification performance appeared to be correlated with *Nitrospira* cell numbers for the plants investigated. An exception to this correlation was noted for one plant in which low *Nitrospira* numbers (1.2×10^4 Nitrospira cells/ mL) were measured, but a high degree of nitrification (99.7%) occurred, suggesting that organisms other than *Nitrospira* were responsible for nitrite oxidation in this plant. Harms et al. (2003) reported cell densities of 1.7×10^7 to 1.2×10^8 *Nitrospira* cells/ mL of mixed liquor when using a real-time PCR assay for *Nitrospira* 16S rDNA on 12 monthly samples from a full-scale municipal WWTP operating at an average SRT of 12 days. These values are comparable to those measured by Yuan and Blackall (2002).

2.8 Attempts to Correlate Nitrifier Cell Densities with Process Performance

Thus far, few attempts have been made to correlate the number and type of nitrifying populations in wastewater treatment systems with observed nitrification rates

(Urbain et al., 1997; Rittmann et al., 1999; Biesterfeld et al., 2001; Biesterfeld and Figueroa, 2002) other than the assessment of specific in situ activity rates as previously discussed (Wagner et al., 1996; Daims et al., 2001a,b). Urbain et al. (1997) presented the first example of an integrated analysis of activated sludge process performance using chemical, molecular, and mathematical tools. In the study, influent and effluent wastewater quality and sludge concentration were measured in a pilot-scale aerobic membrane bioreactor (MBR) operated at different SRTs in a municipal WWTP, and compared with predicted values obtained using the multispecies mathematical model published Furamai and Rittmann (1992). The accuracy of the model was demonstrated by comparing COD, ammonia-N and nitrate-N values at steady state. The proportion of nitrifiers and heterotrophs in the system were predicted by the model and compared to values measured using the slot-blot technique with oligonucleotide probes targeted towards the 16S rRNA. Urbain et al. (1997) found that there was good agreement between the model-predicted community structure and the slot-blot results. The percentages of nitrifiers predicted by the model were 7.1%, 8.9%, and 7.5% for SRTs of 5, 10, and 20 days, respectively, while the results of the molecular analysis showed that nitrifiers comprised 5.3%, 6.6%, and 12.1% of the total bacterial population for the 5-, 10- and 20-day SRTs, respectively.

Rittmann et al. (1999) also used the mathematical model of Furamai and Rittmann (1992) to link community structure with traditional measures of process performance for full-scale activated sludge WWTPs. In this study, mixed liquor samples from activated sludge WWTPs in France and the Netherlands were analyzed with oligonucleotide probes targeted to the 16S rRNA of ammonia-oxidizers and all active bacteria. Slot-blot assays with oligonucleotide probes and FISH gave direct measurements of the ratio of ammonia-oxidizers to heterotrophs and were found to be consistent with the same ratio deduced from the operating data using the mathematical model.

Biesterfeld et al. (2001) examined ammonia oxidation rates in a full-scale nitrifying trickling filter and found that a reasonable correlation existed between the ammonia-oxidizing populations quantified by FISH and the observed ammonia removal. Correlation coefficients obtained from the application of a simple linear regression of the

AOB FISH signal area and ammonia removal rate ranged from 0.72 to 0.98 for the six sample dates investigated. In a similar study, Biesterfeld and Figueroa (2002) showed that the percentage of AOB in bench-scale nitrifying trickling filters tracked the nitrate plus nitrite generation rates. The researchers defined tracking as having a correlation coefficient greater than 0.500 between nitrate plus nitrite generation rates and percentages of AOB FISH signal area. The correlation coefficients calculated by simple linear regression between the two parameters ranged from 0.54 to 0.78 throughout their sampling campaign.

Chapter 3.0
Materials and Methods

3.1 Experimental Treatment System

3.1.1 Equipment Design and Configuration

The experimental treatment system, shown in Figure 3-1, consisted of four identical bench-scale treatment units operated in parallel. Each treatment unit (Figure 3-2) was composed of an aerated continuous-stirred tank reactor (CSTR) and an external secondary clarifier. The system was designed to simulate a conventional activated sludge wastewater treatment process (Hawkins, 2000).

As illustrated in Figure 3-2, each CSTR consisted of a top plate, a body section and a bottom plate. The reactor body was fabricated from a 30.48 cm (12") section of clear acrylic tubing that was 25.4 cm (10") in diameter and 0.635 cm (¼") thick. The top and bottom plates were made from 30.48 cm (12") x 30.48 cm (12") acrylic sheets, each with a 25.4 cm (10") diameter circular etching to ensure a snug fit onto the tube section. The bottom plate was bonded onto the reactor body to prevent leakage, however, the top plate was removable to facilitate easy access for reactor sampling, cleaning and maintenance. Each CSTR was placed on a large magnetic stir plate, approximately 30.48 cm (12") square, which was used to turn a 5.08 cm (2") magnetic stir bar inside the reactor. During reactor operation, the stir plates were operated at one-half their maximum turning speed to keep the activated sludge in suspension and the reactor contents completely mixed. At this speed, the stir plates were able to provide a volumetric power input of approximately 1500 kW/1000 m^3 (Parker, 2001) well above the required 14 kW/1000 m^3 to ensure complete mixing in an activated sludge CSTR using mechanical mixing devices (Grady et al., 1999). Aeration was provided to each reactor from in-house laboratory compressed air supplied through two 15.24 cm (6") long non-clogging porous aquarium aerator tubes mounted to the bottom plate of each reactor with suction cups. The oxygen delivery and control system is described in detail in Section 3.1.3.

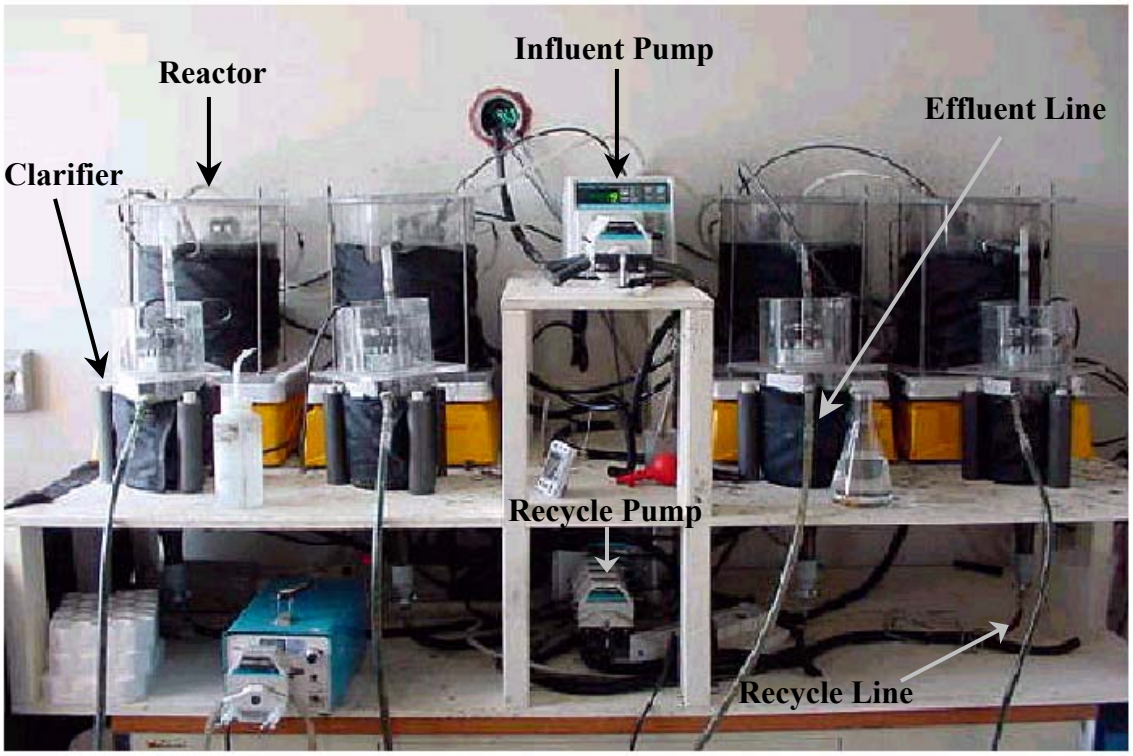

Figure 3-1. Experimental Treatment System Containing Four Parallel Treatment Units (reproduced from Parker, 2001)

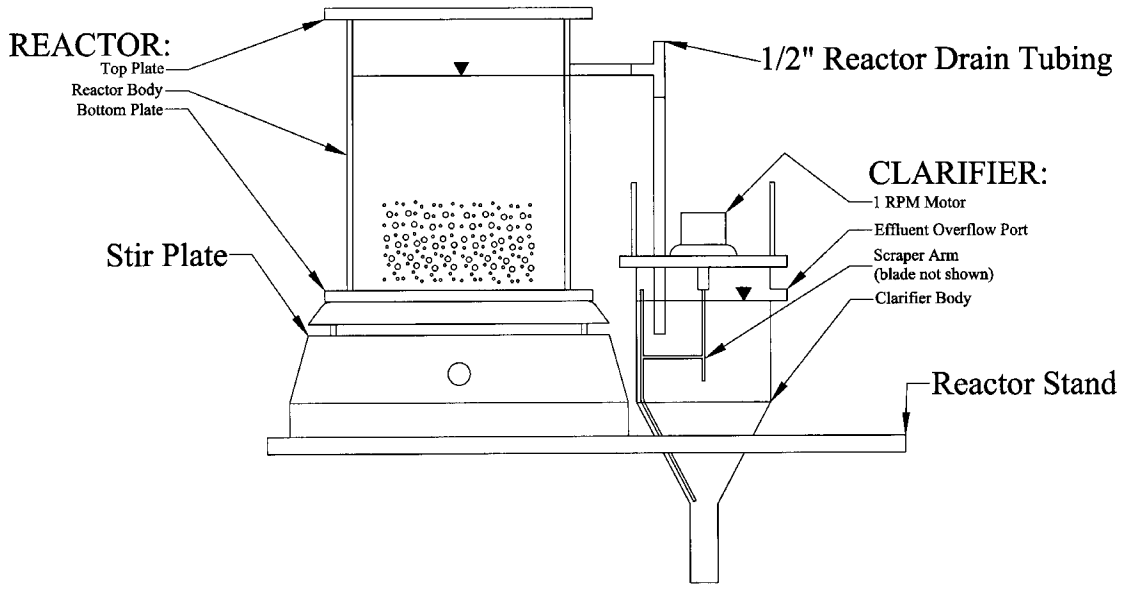

Figure 3-2. Diagram of One of the Treatment Units, which Consisted of a Continuous-Stirred Tank Reactor and an External Secondary Clarifier

The fluid volume of each CSTR was maintained at 10 L by gravity overflow through a 1.27 cm (½") diameter drainage port that was connected to the secondary clarifier with nylon tubing. Each clarifier was made up of a main body and a scraper arm assembly. The main body was constructed of blown glass and measured 15.24 cm (6") in diameter at the top. The bottom of the clarifier was drawn into a conical section sloping approximately 70º from horizontal to a diameter of 3.18 cm (1 ¼") at the bottom. A reservoir for accumulated sludge was constructed by welding a section of glass tubing 7.62 cm (3") in length and 3.18 cm (1 ¼") in diameter onto the bottom of the conical section of the clarifier. The reactor drain tubing, which served as the influent line to the clarifier, was submerged inside the clarifier to minimize mixing and disruption of settling. Treated wastewater exited the clarifier by gravity overflow through a 0.953 cm (⅜") diameter, 2.54 cm (1") long glass tube welded over a precut hole in the side of the clarifier. The effluent drain was positioned to yield a fluid volume of 2.9 L within the clarifier's main body.

A scraper arm assembly was added to each clarifier to prevent sludge from accumulating on the clarifier walls. To mount the assembly, a grooved circular trough was cut into a 17.78 cm (7") square 1.27 cm (½") thick acrylic base plate so that it would fit snuggly on to the top of the clarifier's main body. A 10.16 cm (4") long section of 15.24 cm (6") diameter acrylic tubing was bonded to the top of this base plate to form a protective housing for the scraper arm motor. The 1- rpm motor was bolted to the base plate with the motor shaft penetrating into the clarifier's main body through a hole drilled into the base plate. The sludge scraper arm was constructed from 0.318 cm (⅛") diameter stainless steel wire shaped to conform to the side of the clarifier wall. This scraper arm was mounted to the motor shaft with setscrews. Automobile wiper blades were cut to the appropriate length and attached to the scraper arms to provide a snug fit against the clarifier wall. A timer was used to engage the scraper arm motor every five minutes for the length of time required to rotate the scraper arm approximately one-half turn.

Figure 3-3 shows a schematic diagram of the experimental treatment system. Two identical Cole Parmer, Inc. continuous duty Standard Drive® peristaltic pumps conveyed the influent and sludge recycle flows to the reactors. The pump rotors were fitted with

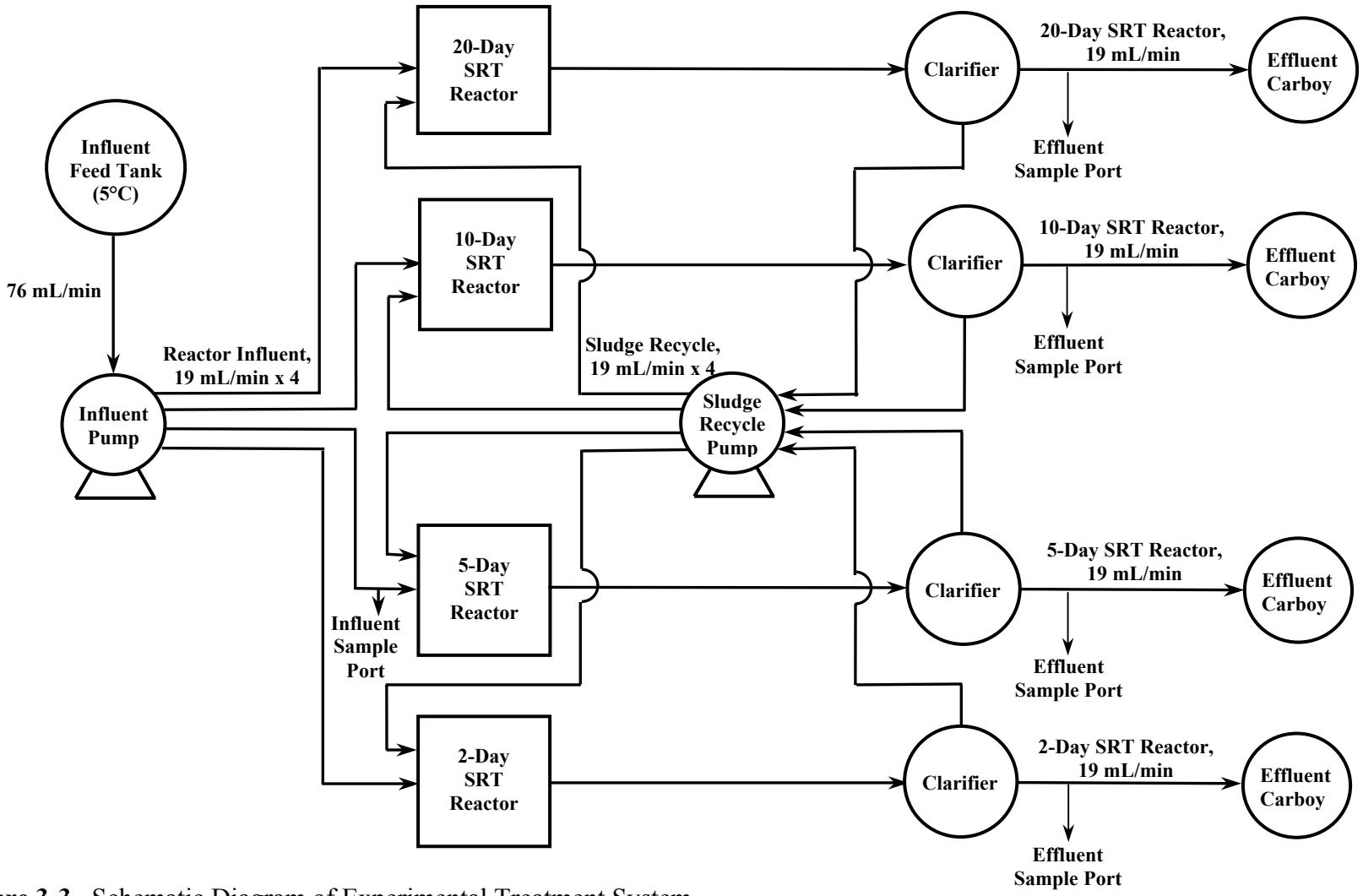

Figure 3-3. Schematic Diagram of Experimental Treatment System

four pump heads so that each reactor would receive influent and recycle flows at exactly the same rate. The influent line from the feed tank was split into four lines just before the pump head assembly while the recycle lines were plumbed from the base of each clarifier to the recycle pump. The influent and sludge recycle flows were introduced continuously into the reactors through separate 0.635 cm (¼") diameter ports that were located 5.08 cm (2") above the surface level of the reactor mixed liquor. Attached to these ports were taps that extended approximately 3.8 cm (1.5") from the sidewall of the reactor that allowed the influent and recycle sludge flows to drip into the reactor in order to avoid short-circuiting in the reactor and to prevent bacterial growth in the influent lines. The influent flow rate was set to 19 mL/min, which provided an HRT of 8.8 hours in the reactor and 2.5 hours in the clarifier. An influent sampling port was plumbed into the influent line to the 5-day SRT reactor with a tee. The placement of this sampling port effectively eliminated concerns about the degradation in the storage tank and influent lines. Effluent grab sample ports were located immediately following the clarifier overflow. This placement avoided collection of the effluent after it had passed through several feet of tubing prone to photosynthetic growth.

3.1.2 Collection and Storage of Influent Wastewater

Municipal wastewater, collected from the Knoxville Utilities Board (KUB) Kuwahee WWTP, served as the influent for this study. The wastewater was collected in batches using two steel 208.2 L (55-gallon) drums, which were filled using a sump pump submerged in the plant's primary clarifier effluent stream. The drums were subsequently transported to the laboratory and placed in a 5°C constant temperature room where the wastewater was allowed to cool overnight before transfer to the experimental treatment system feed tank. At an influent flow rate of 19 mL/min to each of the four reactors, the combined volume of the two drums was sufficient to feed the reactors for four days. Therefore, this procedure was repeated every four days throughout the treatment study. The influent line to the reactors was placed at the bottom of the feed tank, which was maintained at 5°C to minimize degradation of the wastewater during storage. The

feed tank (Figure 3-4) was a steel 208.2 L (55-gallon) drum raised 5.1 cm (2") off the floor using two 61 cm (2') sections of 2x6 lumber and fitted with a Tranter, Inc. Platecoil cooling sleeve and a plastic-coated insulation jacket. A 50/50 blend of ethylene glycol and water was cooled to -20°C using a Forma Scientific, Inc. circulating chiller unit and then pumped through the cooling sleeve in a closed loop using an external peristaltic pump and insulated tubing. The temperature of the wastewater in the feed tank was measured daily throughout the course of the study to confirm that the cooling system was working properly. A small, submersible aquarium pump was placed at the bottom of the feed tank to gently circulate the wastewater in order to minimize solids settling and maintain a homogeneous feed stream.

3.1.3 DO Delivery and Control System

As mentioned in Section 3.1.1, the air supply for the DO delivery system was derived from laboratory in-house compressed air. Before entering the reactors, the compressed air passed through a pressure regulator, a filter assembly, and a humidifier. The humidifier was fabricated using a 20-L carboy with an airtight cap that was partially filled with water. The air entered the humidifier through a submerged tube and bubbled through the water column before exiting the humidifier at the top. This process was used to humidify the air and equalize the air temperature in order to prevent excessive evaporation of the mixed liquor in the reactors during aeration. After exiting the humidifier, the air flowed through a condensate trap to a constant pressure valve where it was regulated to approximately 104.4 kPa (15 psi) and finally through a four-way airflow control and metering manifold before flowing to the aerator tubes. This system allowed the airflow rate in each reactor to be controlled independently, which was necessary as the oxygen requirement for each reactor differed.

In order to monitor and regulate the DO concentration in each reactor, a control system (Great Lakes Instruments) was purchased and installed. Included in the system were four Model 5500-Series DO probes, two Model D53 DO analyzers, four solenoid valves and four air-blast units. The analyzers, air-blast units, and solenoid valves were

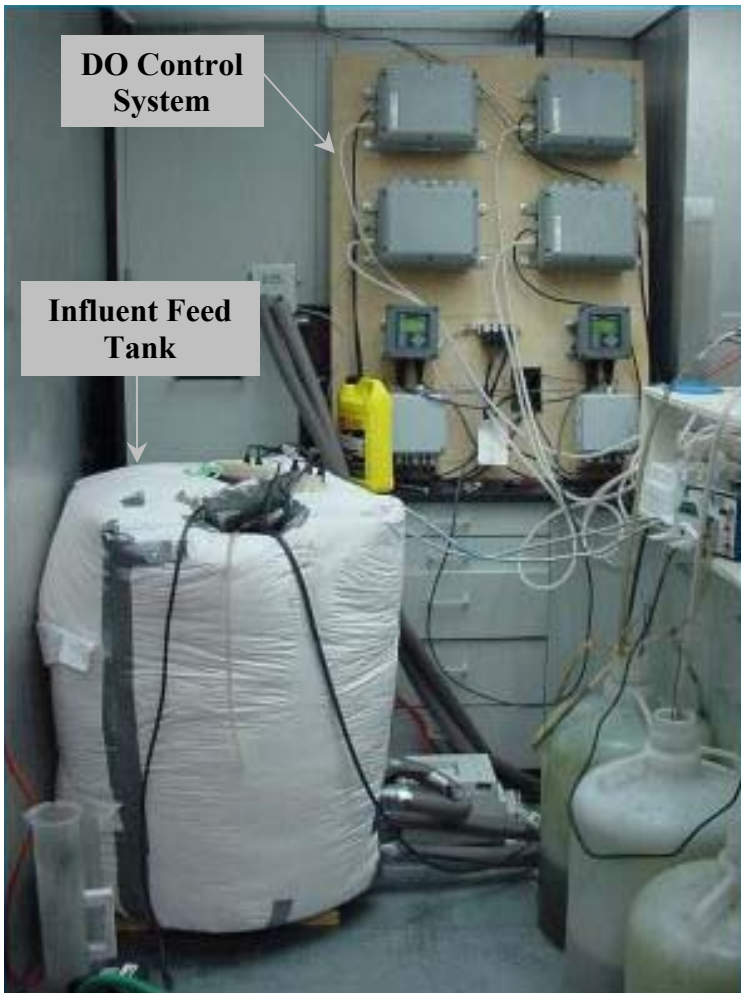

Figure 3-4. Influent Feed Tank and DO Control System (reproduced from Wood, in preparation)

mounted on a 1.52 m (5') x 0.91 m (3'), 0.15 cm (⅜") thick birch plywood base, which is shown in Figure 3-4.

The DO probes contained a hydrophobic membrane, an electrolyte solution, a gold anode, a silver cathode, and a silver reference electrode. The DO in a reactor passed through the hydrophobic membrane and into the electrolyte solution, where a constant voltage was applied to reduce the DO at the cathode. This produced a current between the cathode and anode that was directly proportional to the DO concentration in solution. The probes were calibrated periodically throughout the course of the study to ensure accuracy of measurements. Prior to calibration, the probes were removed from the reactor and rinsed with deionized water and gently wiped with a damp cloth to remove any attached bacterial growth on the membrane. Each probe was then placed in a sealed plastic calibration bag and allowed to equilibrate to the conditions inside the bag. The analyzer computed the DO concentration based on the atmospheric pressure and temperature of the air surrounding the probe and made the necessary adjustments to the probe's internal calibration curve.

Each DO probe was equipped with an air-blast apparatus to minimize attached growth by periodically blowing air across the membrane. However, it was discovered that this procedure resulted in a large increase in the DO measurements for several minutes following the blast. This was undesirable especially for the low DO portions of the study; therefore, the air-blast-units were removed from the probes to avoid affecting treatment performance. As an alternative, the probes were cleaned by hand on a daily basis (during solids analysis) to minimize bacterial growth on the membrane.

The control system's two DO analyzers accepted input from two probes and converted the magnitude of the current produced by a probe into DO concentration in mg/L. The analyzer compared the reading with a previously specified set point concentration. If the DO reading exceeded the set point, the analyzer switched a relay closing a solenoid valve, which stopped the airflow to the reactor until the analyzer read a value below the set point. Once the DO concentration fell below the set point, the analyzer opened the solenoid valve, allowing airflow to enter the reactor. In this manner, tight control of the DO concentration in the reactors was maintained.

A computer logging system was developed to monitor the DO concentration in each reactor over time. The system used a Highway Addressable Remote Transducer (HART) protocol to transmit output signals from the DO analyzers to a personal computer (PC) via a Bell 202 loop. The Bell 202 loop consisted of the two analyzers, a current sensing resistor connected in series to a power supply, and an RS232-Bell 202 mini-modem converter connected across the resistor to the PC. The analyzers were connected in series to complete the loop.

The software package H-View, manufactured by Arcom Control Systems, was installed on the PC to read the HART data as it was transmitted. A Dynamic Data Exchange (DDE) interface was installed to store the data collected during the course of the study. The DDE interface allowed the data to be viewed in a Microsoft Excel spreadsheet, from which the DO reading for each reactor was copied every 30 seconds and stored in a database using a Visual Basic macro program.

3.2 Operating Procedures

3.2.1 Selection of Reactor SRTs

As discussed in Section 2.3, the choice of the operating SRT plays a crucial role in determining the efficiency of wastewater treatment, as well as the physical and biological characteristics of the system. SRTs of 20-, 10-, 5-, and 2-days were chosen for this study to bracket the range of SRTs typically observed in full-scale WWTPs. The 20- and 10-day SRTs were representative of full-scale single-stage nitrifying systems, while the 2-day SRT placed one reactor near the maximum specific growth rate for nitrifiers. An SRT of 5 days was selected to fall between these two extremes.

3.2.2 Sampling and Reactor Maintenance Procedures

The selected SRTs were maintained in each reactor using a controlled solids wasting policy. The amount of solids removed each day to maintain a constant SRT was determined using the following equation for each reactor.

$$\text{WastageVolume} = \left(\frac{\text{MLSS} * \text{Volume}}{\text{SRT}} - \text{Q} * \text{ESS} \right) * \text{MLSS} \qquad (3\text{-}1)$$

where: Wastage Volume = mixed liquor volume to be wasted (L)
MLSS = mixed liquor suspended solids (mg/L)
Volume = reactor volume (L) = 10 L
SRT = solids retention time of individual reactor (days)
ESS = effluent suspended solids (mg/L)
Q = influent flow rate (L/day) = 27.36 L/day

This calculation required that solids analysis be performed daily to determine the MLSS, and ESS values. In addition to MLSS and ESS analyses, a number of other physical and chemical analyses were performed daily to monitor the treatment performance in each reactor and provide data necessary for comparison with the genomic information obtained in this study. MLVSS values were measured to obtain a closer approximation of the biological component in each reactor and were expected to correlate better with molecular measures of total bacteria than the MLSS values. The chemical oxygen demand (COD) of the influent and effluent of each treatment unit were measured to document carbon treatment performance in each reactor. In order to assess nitrification performance, analyses were performed on influent and effluent samples to determine the ammonia-N, nitrite-N, and nitrate-N concentrations. Also, since nitrification consumes alkalinity at a high rate, the pH and alkalinity content of the influent and reactor effluent samples were recorded to verify that the wastewater was sufficiently buffered to prevent depression of pH.

The daily sampling and reactor maintenance routine is described below. The sample analysis procedures are described in the following section. Effluent grab samples (except ESS) were collected by removing the tubing that ran from the clarifier effluent ports to the effluent carboy. The effluent wastewater was then allowed to overflow into a sample container placed directly beneath the ports until a volume of 250 mL had been collected. Once the effluent samples were taken, an influent grab sample was obtained by unclamping the tube plumbed into the 5-day SRT reactor feed line and placing it in a sample container until 250 mL had been collected. The influent and effluent samples

were then transported from the constant temperature room that housed the treatment system to the laboratory and allowed to come to room temperature before analysis.

Sample collection for solids analysis occurred after all treatment performance samples had been obtained in order to minimize disruptions in system operation caused by the procedure. By sampling in this manner, treatment performance samples could be collected after nearly 24 hours of undisturbed operation. To ensure that all of the biomass in each treatment unit was retained in the reactor at the time of solids sampling, the influent and recycle pumps, stir plates, and air supply lines were turned off. The effluent port of each reactor was then plugged with a thick wire brush and the recycle pump was turned on at full capacity for approximately 30 seconds, or until all of the sludge from the clarifier and recycle lines was returned to the reactor. At this time, 24- hour composite ESS samples were taken from the 40-L carboys after gently stirring the effluent wastewater to obtain a representative sample. The 400 mL ESS samples were withdrawn with a pump and nylon tubing into 500 mL Erlenmeyer flasks. After all ESS samples had been collected, the air supply lines and stir plates were turned back on to ensure that the solids in the reactors were completely mixed then the wire brushes plugging the effluent lines from the CSTRs were removed. After several minutes of mixing, 10 mL of mixed liquor from the 20-, 10-, and 5-day SRT reactors and 20 mL of mixed liquor from the 2-day SRT reactor were removed using graduated, wide-mouthed serological pipettes. During sampling, the mouth of the pipette was placed near the center of the reactor. Once the grab samples were collected for MLSS/MLVSS analysis, 10 to 50 mL samples of mixed liquor were collected from each reactor and stored in a -80°C freezer for subsequent molecular analysis. This concluded the daily sampling process, after which the reactors were cleaned to remove any attached growth. Cleaning involved removing the top plate from each reactor and scraping the sidewalls with a wire-bristle brush and gently wiping the DO probe with a damp cloth. The DO probe and reactor sidewalls above the fluid level were then rinsed with deionized water. The effluent ports lines from each CSTR were also cleaned daily by passing a small wire-bristle brush through them and flushing with deionized water. Once this was completed, the influent and recycle pumps were restarted.

Upon completion of MLSS/MLVSS and ESS sample analysis, the wastage volume for each reactor was determined using Equation 3-1 as previously described. After accounting for the volume of mixed liquor removed during sampling, waste activated sludge was removed directly from the reactors using a portable peristaltic pump and measured using a 2000-mL graduated cylinder. Wastage volumes were immediately replaced with equivalent volumes of effluent wastewater from each treatment unit. Effluent wastewater was used, rather than tap or deionized water, to maintain homogeneity in the reactors. Except for the 2-day SRT reactor, the total volume of waste activated sludge was removed in a single wasting event. Due to the relatively low MLSS concentration and high wastage volume in the 2-day SRT reactor, a single event was not conducive to proper steady-state operation of the reactor. Therefore, the wastage volume was split into two equal parts that were removed approximately 8-12 hours apart. After the morning wastage procedures were concluded, the effluent wastewater in the carboys was emptied.

3.2.3 Sample Analysis Procedures

MLSS and ESS Sample Analysis

Analyses of reactor MLSS and ESS samples were performed in accordance with Standard Method 2450 D, Total Suspended Solids dried at 103-105°C (APHA, 1998) using 47 mm diameter 1.5 μm glass fiber filters (Proweigh® by Environmental Express). All filters were pre-dried and weighed the day before usage, and pre-wetted with DI water just prior to being used. The samples were gently poured through the filters and washed down with DI water. The filters were then placed in aluminum dishes and dried in a 105°C oven for one hour. At the end of the hour, the filters were removed from the oven and weighed. The values were recorded and used in the following equation to determine the MLSS and ESS in mg/L:

$$SS = \frac{(W_F - W_I)}{V} \times 1000 \qquad (3\text{-}2)$$

where: SS = suspended solids concentration (mg/L)
W_F = final filter weight (mg)
W_I = initial filter weight (mg)
V = sample volume (mL)

MLVSS Sample Analysis

MLVSS analysis was conducted daily in accordance with Standard Method 2540 E, Fixed and Volatile Solids Ignited at 550°C (APHA, 1998). The filters containing dried solids from the MLSS analysis were placed in aluminum dishes and combusted in a 550°C muffle furnace for no less than 15 minutes. The filters were then removed from the oven and reweighed and the MLVSS values were calculated using the following equation:

$$\text{MLVSS} = \frac{\left(W_F - W_{FV}\right)}{V} \times 1000 \qquad (3\text{-}3)$$

where: MLVSS = mixed liquor volatile suspended solids (mg/L)
W_{FV} = final filter weight after MLVSS analysis (mg)

COD Sample Analysis

Analysis of influent and effluent samples for total COD (COD_t) and soluble COD (COD_s) respectively were performed in accordance with Standard Method 5220 D, Closed Reflux Colorimetric Method using high- and low-range micro-COD test vials obtained from Hach, Inc. (APHA, 1998). Effluent samples were analyzed for COD_s to eliminate the variability caused by daily fluctuations in the ESS. Approximately 10 mL of the remaining influent and effluent samples were placed in 15-mL Falcon centrifuge tubes using syringes with the 0.45 μL filters. All samples were then preserved with concentrated H_2SO_4 at the recommended 2 mL per liter of sample and placed into the laboratory's refrigerator at 4°C. COD analyses were performed every two weeks, well under the recommended 28-day maximum storage time.

The influent and effluent COD tests were performed separately because the influent test required the use of Hach's high-range vials (0-1500 mg/L) and the effluent test required the low-range vials (0-150 mg/L). Five standards were prepared for each

test using dried potassium hydrogen phthalate (KHP) to create a standard adsorption curve. For each test, 2 mL of sample were placed into a Hach vial, shaken, and digested on a heating block for 2 hours. After cooling, the digested sample was transferred to a clear spectrophotometer cuvette and analyzed using a spectrophotometer at 600nm. A standard curve was then plotted and values of COD (in mg/L) were recorded.

Ammonia Sample Analysis

Ammonia concentrations in the influent and clarifier effluent grab samples were measured daily using Standard Method 4500 D, Ammonium-Selective Electrode Method (APHA, 1998), with an Orion model 95-12 ammonium-selective probe. Immediately following sample collection, a volumetric pipette was used to transfer 100 mL of to a clean 150-mL Erlenmeyer flask. The sample was allowed to equilibrate to room temperature before analysis. Sample quantities and temperatures were consistent with the ammonium standards used to calibrate the ammonia-selective probe. On rare occasions when ammonia analysis could not be performed immediately following sample collection, the samples were preserved by adding 200 μL of concentrated H_2SO_4, then stoppered and stored at 5°C. The samples were stored in this manner for no longer than 48 hours before analysis. Standard solutions of 0.1, 0.5, 5.0, and 50 mg/L ammonia-N were prepared daily and used to construct the standard curve, which was used to determine ammonia-N concentrations in the grab samples, as well as a quality control sample.

Nitrite-N and Nitrate-N Sample Analysis

The concentration of nitrite-N and nitrate-N in the effluent of each treatment unit was determined using Standard Method 4110 B, Ion Chromatography with Chemical Suppression of Eluent Conductivity (APHA, 1998). A small aliquot was taken with a syringe from the sample collection container and filtered (0.45 μm Gelman glass fiber filters) into Dionex 0.5 mL auto-sample vials . The samples were stored for no longer than 48 hours at 4°C before analysis with a Dionex DX 500 Ion Chromatograph (IC) fitted with an Ionpac® AS9HC 4 mm anion exchange column. For each batch of samples,

calibration of the IC was performed with four standards containing varying concentrations of both nitrite-N and nitrate-N. Additionally, a quality control sample was analyzed during each IC run. After placing the standards and sample vials into the IC's auto sampler, the analysis sequence was initiated. A software program was set up that enabled the IC to automatically plot a calibration curve based on the standards and convert sample measurements into anion concentrations (in mg/L).

Alkalinity and pH Sample Analysis

The daily measurements for alkalinity were determined in accordance with Standard Method 2320 B, Titration Method using an Orion model 91-57 pH probe (APHA, 1998). Volumetric pipettes were used to transfer 50 mL of influent and effluent grab samples from the sample collection containers into clean 150 mL Erlenmeyer flasks. After acclimating to room temperature, initial pH measurements were made with the pH probe and recorded. Each sample was then titrated with 0.02 N HCl to the total alkalinity endpoint (pH=4.5). The volume of acid required to reach this endpoint was recorded and converted to the standard units of $CaCO_3$.

3.3 Real-time PCR

3.3.1 DNA Extraction

In order to obtain sequence information and perform PCR analysis, genomic DNA was extracted from mixed liquor samples ranging in volume from 1 to 25 mL, depending on the MLVSS values, using a FastDNA kit (BIO 101, Vista CA) with minor modifications. These modifications included washing the binding matrix-DNA complex twice with 80% (vol/vol) ethanol after the recommended salt-ethanol wash step and eluting the DNA in 100 μL of 10 mM Tris-HCl buffer (pH 8.0) (Dionisi et al., 2002a). The integrity of the DNA samples was assessed by electrophoresis in 0.8% (wt/vol) agarose (Fisher Scientific, Pittsburgh, PA), 1X TBE and 1X Gelstar® nucleic acid gel stain (FMC Corporation, Rockland, ME) and the DNA was quantified by using a DyNA Quant200 fluorometer (Hoefer Pharmacia Biotech, San Francisco, CA).

3.3.2 Real-Time PCR Assays

Real-time PCR assays were used for the quantification of eubacterial 16S rDNA, *N. oligotropha*-type *amo*A , and *Nitrospira* spp. 16S rDNA in mixed liquor samples.

Real-time PCR for Quantification of Total Eubacteria

Amplification of total eubacterial 16S rDNA was performed using primers 1055f (Ferris et al., 1996) and 1392r (Lane et al., 1991) and the TaqMan probe 16STaq1115f (Table 3-1) as described by Harms et al. (2003). The composition of the PCR mix with a total volume of 25 μL is shown in Table 3-2. Dilutions of plasmid pCR®2.1 vector (Invitrogen, Carlsbad, CA) carrying an uncultured bacterium 16S rRNA gene for *Nitrospira* (GenBank accession number AF420301) (Dionisi et al., 2002a) ranging from 4.5×10^3 to 4.5×10^8 copies of the 16S rDNA gene were used as standards in this assay. The PCR program consisted of 3 min at 50°C, an initial denaturation at 95 ºC for 10 min, followed by 45 cycles of denaturation at 95 ºC for 30s, annealing at 50 ºC for 60s and extension at 72 ºC (Harms et al., 2003). Fluorescence was detected during the annealing step of each cycle of the PCR run.

Real time PCR for Quantification of *N. oligotropha*-type AOB

The *amoA* gene was selected for analyzing ammonia-oxidizing communities in this study due to (i) its specificity, (ii) its fine-scale resolution of closely related populations, and (iii) the fact that it is a functional trait rather than a phylogenetic trait (Rotthauwe *et al.,* 1997). The primers *amo*No550D2f and *amo*No754r were designed to target the *amoA* gene of ammonia-oxidizing bacteria found in the full-scale municipal WWTP used to seed the reactors (Dionisi et al., 2002a) based on alignment of *amoA* gene sequences using the CLUSTAL W program (Purkhold et al., 2000). Alignments consisted of *amoA* sequences from clonal libraries obtained from the municipal WWTP, an industrial WWTP (Dionisi et al., 2002a), the four bench-scale reactors used in the current study (Dionisi et al., 2002b) and *amoA* sequences available in GenBank (Purkhold et al., 2000). The forward primer *amo*No550D2f contained two degenerate bases in order to amplify

Table 3-1. Primers and Probes Used in This Study

Assay	Target	Primer/Probe[a]	Sequence (5'-3')[b]	Reference
Eubacterial 16S rDNA	Eubacteria 16S rDNA	1055f	4 5'-ATGGCTGTCGTCAGCT-3'	Ferris et al., 1996
		1392r	5'-ACGGGCGGTGTGTAC-3'	Lane, 1991
		16STaq1115f	5'-(6-FAM)-CAACGAGCGCAACCC-(TAMRA)-3'	Harms et al., 2003
N. oligotropha -type *amo*A	*N. oligotropha amoA* gene	*amo*No550D2f	5'-TCAGTAGCYGACTACACMGG-3'	Harms et al., 2003
		*amo*No754r	5'-CTTTAACATAGTAGAAAGCGG-3'	Harms et al., 2003
		*amo*NoTaq729r	5'-(6-FAM)-CCAAAGTACCACCATACGCAG-(TAMRA)-3'	Harms et al., 2003
Nitrospira 16S rDNA	*Nitrospira* spp. 16S rDNA	NSR1113f	5'-CCTGCTTTCAGTTGCTACCG-3'	Dionisi et al., 2002a
		NSR1264r	5'-GTTTGCAGCGCTTTGTACCG-3'	Dionisi et al., 2002a
		NSR1143fTaq	5'-(6-FAM)-AGCACTCTGAAAGGACTGCCCAGG-(TAMRA)-3'	Harms et al., 2003

[a] Primer/Probe abbreviations: f= forward primer, r= reverse primer, Taq= TaqMan probe.
[b]5'-fluorophore-probe-quencher-3' in case of TaqMan probe. 6-FAM = 6-carboxyfluorescein; TAMRA = carboxytetramethylrhodamine.

Table 3-2. PCR Mix for the Quantification of Total Eubacteria

Ingredient	Volume in one 25 μL reaction (in μL)
Platinum® Quantitative PCR SuperMix-UDG (Life Technologies, Inc., Gaithersburg, MD)	12.5
Primer 1055f (20 μM stock)	0.75
Primer 1392r (20 μM stock)	0.75
$MgCl_2$ (50 mM stock)	1.0
16STaq1115f TaqMan probe (10 μM stock)	0.625
sterile HPLC water	4.375
Sample DNA or dilutions of standard	5.0

all *amoA* clones from the libraries, as well as *N. urea* (AJ388585) and *N. oligotropha* (AF272406) *amoA* genes. The TaqMan probe *amo*NoTaq729r was derived from a conserved sequence region within the primer pair *amo*No550D2f and *amo*No754r (Harms et al., 2003). The composition of the PCR mix with a total volume of 25 μl is shown in Table 3-3. Standards consisted of the plasmid pCR®2.1 carrying the M-20 *amoA* gene (GenBank accession number AF420299) (Dionisi et al., 2002a) adjusted to 10 to 1.0×10^7 copies per PCR reaction. The PCR amplification program consisted of 2 min at 50°C, 10 min at 95°C, 55 cycles at 95°C for 30 s, 56°C for 60 s.

Real-time PCR for Quantification of *Nitrospira*

The target for detecting *Nitrospira* was the 16S rDNA molecule since the genes for nitrite oxidation have not been cloned and sequenced from this microorganism. In addition, the *Nitrospira* found in activated sludge appear to be monophylogenetic and

Table 3-3. PCR Mix for the Quantification of *Nitrosomonas oligotropha*-type AOB

Ingredient	Volume in one 25 μL reaction (in μL)
TaqMan® Universal PCR Master Mix (PE Applied Biosystems, Foster City, Calif.)	12.5
Primer amoNo550D2f (20 μM stock)	0.375
Primer amoNo754r (20 μM stock)	0.375
TaqMan probe *amo*NoTaq729r (10 μM stock)	0.625
sterile HPLC water	6.125

conserved between municipal and industrial wastewater treatment plants (Burrell et al., 1998, Dionisi et al., 2002a). The *Nitrospira* 16S rDNA primers NSR1113f and NSR1264r (Table 3-1) were designed and tested using genomic DNA extracted from municipal and industrial MLSS as templates (Dionisi et al., 2002a).

The TaqMan probe NSR1143fTaq was derived from a conserved sequence region between the primers NSR1113f and NSR1264r (Table 3-1). Real-time PCR assays using NSR1143fTaq were performed in a total volume of 25 μL with the composition of the PCR mix shown in Table 3-4. Standards consisted of 151 bp fragment of *Nitrospira* 16S rDNA from (Dionisi et al., 2002a) adjusted to 30 to 3×10^7 copies. The PCR amplification consisted of 2 min at 50°C, 10 min at 95°C, 55 cycles at 95°C for 30 s, 63°C for 60 s (Harms et al., 2003).

3.3.3 Data Acquisition and Analysis

Real-time PCR assays for bacterial 16S rDNA and *Nitrospira* 16S rDNA were run on a Bio-Rad iCycler with the iCycler iQ™ fluorescence detector and iCycler software version 2.3 (Bio-Rad, Hercules, CA). Plate well factors were determined prior to each

Table 3-4. PCR Mix for the Quantification of *Nitrospira*

Ingredient	Volume in one 25 μL reaction (in μL)
Platinum® Quantitative PCR SuperMix-UDG (Life Technologies, Inc., Gaithersburg, MD)	12.5
Primer NSR1113f (20 μM stock)	0.75
Primer NSR1264r (20 μM stock)	0.75
$MgCl_2$ (50 mM stock)	1.0
NSR1143fTaq (10 μM stock)	0.625
sterile HPLC water	4.375

PCR run to normalize background fluorescence intensities from each single well. *AmoA* real-time PCR assays were run using a DNA Engine Opticon™ Continuous fluorescence Detection System (MJ Research, Waltham, MA). The threshold was determined by the computer software as 10 times the standard deviation of the background fluorescence averaged over at least 5 cycles at the start of the run. The threshold cycle (C_T) of each PCR reaction was automatically determined by detecting the cycle at which the fluorescence exceeded the calculated threshold. During each PCR run, the C_T values obtained from the DNA standards were used for the construction of standard curves.

3.3.4 Application of Real-time PCR Assays to Mixed Liquor Samples

All real-time PCR assays were performed using three replicates per sample and all PCR runs included control reactions without template. The effect of sample concentration on PCR performance was determined using dilutions of sample DNA (initial concentration of 50 ng/uL) containing 5 pg to 50 ng in sterile water followed by real-time PCR analysis for 16S rDNA, *Nitrospira* 16S rDNA, and *N. oligotropha*-like *amoA* as described above.

Gene copies were initially calculated by comparison of threshold cycles obtained in each PCR run from known standard DNA concentrations. To reduce variability between PCR runs, data were recalculated using a second standard curve generated from 11 standard curves for bacterial 16S rDNA ($r^2 = 0.94$), 22 standard curves for *Nitrospira* 16S rDNA ($r^2 = 0.84$), and 5 standard curves for *N. oligotropha*-like *amoA* ($r^2 = 0.90$). In the case of the *Nitrospira* 16S rDNA and eubacterial 16S rDNA assays, one universal standard curve was applied for calculations, because both assays were shown to function alike with standard plasmid AF420301 as template.

3.4 Computation of Process Performance Parameters

3.4.1 Carbon Treatment Performance

COD removal efficiency was used as a measure of carbon treatment performance in this study and was computed according to the following equation.

$$\%\,\text{COD Removal} = \frac{\text{COD}^0 - \text{COD}^e}{\text{COD}^0} \times 100\% \qquad (3\text{-}4)$$

where: COD^0 = influent COD concentration (mg/L)
COD^e = effluent COD concentration (mg/L)

3.4.2 Nitrification Performance

Influent ammonia and reactor effluent ammonia, nitrite, and nitrate concentrations (as N) were used to calculate ammonia oxidation rates and efficiencies. Nitrite- and nitrate-N are products of the nitrifying bacteria, while ammonia-N in the effluent represents nitrogen not biologically utilized. Thus, the ammonia oxidation rate for the AOB can be calculated using these effluent inorganic nitrogen concentrations as shown in Equation 3-5.

$$NH_4^+ \text{ Oxidation Rate} = \frac{Q\left(\text{Eff. } NO_2^- + \text{Eff. } NO_3^-\right)}{V} \quad (3\text{-}5)$$

where: NH_4^+ Oxidation Rate = rate of ammonia oxidation (mg N/L/day)
Q = volumetric flow rate (L/day) = 27.4 L/day
Eff. NO_2^- = effluent nitrite (mg/L as N)
Eff. NO_3^- = effluent nitrate (mg/L as N)
V = reactor volume = 10 L

The conversion efficiency for the AOB can be calculated using these effluent inorganic nitrogen concentrations as shown in Equation 3-6.

$$NH_4^+ \text{ Oxidation Eff.}(\%) = \frac{\left(\text{Eff. } NO_2^- + \text{Eff. } NO_3^-\right)}{\left(\text{Eff. } NH_4^+ + \text{Eff. } NO_2^- + \text{Eff. } NO_3^-\right)} \times 100\% \quad (3\text{-}6)$$

where: Eff. NO_2^- = effluent nitrite (mg/L as N)
Eff. NO_3^- = effluent nitrate (mg/L as N)
Eff. NH_4^+ = effluent ammonia (mg/L as N)

Similarly, nitrite oxidation rates were computed using Equation 3-7 and nitrite oxidation efficiencies were calculated using Equation 3-8.

$$NO_2^- \text{ Oxidation Rate} = \frac{Q\left(\text{Eff. } NO_3^-\right)}{V} \quad (3\text{-}7)$$

where: NO_2^- Oxidation Rate = rate of nitrite oxidation (mg N/ L•day)
Q = volumetric flow rate (L/day) = 27.4 L/day
Eff. NO_3^- = effluent nitrate (mg/L as N)
V = reactor volume = 10 L

$$NO_2^- \text{ Oxidation Eff.}(\%) = \frac{\left(\text{Eff. } NO_3^-\right)}{\left(\text{Eff. } NO_2^- + \text{Eff. } NO_3^-\right)} \times 100\% \quad (3\text{-}8)$$

where: Eff. NO_2^- = effluent nitrite (mg/L as N)
Eff. NO_3^- = effluent nitrate (mg/L as N)
Eff. NH_4^+ = effluent ammonia (mg/L as N)

3.5 Statistical Analysis

Multiple linear regression analyses were performed on the physical/chemical and molecular data generated in this study using the SPSS 11.0 (SPSS, Inc., Chicago, IL) statistical analysis software package. This type of analysis was used to estimate models to describe the distribution of a response (or independent) variable with a number of predictors (or dependent variables). A function of the analysis was to search for predictor variables that explain significant variation in the response variable. If a number of significant predictors could be identified, the model provided information as to the relative influence each parameter had on the response variable.

In this study, the predictor variables were the controlled parameters, SRT, temperature and DO concentration, while the response variables were the measured parameters MLVSS, total eubacteria concentration, ammonia and nitrite oxidation rates, and the *N. oligotropha*-type AOB and *Nitrospira* NOB concentrations. In addition to these main effect predictor variables, interaction terms were included in the models to incorporate the joint effect of two variables (e.g. temperature and DO) on a dependent variable (e.g. ammonia oxidation rate) over and above their separate effects. The two-way interactions of SRT and temperature, SRT and DO, and temperature and DO, as well as the three-way interaction of SRT, temperature, and DO were included in the multiple linear regression analyses performed in this study. The interaction terms were added to the models as cross products of the individual independent variables. When studying the measures of biomass (MLVSS and total eubacteria concentration) the influent COD level was also considered in the linear regression models since this parameter did vary with each batch of influent wastewater. When studying nitrification, the influent ammonia level was incorporated into the analysis.

In order to perform multiple linear regression analyses, it was necessary to assume that the relationship between the dependent and the independent variables were linear and that for each combination of independent variable values the distribution of the dependent variable was normal with a constant variance (Norušis, 2000). To meet these requirements it was necessary to first transform some of the data. The logarithm of the

molecular data (total eubacteria, *N. oligotropha*-type AOB, and *Nitrospira* concentrations) had to be computed before inputting this data into the analyses.

Multiple linear regression fits a response variable as a linear combination of multiple X variables by the method of least squares analysis. This hypothetical relationship is described in the following equation.

$$Y = C + B_1X_1 + B_2X_2 + \ldots B_kX_k \qquad (3\text{-}9)$$

where: Y = independent (response) variable
C = constant
B_1, B_2, B_k = partial regression coefficients of predictors
X_1, X_2, X_k = dependent (predictor) variables

In the multiple linear regression model, the constant (C) is determined by the intercept of the regression line with the y-axis. This number represents the value of Y when all independent variables are zero. The partial regression coefficient (B) of a predictor quantifies the amount of linear trend in Y. It is the average amount the dependent variable increases when the independent parameter increases one unit and other independents are held constant (Norušis, 2000). In other words, the B coefficient is the slope of the regression line. The larger the value of B, the steeper the slope, and the more the dependent variable changes for each unit change in the independent variable. A positive coefficient means that the predicted value of the dependent variable increases when the value of the dependent variable increases. Conversely, a negative coefficient means that the predicted value of the dependent variable decreases when the value of the independent parameter increases.

The null hypothesis that the partial regression coefficient for a variable is zero is tested using the t-statistic and its observed significance level (Norušis, 2000). If the confidence interval for the partial regression coefficient includes 0, then there is no significant linear relationship between X and Y, and the null hypothesis cannot be rejected. A partial regression coefficient of zero would indicate that the predictor had no effect on the response variable.

Standardized partial regression coefficients, called beta coefficients, can be compared to judge the relative importance of each independent variable in the model. These coefficients enable the comparison of variables of differing magnitudes and measurement units and are equal to the average amount the dependent variable increases when the independent variable increases one standard deviation and the other independent variables are held constant (Norušis, 2000).

Before generalizations can be made about the experimental data based on the results of the multiple linear regression analysis, it is necessary to confirm how well the model fits the data. One measure of goodness of fit is the coefficient of multiple determination, R^2. This parameter indicates how much of the observed variability in the dependent variable can be explained collectively by all of the independent variables (Norušis, 2000). An R^2 value close to 1.0 indicates that almost all of the variability has been accounted for with the variables specified in the model. The degree to which two or more predictors are related to the dependent variable is expressed in the correlation coefficient R, which is the square root of R^2. R is the correlation coefficient between the observed value and the predicted value based on the regression model. A value of one indicates the dependent variable can be perfectly predicted from the independent variables. A value close to zero tells you that the independent variables are not linearly related to the depended variable.

Analysis of variance is used to test several equivalent null hypotheses. The first is that there is no linear relationship to the population between the dependent and independent variables. The second is that all of the partial regression coefficients are zero. The last is that the population value for multiple R^2 is zero. The test of the null hypotheses is based on the ratio of the regression mean square to the residual mean square and is called the overall regression F test (Norušis, 2000). The F test is used to test the significance of R, which is the same as testing the significance of the model as a whole. If the observed significance level of F is less than 0.05, then the model is considered significantly better than would be expected by chance and the null hypothesis that no linear relationship exists between the dependent and independent variables can be rejected.

Chapter 4.0
Results and Discussion

Four activated sludge reactors with different SRTs, were operated at three constant temperature levels (20°C, 15°C, and 10°C) and varying DO levels to assess the impact of these parameters on the effectiveness of activated sludge performance and microbial dynamics. The study of DO effects on treatment performance at 20°C was conducted between June 2000 and January 2001. The DO was initially set at 4.0 mg/L to minimize the impact of DO on nitrification and lowered in discrete increments to a final value of 0.5mg/L for the 2-day SRT reactor and 0.2 mg/L for the 5-, 10-, and 20-day SRT reactors (Parker, 2001). The study at 15°C took place between March and September of 2001. The DO concentration was set at 3.0 mg/L to begin the experiment and was then lowered in discrete increments to a final DO level of 0.2 mg/L. The 10°C study occurred between October 2001 and January 2002 and included DO concentrations of 2.0, 1.0, and 0.5 mg/L. For analysis purposes, the DO levels were collapsed into 3 groups: high (DO = 2.0 and 3.0 mg/L), intermediate (DO = 1.0 and 1.5 mg/L) and low (DO = 0.2 and 0.5 mg/L). The time frames for operation of each reactor at various DO levels are reported in Tables 4-1, 4-2, and 4-3 for 20°C, 15°C, and 10°C temperatures, respectively.

4.1 Selection of Samples for Real-time PCR Analysis

Because it was not feasible to perform real-time PCR analysis on all reactor samples (collected daily throughout the course of the study), it was necessary to select subsets of samples representative of each experimental phase. Listings of the selected sample dates for each SRT and DO level are shown in Tables 4-4, 4-5 and 4-6 for the 20°C, 15°C and 10°C systems, respectively. Sample dates denoted in bold indicate apparent steady-state samples. Steady-state periods were defined as time intervals in which stable nitrification occurred after the reactors were operated for a minimum of twice the SRT following a change in environmental or operational conditions.

Table 4-1. DO Levels and Operational Dates for 20°C Study

DO Level	High	Intermediate	Low
20-day SRT	6/6/00-9/6/00	9/7/00-11/2/00	11/3/00-1/10/01
10-day SRT	6/6/00-9/6/00	9/7/00-11/2/00	11/3/00-1/10/01
5-day SRT	6/6/00-9/6/00	9/7/00-11/2/00	11/3/00-1/10/01
2-day SRT	6/6/00-10/27/00	10/28/00-12/27/00	12/28/00-1/10/01

Table 4-2. DO Levels And Operational Dates for 15°C Study

DO Level	High	Intermediate	Low
20-day SRT	3/1/01-4/25/01	4/26/01-8/1/01	8/2/01-9/29/01
10-day SRT	3/1/01-4/25/01	4/26/01-8/1/01	8/2/01-9/29/01
5-day SRT	3/1/01-4/25/01	4/26/01-8/1/01	8/2/01-9/29/01
2-day SRT	3/1/01-4/25/01	4/26/01-8/1/01	8/2/01-9/29/01

Table 4-3. DO Levels and Operational Dates for 10°C Study

DO Level	High	Intermediate	Low
20-day SRT	10/23/01-11/29/01	11/30/01-12/12/01	12/13/01-1/6/02
10-day SRT	10/23/01-11/29/01	11/30/01-12/12/01	12/13/01-1/6/02
5-day SRT	10/23/01-11/29/01	11/30/01-12/12/01	12/13/01-1/6/02
2-day SRT	10/23/01-11/29/01	11/30/01-12/12/01	12/13/01-1/6/02

Table 4-4. Real-time PCR Sampling Dates for the 20°C Study

	SRT			
D.O. (mg/L)	2 day	5 day	10 day	20 day
High	**07/28/00** 08/03/00 **08/20/00** **09/01/00** **09/04/00** **10/05/00** **10/19/00**	**07/28/00** 08/03/00 08/04/00 **08/16/00** **08/21/00**	08/04/00 **08/13/00** **08/20/00** **08/21/00** **09/01/00** **09/04/00**	**08/04/00** **08/13/00** **08/20/00** **08/21/00** 09/01/00 **09/04/00**
Intermediate	**12/05/00** **12/06/00** **12/07/00** **12/11/00**	10/05/00 **10/19/00** **10/22/00** **10/24/00** **10/26/00**	10/05/00 **10/19/00** **10/22/00** **10/24/00** **10/26/00**	10/05/00 10/19/00 **10/22/00** **10/24/00** **10/26/00**
Low	**01/03/01** **01/05/01** **01/06/01** **01/07/01** **01/09/01**	11/08/00 11/16/00 11/28/00 **12/01/00** **12/05/00** **12/06/00** **12/07/00** **12/11/00**	11/08/00 11/16/00 11/28/00 12/01/00 12/05/00 12/06/00 12/07/00 12/11/00	11/08/00 11/16/00 11/28/00 12/01/00 12/05/00 12/06/00 12/07/00 12/11/00

*Dates in bold denote steady-state samples

Table 4-5. Real-time PCR Sampling Dates for the 15°C Study

	SRT			
D.O. (mg/L)	2 day	5 day	10 day	20 day
High	**03/06/01** **03/14/01** **04/03/01** **04/18/01** **04/23/01**	03/06/01 03/14/01 **04/03/01** **04/18/01** **04/23/01**	03/06/01 03/14/01 **04/03/01** **04/18/01** **04/23/01**	03/06/01 03/14/01 04/03/01 **04/18/01** **04/23/01**
Intermediate	**07/14/01** **07/16/01** **07/25/01** **07/27/01** **07/29/01**	**07/14/01** **07/16/01** **07/25/01** **07/27/01** **07/29/01**	**07/14/01** **07/16/01** **07/25/01** **07/27/01** **07/29/01**	**07/14/01** **07/16/01** **07/25/01** **07/27/01** **07/29/01**
Low	**09/11/01** **09/13/01** **09/18/01** **09/21/01** **09/24/01**	**09/11/01** **09/13/01** **09/18/01** **09/21/01** **09/24/01**	**09/11/01** **09/13/01** **09/18/01** **09/21/01** **09/24/01**	**09/11/01** **09/13/01** **09/18/01** **09/21/01** **09/24/01**

*Dates in bold denote steady-state samples

Table 4-6. Real-time PCR Sampling Dates for the 10°C Study

	SRT			
D.O. (mg/L)	2 day	5 day	10 day	20 day
High	**11/18/01** **11/20/01** **11/21/01** **11/24/01** **11/27/01**	**11/18/01** **11/20/01** **11/21/01** **11/24/01** **11/27/01**	**11/18/01** **11/20/01** **11/21/01** **11/24/01** **11/27/01**	11/18/01 11/20/01 11/21/01 11/24/01 11/27/01
Intermediate	**12/03/01** **12/05/01** **12/07/01** **12/09/01** **12/12/01**	12/03/01 12/05/01 12/07/01 **12/09/01** **12/12/01**	12/03/01 12/05/01 12/07/01 12/09/01 12/12/01	12/03/01 12/05/01 12/07/01 12/09/01 12/12/01
Low	**12/23/01** **12/26/01** **12/27/01** **01/02/02** **01/04/02**	**12/23/01** **12/26/01** **12/27/01** **01/02/02** **01/04/02**	12/23/01 12/26/01 12/27/01 01/02/02 01/04/02	12/23/01 12/26/01 12/27/01 01/02/02 01/04/02

*Dates in bold denote steady-state samples

4.2 Carbon Treatment Performance

Nitrification performance was of primary interest in this study. However, because nitrifying bacteria in single-stage nitrification systems are indirectly affected by the heterotrophic organisms present, it was desirable to monitor their activity as well. Carbon treatment performance was used to indicate heterotrophic activity in the reactors and was documented by performing COD analyses of the influent and reactor effluents. While total COD (COD_t) was used to monitor influent strength, effluent samples were filtered to minimize the influence of suspended solids on effluent COD values. The influent wastewater was originally filtered as well; however, a large fraction of the COD was removed during this process so filtration of influent wastewater was not performed during this study (Parker, 2001). Therefore, carbon treatment performance measures reported here are indicative of each treatment unit's effectiveness in removing soluble, degradable COD from the influent wastewater.

4.2.1 20°C Operation

Figure 4-1 shows influent and effluent COD levels over the time course of the 20°C study. Effective COD removal was consistently achieved at all four SRTs throughout this operational period except for the week of July 28 to August 5, 2000. The spike in effluent COD during this time is believed due to the presence of a surfactant-type material in a batch of influent wastewater collected from the municipal treatment plant. The material appeared to decrease the degradability of the waste, which resulted in a disruption in treatment performance in all four SRT reactors. COD removal efficiency rapidly recovered once the surfactant had passed through the system. A similar process upset occurred at the full-scale municipal WWTP during the week in which this material was present in the influent, causing the design maximum daily BOD discharge level to be exceeded four times during this period (Parker, 2001).

Table 4-7 summarizes carbon treatment performance for the four reactors during the high, intermediate, and low DO time periods. The 20-day SRT reactor consistently

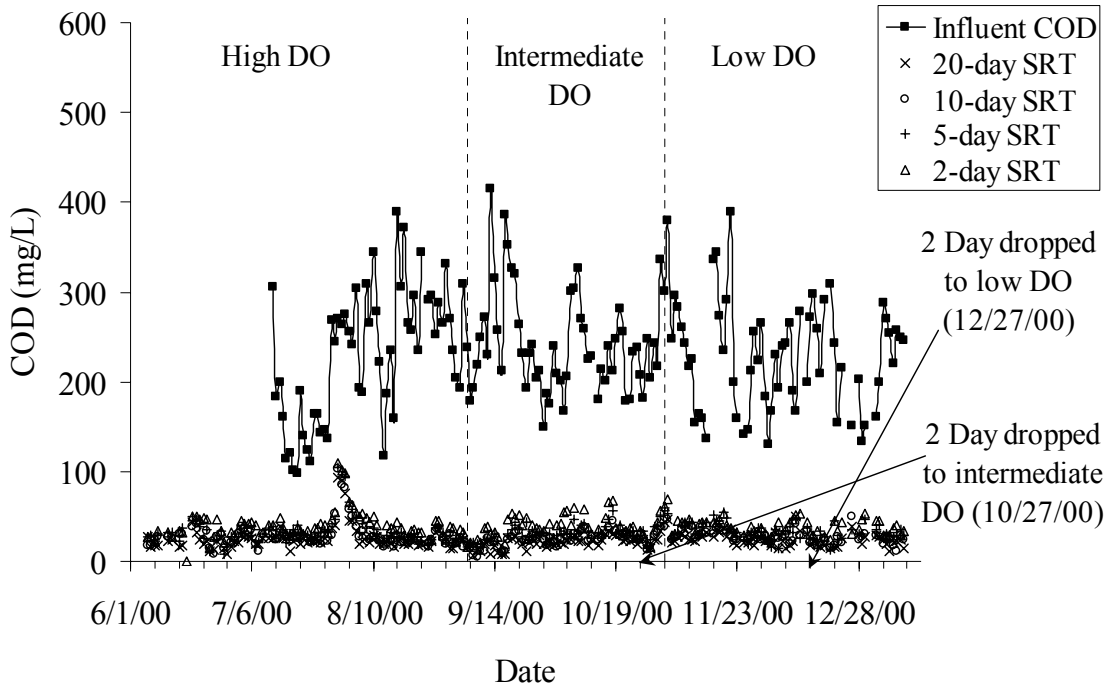

Figure 4-1. Effect of DO Concentration on COD Treatment Performance During 20°C Operation

Table 4-7. Average COD Treatment Performance During Operation at 20°C

DO Level	High		Intermediate		Low	
	Avg. (mg/L)	% COD Removal	Avg. (mg/L)	% COD Removal	Avg. (mg/L)	% COD Removal
Influent	226 (±78)	n/a	242 (±56)	n/a	229 (±61)	n/a
20-Day SRT	23 (±5)	88 (±5)	22 ±(7)	91 (±3)	25 (±8)	88 (±5)
10-Day SRT	25 (±5)	87 (±6)	25 (±8)	89 (±4)	27 (±7)	87 (±5)
5-Day SRT	29 (±6)	85 (±7)	31 (±10)	87 (±5)	33 (±10)	85 (±6)
2-Day SRT	35 (±8)	83 (±7)	38 (±10)	83 (±5)	38 (±8)	81 (±9)

provided the highest average treatment efficiency throughout all phases of 20°C operation. The 2-day SRT reactor provided somewhat poorer average treatment; however, COD removal remained above 80% in this reactor and did not vary substantially with changes in DO.

4.2.2 15°C Operation

Influent and effluent COD levels are plotted over time for the 15°C study (Figure 4-2). Table 4-8 summarizes the average carbon treatment performance at each operational phase. These results were very similar to those obtained during 20°C operation, suggesting that the decrease in temperature did not inhibit carbon oxidation. In general, average treatment performance decreased with decreasing SRT, but was unaffected by decreasing DO conditions during operation at 15°C.

4.2.3 10°C Operation

Figure 4-3 shows influent and effluent COD levels throughout the 10°C study period, while Table 4-9 depicts average COD treatment performance for each DO level. Inspection of Figure 4-3 reveals that the strength of the influent wastewater declined throughout the course of the 10°C study, so much so that the average influent COD during the low DO phase was only one-half of that during the high DO phase. Inspection of Tables 4-8 and 4-9 indicates that average percent COD removal decreased at all SRTs for the intermediate and low DO levels when the temperature was decreased from 15°C to 10°C. However, this trend can be attributed to the decrease in influent COD values, rather than a decline in treatment performance. The impact of influent COD concentration on percent COD removal can be shown by rearranging Equation 3-4 as follows.

$$\%\,\text{COD Removal} = \left(\frac{\text{COD}^0}{\text{COD}^0} - \frac{\text{COD}^e}{\text{COD}^0}\right) \times 100\% = \left(1 - \frac{\text{COD}^e}{\text{COD}^0}\right) \text{x}\, 100\% \,. \qquad (4\text{-}1)$$

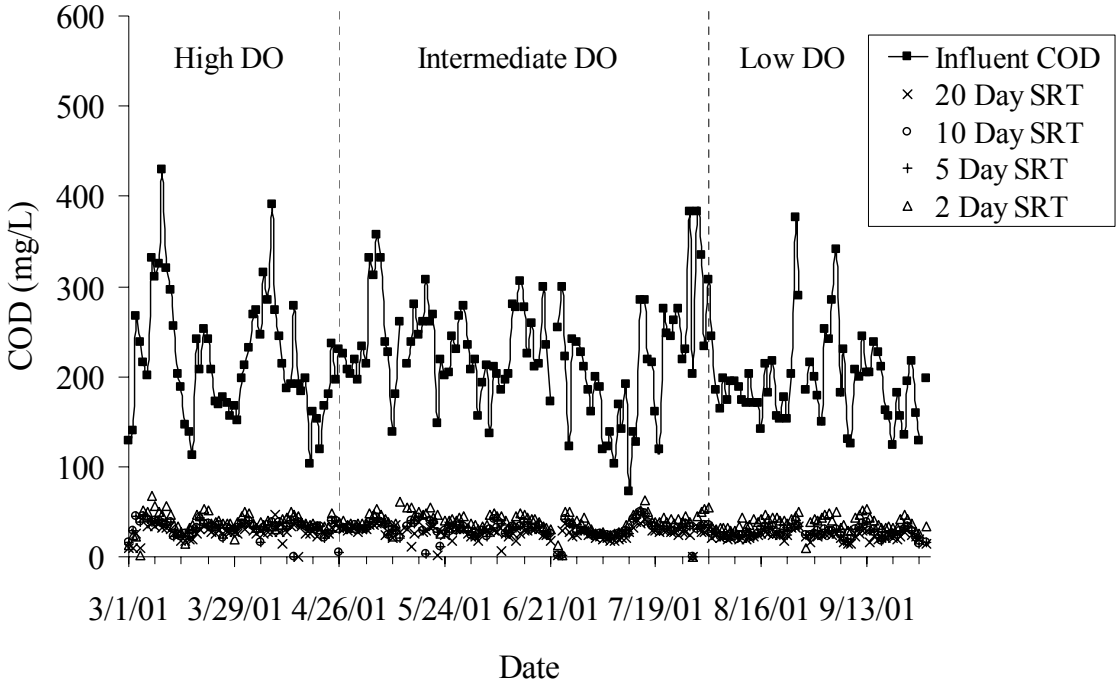

Figure 4-2. Effect of DO Concentration on COD Treatment Performance During 15°C Operation

Table 4-8. Average COD Treatment Performance During Operation at 15°C

DO Level	High		Intermediate		Low	
	Avg. (mg/L)	% COD Removal	Avg. (mg/L)	% COD Removal	Avg. (mg/L)	% COD Removal
Influent	219 (±68)	n/a	227 (±82)	n/a	204 (±72)	n/a
20-Day SRT	27 (±8)	87 (±5)	27 (±7)	86 (±13)	23 (±5)	88 (±3)
10-Day SRT	33 (±8)	84 (±5)	31 (±9)	84 (±17)	27 (±6)	86 (±3)
5-Day SRT	36 (±10)	82 (±5)	38 (±10)	81 (±18)	32 (±7)	84 (±4)
2-Day SRT	39 (±11)	81 (±6)	39 (±11)	81 (±8)	38 (±8)	80 (±5)

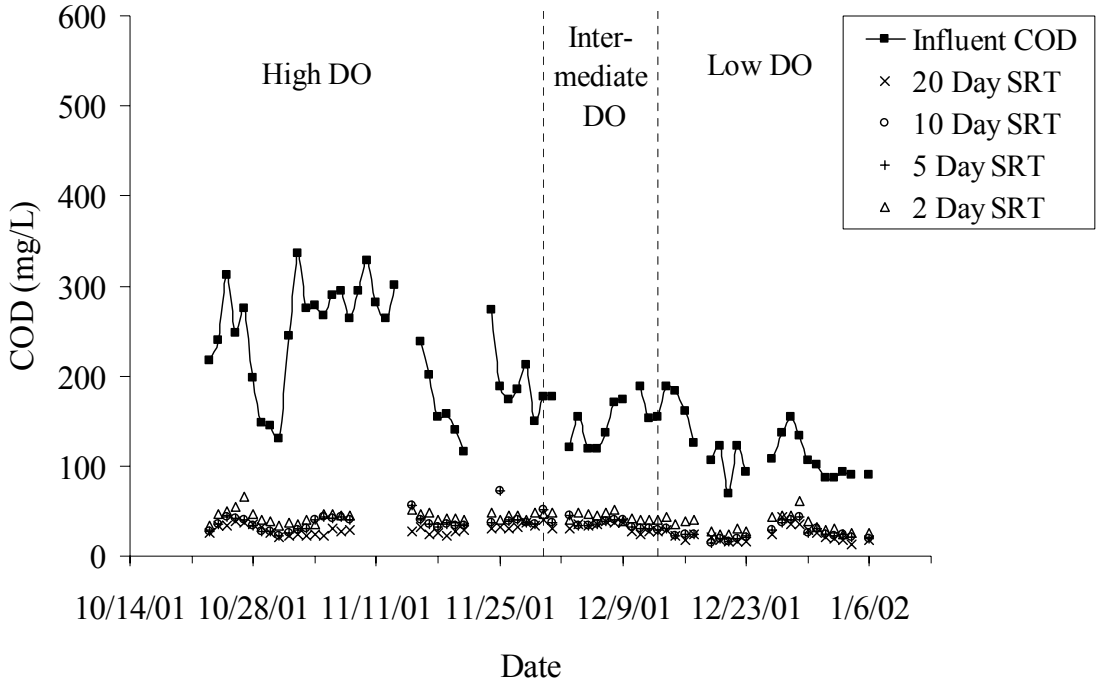

Figure 4-3. Effect of DO Concentration on COD Treatment Performance During 10°C Operation

Table 4-9. Average COD Treatment Performance During Operation at 10°C

DO Level	High		Intermediate		Low	
	COD (mg/L)	% Removal	COD (mg/L)	% Removal	COD (mg/L)	% Removal
Influent	230 (±63)	n/a	154 (±26)	n/a	120 (±33)	n/a
20-Day SRT	29 (±5)	88 (±7)	33 (±5)	78 (±5)	23 (±8)	80 (±5)
10-Day SRT	37 (±10)	85 (±8)	37 (±6)	75 (±6)	26 (±8)	78 (±6)
5-Day SRT	40 (±8)	83 (±9)	40 (±4)	73 (±7)	30 (±7)	74 (±6)
2-Day SRT	44 (±7)	82 (±9)	45 (±4)	70 (±6)	35 (±10)	70 (±6)

Equation 4-1 indicates that for a constant COD^e value, a decrease in COD^0 would yield a larger value for the ratio of COD^e/COD^0, which when subtracted from 1 would result in a lower reported COD removal efficiency. As shown in Table 4-9, average effluent COD levels during intermediate and low DO operation 10°C were similar to values measured at high DO for this temperature. Therefore, while the effluent COD concentrations were stable during the latter stages of this experiment, the large decrease in influent COD levels could result in lower COD removal efficiencies according to Equation 4-1. Effluent COD concentrations during the low DO phase are somewhat lower than those observed during the intermediate and high DO phases at this temperature, suggesting that DO did not negatively impact carbon treatment performance. Additionally, the average residual COD concentrations measured during 10°C operation at the low DO level are similar to those measured during 20°C and 15°C operation at the low DO level, indicating that temperature did not significantly affect carbon oxidation.

4.2.4 Overall Carbon Treatment Performance

Efficient COD removal was achieved throughout all phases of the experiment except for the minor process upset that occurred during July 28 to August 5, 2000, which was caused by factors outside of those controlled during the experiment. Excluding this time period, average effluent COD levels remained below 50 mg/L for all SRTs. A large portion of this residual COD is most likely comprised of soluble organic materials that are resistant to biological breakdown (i.e. refractory organics). Davis and Cornwell (1998) reported that refractory organics can result in effluent soluble COD values in the range of 30-60 mg/L for full-scale municipal WWTPs. These biologically resistant materials do not impact the five-day biochemical oxygen demand (BOD_5) measurement, since BOD_5 only detects the oxygen requirement of biologically oxidizable organic materials. As a result, the COD of an effluent sample will generally be greater than the BOD_5 for the same sample. Currently in the United States, effluent requirements are stipulated in terms of BOD_5 rather than COD. In Tennessee, municipal and domestic WWTPs are required to achieve maximum average monthly discharges of 30 mg/L BOD_5 (TDPH, 1999). Conversion of this value into units of COD assuming the COD_t:BOD_5

ratio of 2.1:1 suggested by Grady and co-workers (1999) yields a value of 63 mg/L COD. Since the concentration of COD discharged from the reactors remained below 50 mg/L throughout all operating periods, the results of this study indicate that the bench-scale system could meet the carbon treatment goals of a full-scale WWTP.

While a high degree of carbon oxidation occurred even at the 2-day SRT, average COD removal efficiency increased with increasing SRT. This trend was expected based on Equation 2-8, which shows the relationship between SRT and effluent substrate concentration, and is in agreement with the results of other studies reported in the literature. For example, when operating a pilot-scale activated sludge system treating domestic wastewater with an average influent COD of 288 mg/L, McClintock et al. (1993) noted COD removal efficiencies of 88%, 89%, and 93% for SRTs of 1.2, 2.7, and 5 days, respectively. Urbain et al. (1998) obtained similar results in a pilot-scale membrane bioreactor. When operated at SRTs of 5, 10, and 20 days, average effluent COD concentrations were 19, 18, and 17 mg/L, respectively, resulting in COD removal efficiencies of 94%, 94%, and 96%. These results, which show that effluent quality improved with increasing SRT are consistent with those obtained in the current study.

DO concentration did not appear to affect carbon removal efficiency in the reactors, which was not surprising since, as discussed in Section 2.5.1, the oxygen half-saturation constant for heterotrophic bacteria is in the range of 0.01-0.15 mg/L (Henze et al., 1987). Several studies have reported effective carbon treatment at low DO. Chuang et al. (1997) found that at SRTs of 5, 10, and 15 days, carbon treatment performance was not impacted by changes in DO concentrations between 0.1 and 2.0 mg/L in a combined activated sludge-biofilm process. For example, when the system was operated at a 10-day SRT and used to treat a synthetic feed with an influent COD concentration of 300 mg/L, COD removal efficiencies of 96.7%, 96.3%, and 96.3% were achieved at DO concentrations of 2.0, 0.5, and 0.1 mg/L DO, respectively. Similar findings were reported by Lau et al. (1984), who found that effective carbon removal could be achieved at DO concentrations as low as 0.088 mg/L. When operated at an SRT of 0.308 days and DO concentrations of 6.16, 0.352, and 0.088 mg/L, 98.0%, 96.3%, and 97.2% COD removal, respectively, were achieved in a chemostat treating synthetic wastewater.

Based on residual COD values for each of the treatment units, changes in temperature did not significantly affect COD levels discharged under the range of conditions studied. These results are consistent with empirical evidence indicating the process of carbon oxidation by heterotrophic bacteria is fairly insensitive to temperature because of the high solids levels maintained in activated sludge systems (Benefield and Randall, 1980). In a set of bench-scale activated sludge experiments, Sayigh and Malina (1978) found that, at SRTs of 3 days or more, BOD removal efficiency was relatively independent of temperature variations between 4°C and 31°C. McClintock et al. (1993) obtained similar results in their investigation of the effects of temperature and SRT on biological nutrient removal (BNR). In their study, COD removal efficiencies of 88%, 91% and 87% were achieved at 20°C, 15°C, and 10°C, respectively, in a pilot-scale activated sludge system operated at an SRT of 15 days. Lishman et al. (2000) also found that residual COD concentrations were not significantly impacted by temperature changes in a sequencing batch reactor (SBR) operated at a 10-day SRT. When treating a synthetic feed with an influent COD level of 400 mg/L, effluent COD values ranged between 25 and 50 mg/L and did not vary substantially when the operating temperature was lowered from 19°C to 14°C.

4.3 Measures of Total Biomass

4.3.1 MLVSS

The MLVSS concentration is the parameter traditionally used in wastewater treatment as a surrogate measure of the microbial population. As demonstrated in Equation 2-13, MLVSS is a function of SRT and influent substrate concentration. Because heterotrophic bacteria comprise the majority of the biomass content in a combined carbon removal/nitrification activated sludge system (Benefield and Randall, 1980), the concentration of biomass in the reactor can be sensitive to changes in the influent COD level. Since municipal wastewater was used as the influent feed to the experimental treatment system, the strength of the wastewater varied with each collection

date. Although MLVSS levels were maintained at fairly stable levels, strict steady state conditions were difficult to maintain due to the variability of the influent waste stream.

20°C Operation

For the 20°C operational period, several abrupt changes in MVLSS concentration were noted over time (Figure 4-4). A substantial drop in MLVSS concentration occurred on August 27, 2000, due to a tubing change in the influent pump (Parker, 2001). A thick walled type of tubing was used to replace worn tubing; however, it was soon discovered that this tubing did not allow the full flow of influent wastewater to pass into the reactors. The 20-day SRT reactor was most affected by the change in tubing, dropping from a MLVSS concentration of 1910 mg/L to 1090 mg/L in three days. Solids in the 10-day SRT reactor decreased from 1460 mg/L to 1040 mg/L while the 2- and 5-day SRT reactors were only marginally affected. Once this problem was realized, the tubing was again replaced, and installation of the proper tubing resulted in an increased MLVSS level in all four reactors.

A foaming problem occurred during the period from October 5 to November 2, 2000, which also led to fluctuations in MLVSS concentrations, particularly in the 20-day and 10-day SRT reactors (Parker, 2001). The foaming caused the reactor effluent ports to clog several times. When this occurred solids would remain in the reactor until the foam at the overflow dispersed, at which time a significant amount of liquid would flood into the clarifier. This overloading of the clarifier resulted in high effluent solids loss on several occasions, thereby affecting MLVSS concentrations. Aside from these exceptions, the MLVSS values in each reactor remained fairly stable, with minor fluctuations following the same trends as influent COD (Figures 4-1 and 4-4). Averages and standard deviations during 20°C operation, excluding the two problem events, are reported in Table 4-10.

A linear regression analysis was performed on the MLVSS data, as discussed in Section 3.5, to determine how much of the variability in measured values could be attributed to changes in the controlled variables and which variables had the largest relative effect on solids levels. The developed model fit the experimental data quite well,

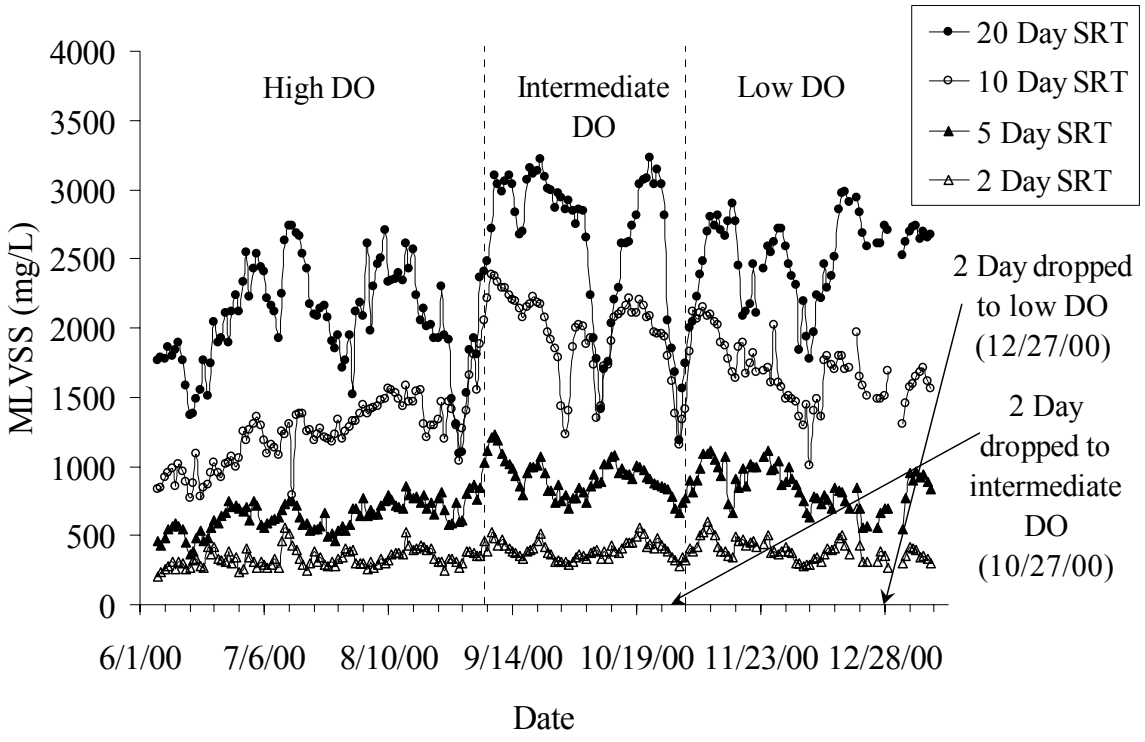

Figure 4-4. Fluctuations in MLVSS Concentration Due to Changing DO and Influent COD Concentrations Throughout the 20°C Study

Table 4-10. Average MLVSS Concentrations (mg/L) During Operation at 20°C

DO Level	High	Intermediate	Low
20-Day SRT	2113 (±331)	2941 (±173)	2515 (±295)
10-Day SRT	1238 (±252)	2041 (±289)	1686 (±234)
5-Day SRT	644 (±73)	932 (±151)	854 (±149)
2-Day SRT	358 (±73)	407 (±83)	345 (±49)

as evidenced by a correlation coefficient of 0.926, and indicated that 85.8% of the observed variability in MLVSS concentrations could be explained by changes in the influent COD, SRT, DO, and the compound effects of DO and SRT.

Of the four independent variables included in the model, the null hypothesis (that the partial regression coefficient was zero) could only be rejected for the SRT at a 95% confidence interval. This result indicated that SRT was the prime determinant of the MLVSS concentration and that variations in DO and influent COD levels did not significantly affect the MLVSS during 20°C operation. This result was anticipated since, as discussed in section 2.3.1, for a fixed reactor volume, selection of the SRT determines the total biomass concentration in the system. Because the influent COD concentration remained fairly stable throughout the 20°C study (Figure 4-1), influent COD level would not be expected to cause large variations in the MLVSS values. As noted in previous sections, changes in DO level were not likely to yield a significant impact on MLVSS concentrations, since the oxygen half-saturation constant for heterotrophs is quite low.

15°C Operation

MLVSS concentrations measured during 15°C operation are shown in Figure 4-5 over time. As with the 20°C study, there were several incidences in which external factors impacted the MLVSS concentration in the reactors. The first major change in solids concentration occurred between May 3 and May 24, 2001, when an ink-like material was observed in the collection system of the full-scale municipal WWTP (Wood, in preparation). A foaming problem also occurred between July 17 and July 26, 2001, resulting in a drastic drop in MLVSS concentrations with a concurrent rise in effluent suspended solids (ESS) for all reactors. Another anomaly occurred in the 5-day SRT reactor during the time period of September 2 and September 9, 2001. The cleaning arm in the external clarifier malfunctioned causing the recycle lines to clog with solids. This problem was not discovered for three days causing unusually low solids concentrations in the mixed liquor. Once the problem was corrected, however, the solids concentrations rapidly increased and returned to apparent steady-state levels.

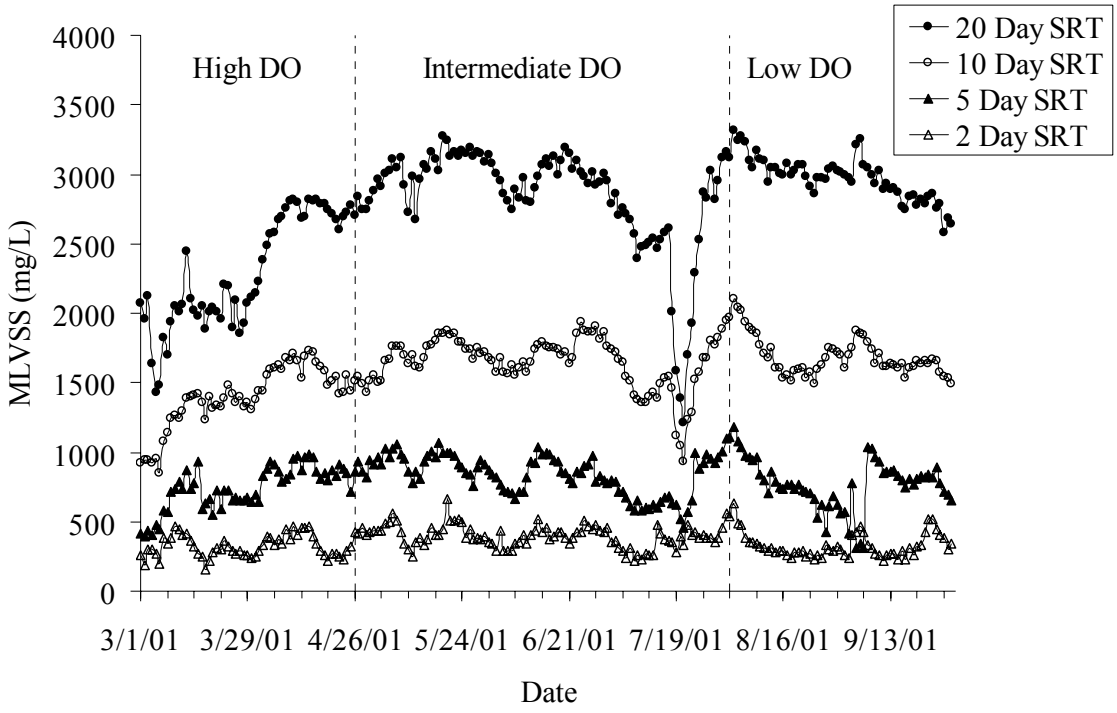

Figure 4-5. Fluctuations in MLVSS Concentration Due to Changing DO and Influent COD Concentrations Throughout the 15°C Study

With the exclusion of the previously described problem events, the MLVSS concentration in the 2-day SRT reactor remained fairly stable throughout the 15°C study. In the 20-, 10-, and 5-day SRT reactors, the MLVSS concentrations increased throughout operation at the high DO level, and then remained fairly stable throughout operation at the intermediate and low DO level periods. Averages and standard deviations for the MLVSS concentrations at 15°C (excluding the three anomalies) are shown in Table 4-11. The average MLVSS concentrations reported in Table 4-11 are very similar to those reported in Table 4-10, suggesting that temperature did not significantly affect MLVSS values.

Linear regression analysis of the 15°C MLVSS data yielded a model which described the experimental data very well (R=0.974) and revealed that 95% of the variability in MLVSS could be attributed to changes in the influent COD, SRT, DO and the interaction between SRT and DO.

Table 4-11. Average MLVSS Concentrations (mg/L) During Operation at 15°C

DO Level	High	Intermediate	Low
20-Day SRT	2293 (±398)	2894 (±208)	2974 (±156)
10-Day SRT	1398 (±223)	1660 (±153)	1691 (±141)
5-Day SRT	739 (±158)	787 (±167)	791 (±146)
2-Day SRT	321 (±79)	382 (±73)	330 (±90)

Again the SRT was found to have the greatest impact on MLVSS, however, in this case the interaction term describing the joint effect of SRT and DO also contributed significantly to the model. To study this interaction, the data was subdivided by DO level and additional linear regression analyses were performed for each data subset. The resulting linear models showed that the impact of SRT on the MLVSS increased as the DO level decreased. The partial regression coefficients indicated that an increase in the SRT of 1 day resulted in an increase in MLVSS concentration of 110 mg/L, 125 mg/L and 139 mg/L at the high, intermediate and low DO levels, respectively. This can be seen in Figure 4-5 as well, which shows that throughout the course of the treatment study, the difference in MLVSS concentrations between each SRT increases. The influent COD concentration was not found to significantly affect the MLVSS concentration, which is not surprising since the strength of the influent wastewater did not vary substantially throughout the 15°C study period (Figure 4-2).

10°C Operation

During 10°C operation of the municipal bench-scale reactors, the MLVSS levels appeared to mirror the trend in influent COD concentration as indicated by a comparison of Figures 4-3 and 4-6. The influent COD concentration decreased throughout the 10°C operational period and the MLVSS values decreased in a corresponding fashion. Although inspection of Table 4-12 appears to indicate that lower DO levels decreased MLVSS concentrations, it is believed that the lower influent COD levels were responsible for the changes noted. The average influent COD concentration measured during operation at the high DO level was consistent with values measured throughout

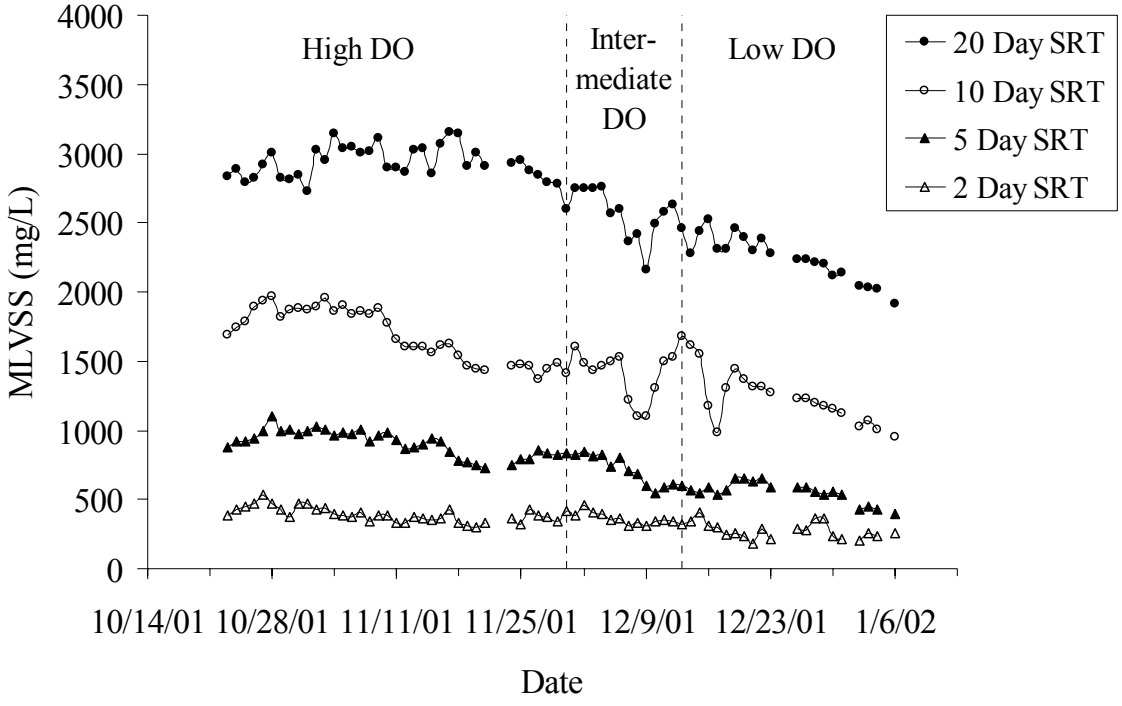

Figure 4-6. Fluctuations in MLVSS Concentration Due to Changing DO and Influent COD Concentrations Throughout the 10°C Study

Table 4-12. Average MLVSS Concentrations (mg/L) During Operation at 10°C

DO Level	High	Intermediate	Low
20-Day SRT	2939 (±114)	2571 (±178)	2252 (±230)
10-Day SRT	1698 (±187)	1398 (±166)	1247 (±201)
5-Day SRT	908 (±92)	724 (±107)	556 (±73)
2-Day SRT	391 (±55)	368 (±43)	276 (±58)
Influent COD	230 (±63)	154 (±26)	120 (±33)

the course of the 15°C and 20°C studies, and the MLVSS levels during these periods were quite similar. This suggests that the decrease in temperature did not affect the MLVSS concentration.

The multiple linear regression model developed for the 10°C MLVSS data described the experimental results very well (R = 0.99), and revealed that 98.3% of the observed variability in MLVSS values could be attributed to changes in controlled variables. Only the SRT and the compound effects of SRT and DO were found to affect the MLVSS in a statistically significant manner. It was expected that the influent COD level would be a significant predictor of MLVSS concentration, however, it is believed that this was not observed in the model due to problems of multicollinearity. Since the influent COD and DO decreased in a corresponding fashion, these parameters were highly correlated. The inclusion of both terms overspecified the model, making the effect of the individual variables on the independent variable unclear. To test this theory, the data was subdivided based on DO and additional analyses were performed. The results of these models showed that the influent COD was not significant at the high DO level, but did impact the MLVSS at the intermediate and low DO levels. This is reasonable since at the high DO level, the influent COD concentration was much more stable than at the other DO levels (Figure 4-3). At the high DO level, only the SRT controlled the MLVSS concentration. Even though the influent COD concentration impacted the MLVSS at the intermediate and low DO levels, SRT exerted much more influence on the solids concentration under these conditions.

As shown in Equation 2-13, the MLVSS concentration is directly proportional to the amount of COD removed in the treatment system.

$$X = \frac{\theta_x}{\theta} \frac{Y\left(S^0 - S\right)}{1 + b\theta_x} \tag{2-13}$$

Throughout the 10˚C study, the decrease in influent COD concentration resulted in a decrease in the amount of COD removed. In turn, a decrease in MLVSS values was observed according to equation 2-13. Several other studies have shown a correlation between influent COD level and MLVSS concentration. Jianlong et al. (2000) conducted a study on the effect of organic loading rates on treatment performance in a hybrid

biological reactor treating domestic wastewater that was supplemented with glucose to control the loading rates. In this hybrid biological reactor system, the activated sludge process was combined with a fixed film biomass process. Average influent COD levels of 190, 365, and 760 mg/L resulted in average MLVSS values in the suspended biomass of 1900, 2050, and 2250 mg/L, respectively, and MLVSS values in the total biomass of 4300, 4850, and 5750 mg/L, respectively. Lee et al. (2000) also performed experiments to investigate the effect of organic loading on treatment performance in hybrid biological reactors and obtained similar results. In their study, a bench-scale conventional activated sludge reactor was used as a control. When the reactor was operated at an SRT of 10 days and used to treat synthetic wastewater with COD levels of 250, 500, and 1000 mg/L, MLVSS concentrations of 2080, 2120, and 2200 mg/L were measured. In these studies, and the current investigation, the MLVSS concentration was positively correlated with influent COD levels.

Comparison of Data from All Three Temperatures

A linear regression analysis was performed on all of the MLVSS data from the 20°C, 15°C, and 10°C operating periods and the results showed that 92% of the observed variability in MLVSS values could be explained by the influent COD, SRT, temperature, DO, and the 2-way and 3-way interactions of these independent variables. The partial correlation coefficients showed that the independent variable that had the greatest impact on the MLVSS was the SRT. This result was expected since more organisms are retained in the system at longer SRTs thereby resulting in larger MLVSS values. The individual effects of temperature, DO, and influent COD were not found to be statistically significant when all the data were considered.

These findings suggest that SRT controls the MLVSS concentration as long as the influent COD level is fairly consistent. However, large variations in influent COD concentrations are reflected in the MLVSS concentration. DO and temperature were not found to significantly impact the MLVSS concentration. These findings are consistent with reported results found in the literature. Chuang et al. (1997) observed that MLSS concentrations in a combined activated sludge-biofilm system were not affected by DO

concentration. When operated at a 5-day SRT, MLSS concentrations in the system were 920, 1010, and 1030 mg/L, at DO levels of 2.0, 0.5, and 0.1 mg/L, respectively. Lau et al. (1984) reported similar findings for an activated sludge CSTR operated at an SRT of 0.33 days. At DO levels of 7.04 and 0.44 mg/L, average MLSS concentrations of 519 mg/L and 491 mg/L, respectively were measured in the system. McClintock et al. (1993) measured MLVSS concentrations of 1,284 mg/L, 1,050 mg/L, and 1,373 mg/L at temperatures of 20°C, 15°C, and 10°C, respectively, in a pilot scale activated sludge system treating domestic wastewater operated at an SRT of 5 days, indicating that temperature did not significantly affect MLVSS concentration.

4.3.2 Total Eubacterial Concentration

In addition to MLVSS, total eubacterial concentration determined from real-time PCR analysis was used as an overall measure of biomass content in each reactor. Real-time PCR data was measured in terms of the number of gene copies in a sample. To allow for a better comparison with the traditional information collected in this study, the real-time PCR data was converted to a cell per liter (mixed liquor) basis. The conversion of total 16S rDNA copy number to cell number can be problematic since bacterial ribosomal operons can vary from 1 to 15 (Condon, 1995; Klappenbach et al., 2000). It has been hypothesized that bacteria with faster growth rates or the ability to respond rapidly to environmental changes have higher ribosomal operon numbers than slow growing bacteria that are sensitive to environmental changes (Condon, 1995, Klappenbach et al., 2000). Therefore, it is possible that the low SRT reactor may select for microbial populations with a different number of ribosomal operons. The reported ribosomal operon copy numbers for bacterial species found in wastewater treatment systems range from a high of 13 in *Bacillus* to 1 in *Nitrosomonas* (Klappenbach et al., 2001). Given that the majority of species in wastewater treatment reactors contain a relatively low number of ribosomal operons, the current average operon number for all bacterial species of 3.6 may be the most reasonable conversion factor (Klappenbach et al., 2001). Therefore, a value of 3.6 16S rDNA gene copies per cell was assumed in this study for the calculation

of total eubacterial cellular concentrations. A sample calculation is provided in Appendix A.

20°C Operation

Table 4-13 lists the average total eubacterial 16S rDNA cell concentrations normalized to mixed liquor volume for the 20°C system. The eubacterial cell densities reported in this table are consistent with those reported in several studies in the literature. Harms et al. (2003) reported an average value of 4.3 (±2.0) x 10^{11} eubacterial cells/L when applying the same real-time PCR assay used in the current study to 12 monthly samples from the full-scale municipal WWTP used to seed the reactors, which operates at an average SRT of 10 days. Lishman et al. (2000) obtained similar results in a sequencing batch reactor (SBR) operated at a 10 day SRT and temperatures of 19°C and 14°C. In their study, the total numbers of bacteria larger than 0.2 μm, enumerated using acridine orange direct counts (AODC), were between 4.9 x 10^{11} and 1.2 x 10^{12} cells/L. Lee et al. (2002) reported biomass densities of 2.32 x 10^{11} to 6.12 x 10^{11} cells/L for a bench-scale activated sludge reactor operated at an SRT of 10 days, a temperature of 20°C, and excess DO. The biomass densities in their study were determined by performing colony counts.

Table 4-13 shows that total eubacterial concentrations follow the expected trends with the highest cell concentrations present in the 20-day SRT samples and the lowest cell concentrations in the 2-day SRT samples. While total eubacterial concentration (cells/L) was found to be highly dependent on SRT, significant trends in bacterial concentration as a function of DO level were not observed. Figure 4-7 provides a

Table 4-13. Average Total Eubacterial Concentrations (cells/L) During Operation at 20°C

DO Level	High	Intermediate	Low
20-Day SRT	1.1 (±0.5) x 10^{12}	6.2 (±1.6) x 10^{11}	7.1 (±4.1) x 10^{11}
10-Day SRT	7.0 (±3.7) x 10^{11}	5.2 (±0.5) x 10^{11}	6.5 (±3.8) x 10^{11}
5-Day SRT	3.8 (±2.9) x 10^{11}	2.0 (±1.2) x 10^{11}	1.8 (±0.8) x 10^{11}
2-Day SRT	1.3 (±0.3) x 10^{11}	7.5 (±4.5) x 10^{10}	3.6 (±0.5) x 10^{10}

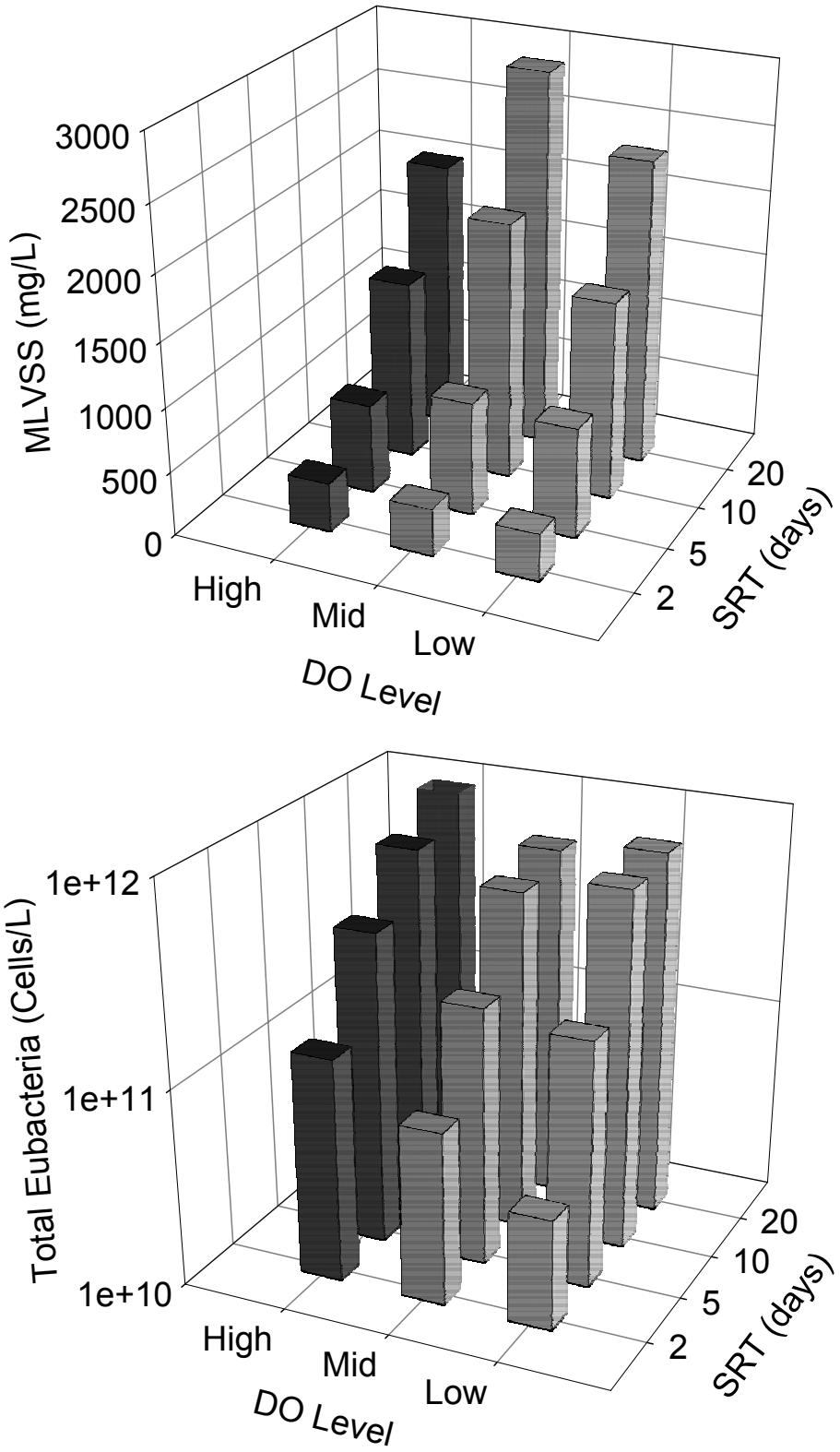

Figure 4-7. Comparison of Trends in MLVSS Concentration and Total Eubacterial Concentration at Varying SRT and DO Levels at 20°C

comparison the average total eubacterial and MLVSS concentrations as a function of SRT and DO level and shows that both measures of biomass followed similar trends with respect to SRT.

Linear regression analysis was performed on the total eubacterial concentrations measured during 20°C operation in the same manner as that used for MLVSS. This model did not describe the data as well as the model developed for MLVSS. The correlation coefficient was 0.769 for total eubacterial concentration, compared to 0.926 for MLVSS. Only 59% of the variability in measured eubacterial concentrations could be explained by changes in controlled variables, in contrast to 86% for the MLVSS. As in the multiple linear regression model for MLVSS, of the four independent variables included in the analysis (SRT, DO, influent COD, and joint effect of SRT and DO) only the SRT was found to significantly affect the concentration of total eubacteria in the reactors.

15°C Operation

The average total eubacterial concentrations measured during 15°C operation are listed in Table 4-14. Again the highest cell concentrations were measured in the 20-day SRT samples and the lowest cell concentrations were present in the 2-day SRT samples. Comparison of Tables 4-13 and 4-14 shows that a clear trend in concentration of total eubacteria based on the decrease in temperature from 20°C to 15°C was not observed. Figure 4-8 compares the average MLVSS and total bacteria concentrations in the reactor during the 15°C study and show similar trends in response to changes in SRT. Average values of both measures of biomass content are shown to increase between the high and

Table 4-14. Average Total Eubacterial Concentrations (cells/L) During Operation at 15°C

DO Level	High	Intermediate	Low
20-Day SRT	$3.7 (\pm 2.0) \times 10^{11}$	$9.8 (\pm 1.5) \times 10^{11}$	$1.6 (\pm 0.3) \times 10^{12}$
10-Day SRT	$3.7 (\pm 1.5) \times 10^{11}$	$7.8 (\pm 2.0) \times 10^{11}$	$1.6 (\pm 0.1) \times 10^{12}$
5-Day SRT	$3.1 (\pm 1.9) \times 10^{11}$	$8.0 (\pm 2.6) \times 10^{11}$	$5.7 (\pm 0.7) \times 10^{11}$
2-Day SRT	$1.5 (\pm 0.7) \times 10^{11}$	$4.3 (\pm 0.5) \times 10^{11}$	$2.6 (\pm 0.6) \times 10^{11}$

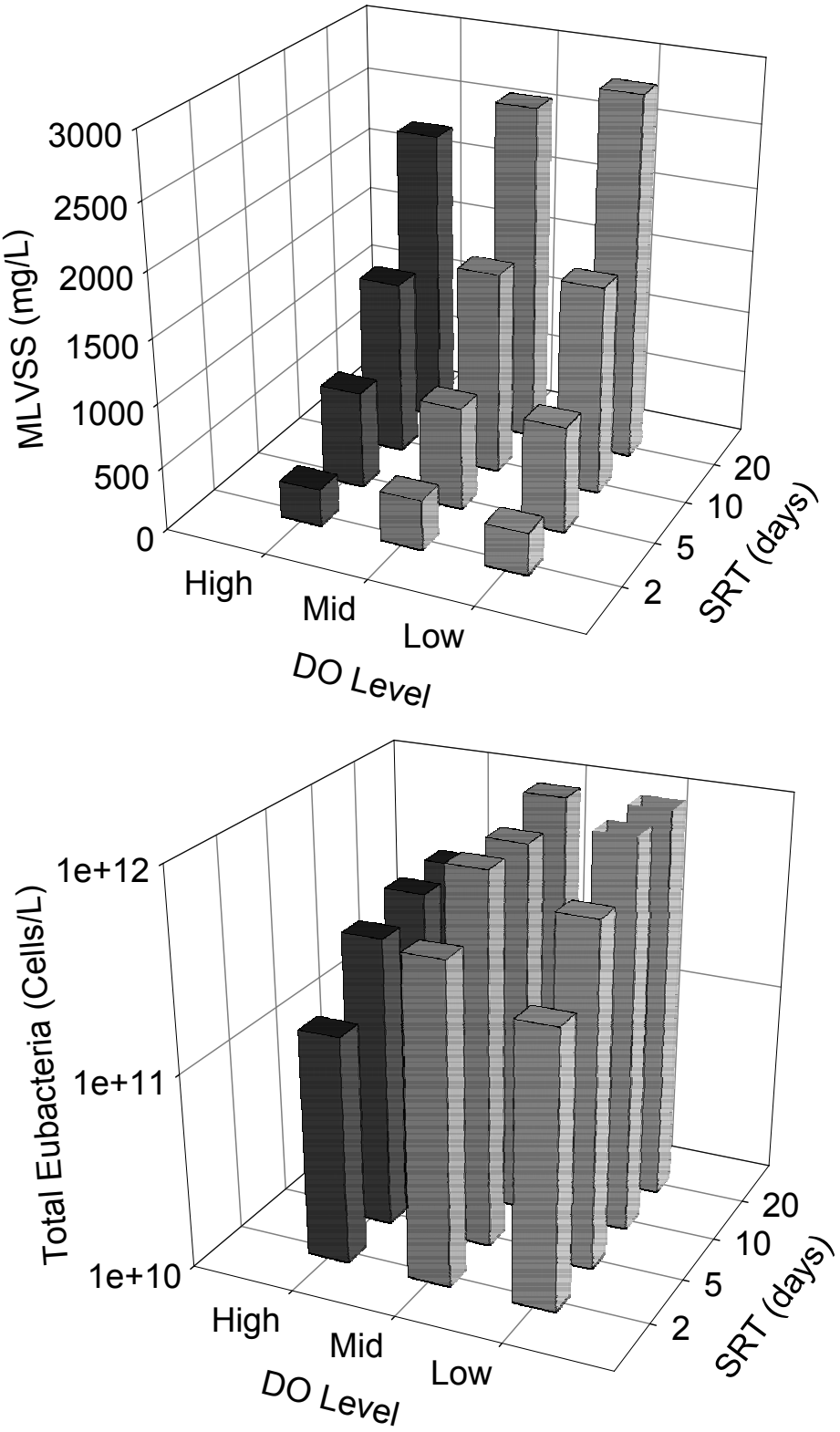

Figure 4-8. Comparison of Trends in MLVSS Concentration and Total Eubacterial Concentration at Varying SRT and DO Levels at 15°C

intermediate DO levels and then remain fairly stable when the DO is dropped to the low DO level.

The linear regression model developed for the 15°C total eubacteria data was similar to that obtained for the 20°C data (R=0.782) and revealed that 61.1% of the observed variability in cell concentrations could be attributed to changes in the influent COD, SRT, DO, and the interaction between SRT and DO. Under these conditions, both the SRT and DO were found to significantly impact the total eubacterial concentration. The SRT was positively correlated with eubacterial concentration, while the DO level was negatively correlated. SRT was found to have the largest relative effect on the total eubacterial concentration.

It is unclear why the eubacterial concentrations increased with decreasing DO level. One possible explanation is that population shifts occurred in the reactors; with dominant bacteria at the lower DO levels having higher yields than those dominant at the high DO levels. It is widely recognized that low DO concentrations favor filamentous organisms (Grady et al., 1999), which is indicative of a population shift. A foaming problem also was noted in the reactors during the intermediate and low DO periods, and excessive foaming is caused primarily by bacteria of the genus *Nocardia* and the species *Microthrix parvicella* (Jenkins et al., 1993). Thus foaming in the reactors also signifies a possible population shift.

10°C Operation

Table 4-15 lists the average total eubacterial concentrations for each DO level during operation at 10°C, which are very similar to those obtained at the higher temperatures. In general, the total eubacteria cell density decreased with decreasing SRT. Total eubacterial concentrations at 10°C appeared to be unaffected by changes in DO concentration. Figure 4-9 provides a graphical representation of this data, as well as the MLVSS data for these operating conditions. The concentration of total eubactiera did not appear to be affected by the changes in influent COD that resulted in decreased MLVSS levels during operation at the low and intermediate DO levels.

Table 4-15. Average Total Eubacterial Concentrations (cells/L) During Operation at 10°C

DO Level	High	Intermediate	Low
20-Day SRT	1.8 (±0.2) x 10^{12}	5.0 (±0.8) x 10^{11}	1.6 (±0.2) x 10^{12}
10-Day SRT	1.0 (±0.2) x 10^{12}	1.0 (±0.3) x 10^{12}	9.5 (±2.4) x 10^{11}
5-Day SRT	4.8 (±1.5) x 10^{11}	4.7 (±0.5) x 10^{11}	6.9 (±2.3) x 10^{11}
2-Day SRT	3.7 (±0.9) x 10^{11}	3.2 (±0.7) x 10^{11}	3.3 (±0.9) x 10^{11}

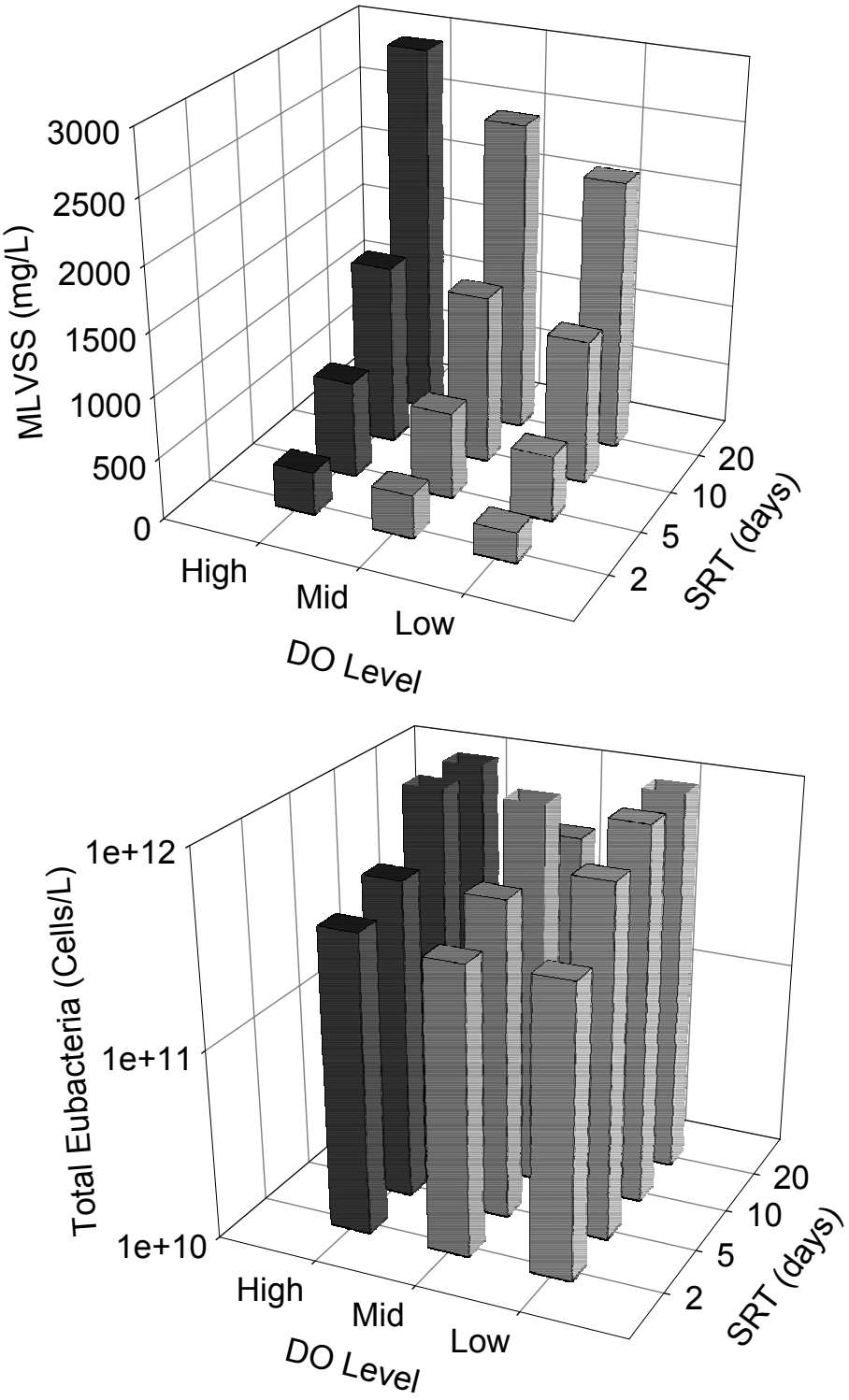

Figure 4-9. Comparison of Trends in MLVSS Concentration and Total Eubacterial Concentration at Varying SRT and DO Levels at 10°C

Linear regression analysis of the 10°C data total eubacterial cell density revealed that only 52.5% of the observed variability in measured values could be explained by changes in the influent COD, SRT, DO, and combined effects of SRT and DO. Only SRT was found to significantly impact the concentration of total eubacteria. In contrast to MLVSS, the total eubacterial cell density was not affected by the large decrease in influent COD concentration throughout this study period.

Comparison of Data from All Three Temperatures

The linear regression model developed for all the total eubacteria data from 20°C, 15°C, and 10°C operating periods described the data fairly well (R=0.734), but showed that only 54% of the observed variability could be explained by changes in the influent COD level, SRT, temperature, DO, and the interactions between these variables. The partial regression coefficients provided unclear results regarding the independent variables yielding the largest influence on total eubacterial concentration. It is believed that this was a result of the strong correlation between the interaction terms and the individual variables, which led to problems of multicollinearity.

At each temperature, the SRT was found to have the most significant impact on concentration of total eubacteria. No clear trends in eubacterial concentration were observed with respect to temperature or DO as shown in Figure 4-10, which includes only steady-state data as identified in Tables 4-4, 4-5 and 4-6. Figure 4-11 shows similar trends for MLVSS. Both total eubacterial and MLVSS concentration were found to increase with SRT between 2 and 10 days and then level off between 10 and 20 days.

Temperature and DO level were not expected to have a significant impact on the MLVSS or total bacterial concentration in the range of operating conditions tested since both of these parameters are largely reflective of the heterotrophic population which is not as sensitive to changes in these conditions as the nitrifying bacteria. In a study on the effects of temperature on wastewater treatment under aerobic and anoxic conditions, Lishman et al. (2000) found that the change in temperature from 19°C and 14°C did not produce a statistically significant difference in the bacterial concentrations in a SBR.

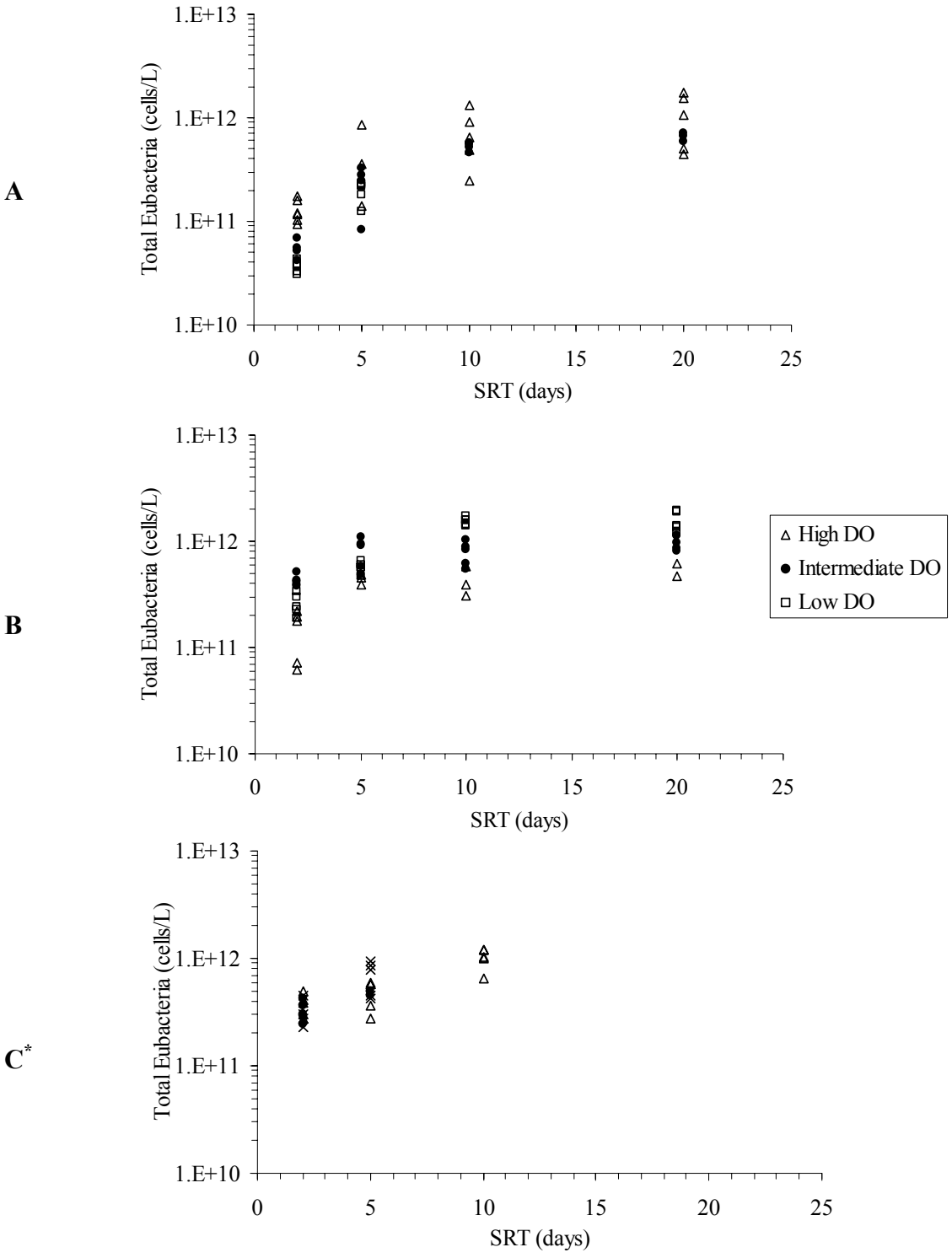

Figure 4-10. Steady-state Concentration of Total Eubacteria as a Function of SRT (A) 20°C, (B) 15°C, (C) 10°C

* 20-day SRT data at 10°C did not fit criteria for steady-state and therefore is not included in Figure-10C

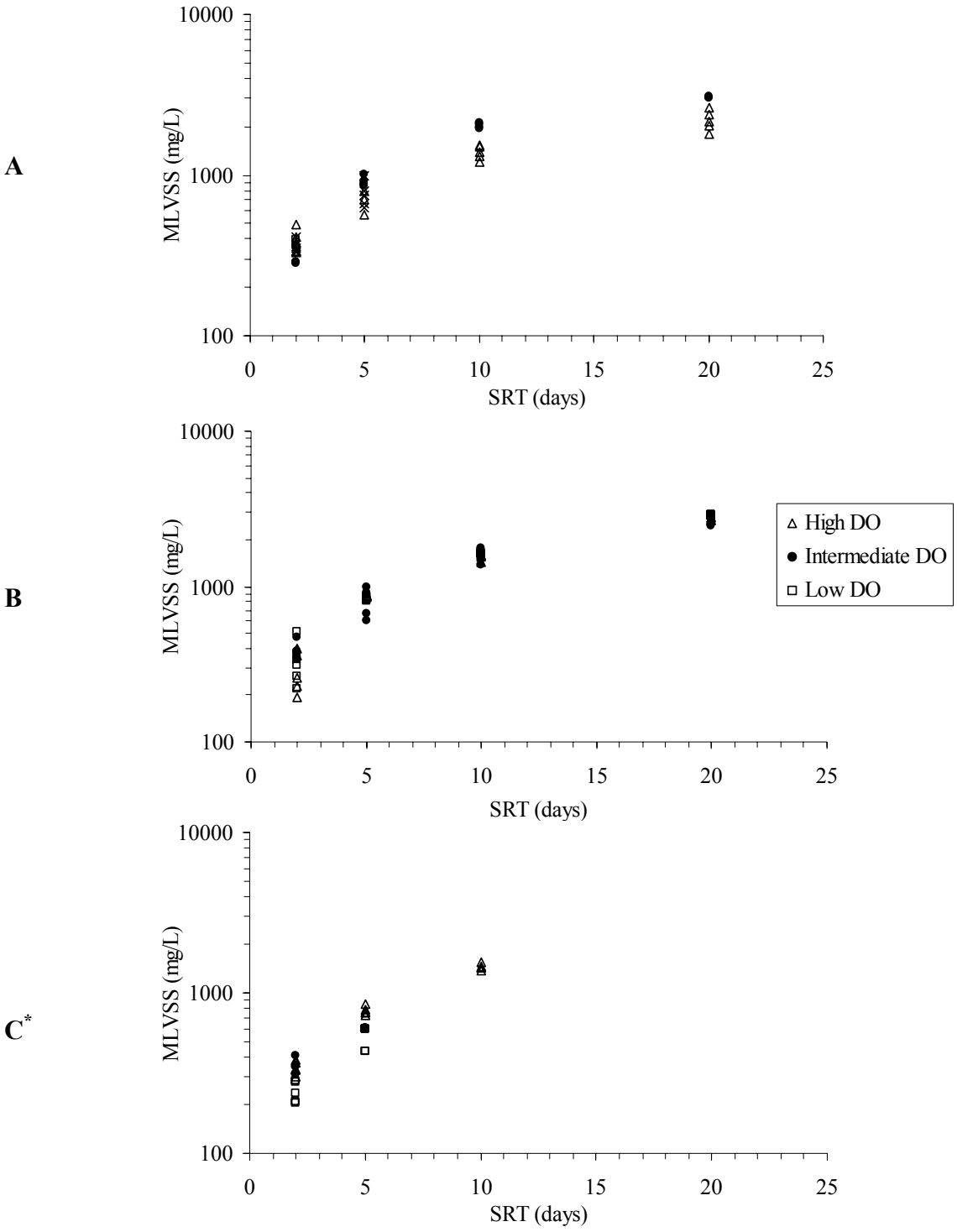

Figure 4-11. Steady-state Concentration of MLVSS as a Function of SRT (A) 20°C, (B) 15°C, (C) 10°C

* 20-day SRT data at 10°C did not fit criteria for steady-state and therefore is not included in Figure-11C

As shown in Table 4-16, between 27% and 46% less of the variability in total eubacterial cell numbers could be explained by the parameters controlled in this study than for the MLVSS. This indicates that one or more additional factors accounting for a substantial portion of the variability in eubacterial concentration were not included in the linear regression analysis. A likely source of the undescribed variability is changes in cell weight in response to variations in operational and environmental parameters. MLVSS is a crude measure of dry cell weight and is maintained at fairly stable levels through biomass wastage to maintain a constant SRT, regardless of temperature or DO level. In contrast, the real-time PCR assay measures copy numbers of eubacterial 16S rDNA. As discussed previously, in this study it was assumed that each cell contained 3.6 copies of 16S rDNA. However, it has been hypothesized that bacteria with higher maximum specific growth rates have higher ribosomal operon numbers than slow growing bacteria (Condon, 1995; Klappenbach et al., 2000), suggesting that lower SRTs may select for microbial populations with a different number of ribosomal operons. In addition, cell size and weight vary from bacterial species to species, and within a species as a result of environmental conditions. Another factor may be that MLVSS is a measure of all organics present in the sample and includes protozoa, fungi, etc. While bacteria are responsible for most carbon oxidation, their contribution to MLVSS may vary for different conditions due to predation by protozoa and metazoa (Rittmann and McCarty, 2001). Undescribed variability could also result from the fact that some of the samples included in the analysis were not taken during steady-state operation.

Table 4-16. Summary of Linear Regression Analyses for MLVSS and Total Eubacterial Concentrations

	MLVSS		Log Total Eubacterial Concentration	
Temperature	R	R^2	R	R^2
All	0.957	0.916	0.734	0.539
20°C	0.926	0.858	0.769	0.591
15°C	0.974	0.949	0.782	0.611
10°C	0.992	0.983	0.724	0.525

4.4 Nitrification Performance

4.1.1 Ammonia Oxidation

Figures 4-12 through 4-15 show the influent ammonia and reactor effluent ammonia, nitrite, and nitrate concentrations (as N) over time as a function of temperature and DO level for the 20-, 10-, 5-, and 2-day SRT systems, respectively.

20°C Operation

Average ammonia concentrations and corresponding ammonia oxidation rates and efficiencies for each DO level in each SRT reactor are presented in Table 4-17 for the 20°C study. The rates shown in Table 4-17 are comparable to the nitrification rates measured by Ydstebo et al. (2000), which ranged from 42.6 to 53.6 mg N/L/day in a Norwegian BNR treatment facility treating domestic wastewater with an average influent total nitrogen concentration of 32 mg/L. Prinčič et al. (1998) reported ammonia oxidation rates of 37- 74 mg N/L/ day for enriched nitrifying bacterial cultures in continuously fed reactors operated under excess oxygen conditions. McClintock et al. (1993) reported similar results in a pilot scale activated sludge system treating domestic wastewater with influent TKN concentrations of 25-37 mg N/ L operated at SRTs between 1.5 and 15 days. In their study, ammonia oxidation rates of 45-81 mg N/L/day were measured in the reactors and corresponded to nitrification efficiencies between 65% and 100%.

High rates and efficiencies of ammonia oxidation were consistently achieved in the 20-, 10- and 5-day SRT reactors during operation at the high and intermediate DO levels (Table 4-17). The multiple linear regression model developed using data obtained under these operating conditions showed that only the influent ammonia significantly affected the ammonia oxidation rate at a 95% confidence level, indicating that nitrification performance was not substantially improved by increasing the SRT above 5 days or the DO concentration above 1 mg/L at a temperature of 20ºC.

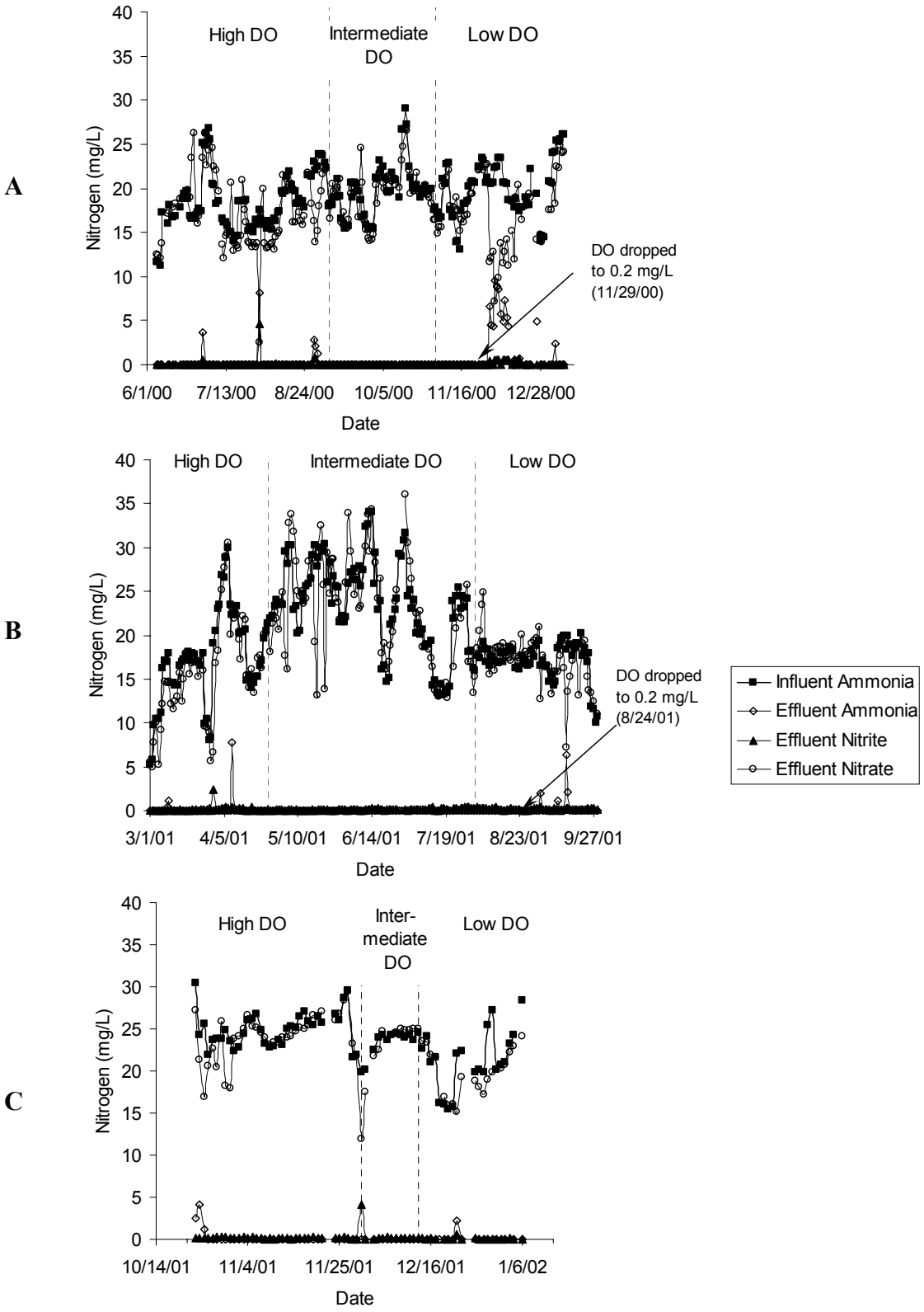

Figure 4-12. 20-day SRT Reactor Nitrogen Results (A) 20°C, (B) 15°C, (C) 10°C

A

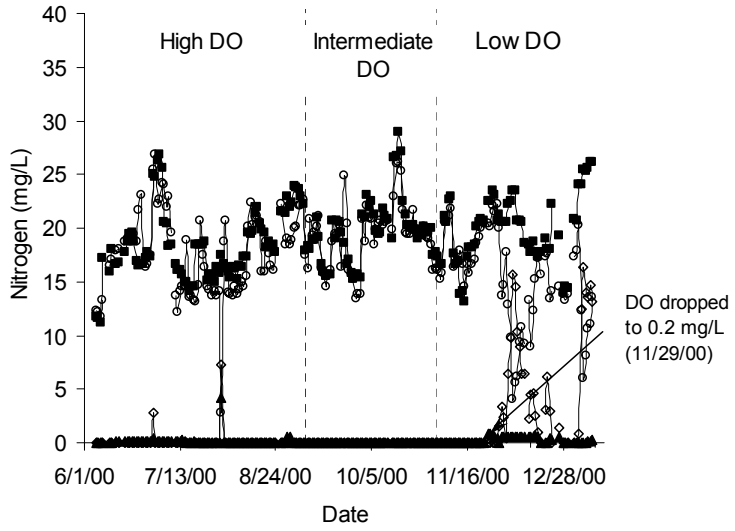

B

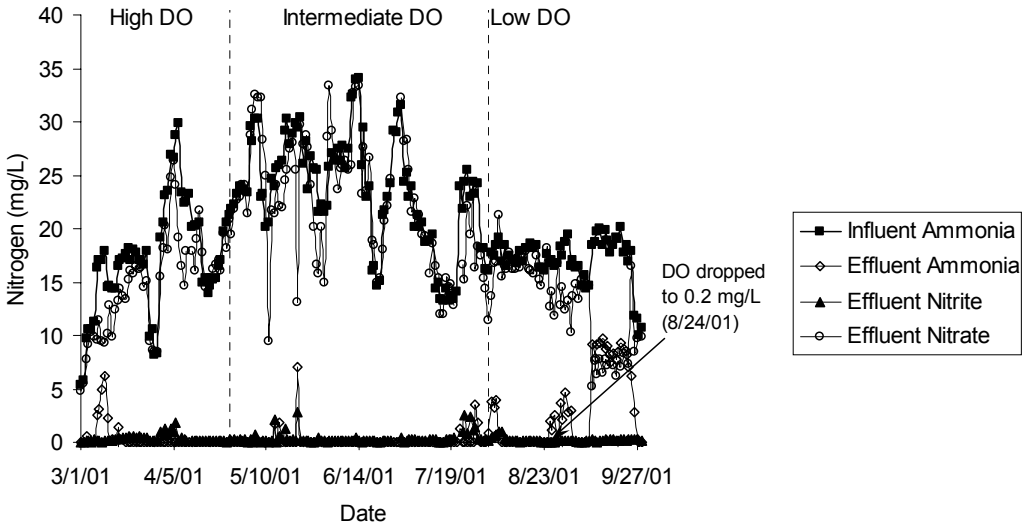

C

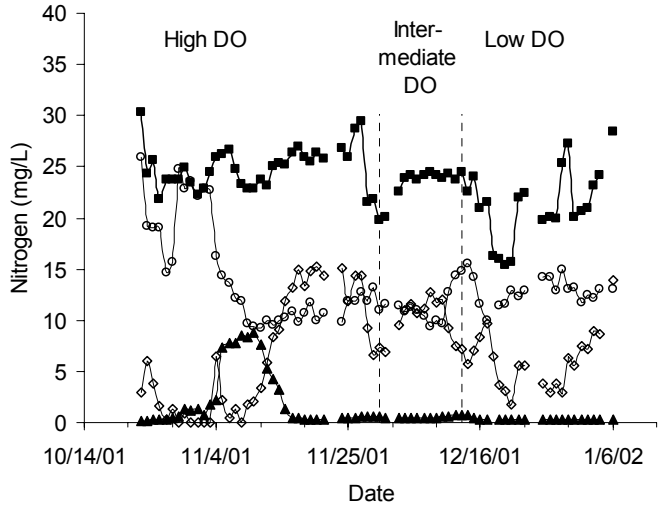

Figure 4-13. 10-day SRT Reactor Nitrogen Results (A) 20°C, (B) 15°C, (C) 10°C

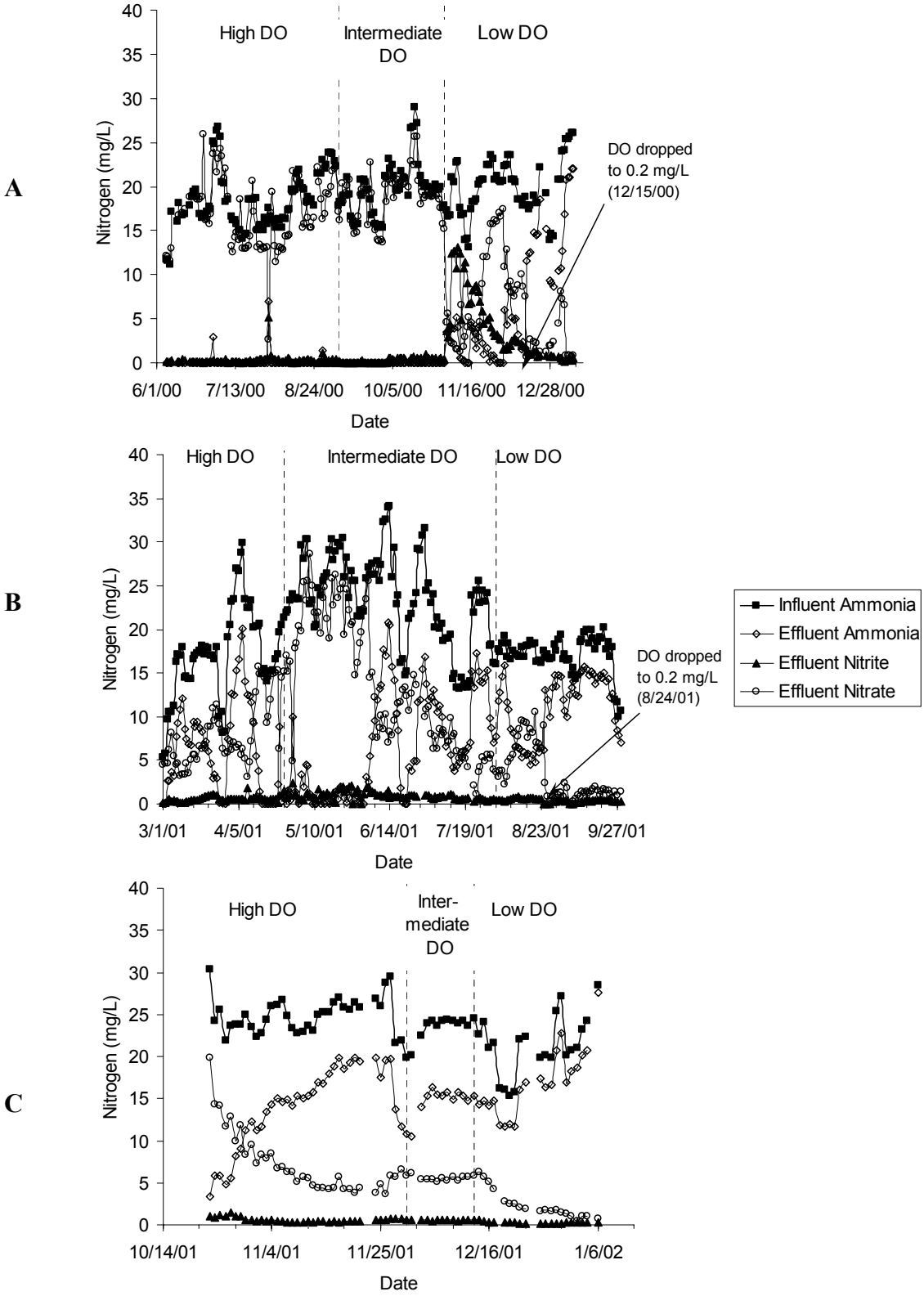

Figure 4-14. 5-day SRT Reactor Nitrogen Results (A) 20°C, (B) 15°C, (C) 10°C

A

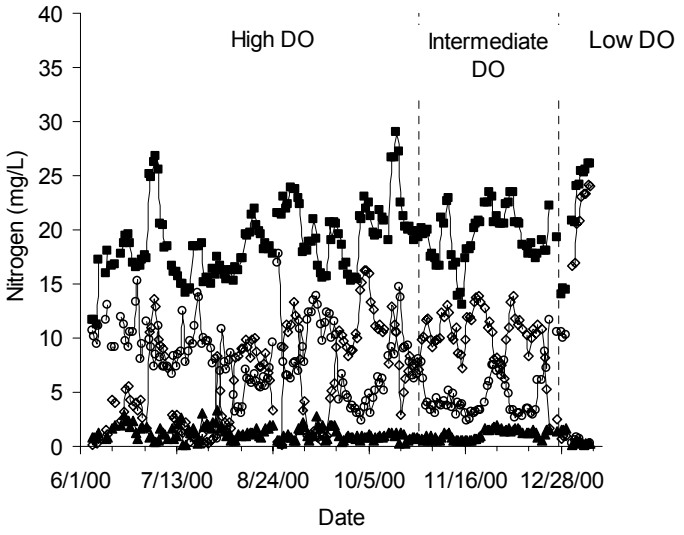

B

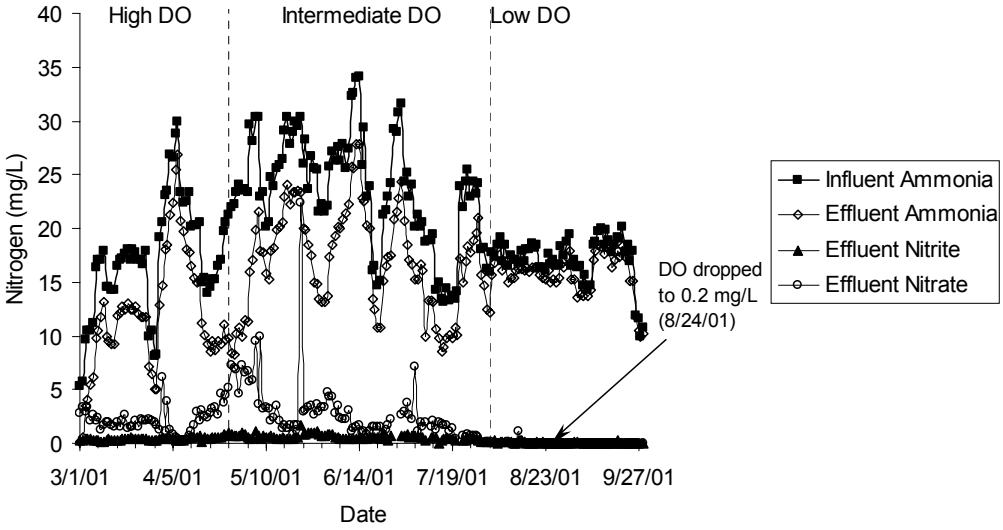

C

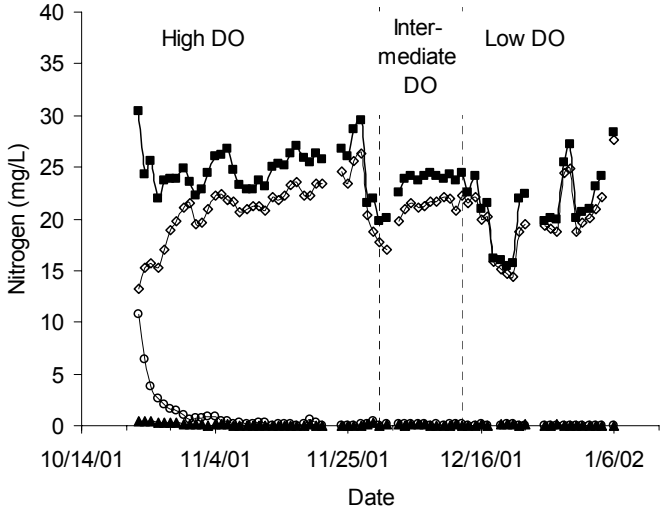

Figure 4-15. 2-day SRT Reactor Nitrogen Results (A) 20°C, (B) 15°C, (C) 10°C

Table 4-17. Average Ammonia Oxidation During Operation at 20°C

DO Level	Parameter	20 day	10 day	5 day	2 day	Influent
High	Avg. NH_4^+ (mg N /L)	0.2 (±1.0)	0.1 (±0.8)	0.1 (±0.8)	6 (±4)	18 (±3)
	NH_4^+Oxidation Rate (mg N/L/day)	46 (±13)	47 (±13)	46 (±13)	26 (±10)	n/a
	NH_4^+ Oxidation Efficiency (%)	99 (±6)%	99 (±6)%	99 (±5)%	64 (±24)%	n/a
Intermediate	Avg. NH_4^+ (mg N /L)	0.0 (±0.0)	0.0 (±0.0)	0.0 (±0.0)	11 (±2)	20 (±3)
	NH_4^+Oxidation Rate (mg N/L/day)	52 (±10)	52 (±11)	51 (±10)	14 (±6)	n/a
	NH_4^+ Oxidation Efficiency (%)	100 (±0)%	100 (±0)%	100 (±0)%	34 (±10)%	n/a
Low	Avg. NH_4^+ (mg N /L)	1 (±3)	3 (±5)	7 (±7)	21 (±3)	20 (±3)
	NH_4^+Oxidation Rate (mg N/L/day)	44 (±17)	39 (±17)	25 (±17)	2 (±1)	n/a
	NH_4^+ Oxidation Efficiency (%)	93 (±14)%	84 (±23)%	62 (±34)%	3 (±2)%	n/a

Ammonia removal did not decline in the 5-day SRT reactor until the DO level was lowered to 0.5 mg/L on November 2, 2000, and in the 20- and 10-day SRT reactors until the DO concentration was decreased to 0.2 mg/L on November 29, 2000. Prior to these changes in operating conditions, there were only a few occasions when ammonia was present in the effluent of these reactors. The first resulted from a spike in the ammonia concentration (from 17.4 to 25.1 mg/L as N) on July 1, 2000, which temporarily affected ammonia removal in all reactors. A second incident occurred on July 31, 2000, when a surfactant material passed through the system and also disrupted COD removal efficiency as previously discussed. Ammonia was also discharged during the time period of August 29 to 31, 2000, when the installation of improper tubing resulted in decreased solids concentration.

Once the reactor DO concentration was dropped to 0.2 mg/L, complete ammonia removal was no longer consistently achieved at SRTs of 20 and 10 days as evidenced by the routine presence of ammonia in the effluent of these reactors (Figures 4-12A, 4-13A). A considerable decrease in average ammonia oxidation rate was observed at an SRT of 5 days during the low DO period (November 3, 2000 to January 10, 2001). When operated at a DO concentration of 0.2 mg/L (January 6 to January 10, 2001) near complete nitrification failure occurred in this reactor (Figure 4-14A). Multiple linear regression analysis was performed on the data from the 20-, 10-, and 5-day SRT reactors obtained during operation at all three DO levels and indicated that both the DO level and influent ammonia concentration significantly impacted the ammonia oxidation rate at a 95% confidence interval. Since DO level did not significantly impact ammonia oxidation rate at these SRTs when only the high and intermediate DO levels were considered, this result suggests that DO levels less than or equal to 0.5 mg/L negatively impacted ammonia oxidation rate at 20ºC.

Nitrification performance at an SRT of 2 days was significantly poorer than at the higher SRTs, as evidenced by the much lower ammonia oxidation rates in this reactor throughout the 20°C study (Table 4-17). Ammonia oxidation in the 2-day SRT reactor was also found to decrease with decreasing DO level (Table 4-17). Multiple linear

regression analysis of only the 2-day SRT reactor data showed that DO level significantly influenced the ammonia oxidation rate at a 95% confidence interval.

Near complete ammonia removal appears to have occurred at an SRT of 2 days from December 23, 2000 to January 1, 2001 (Figure 4-15A); however these results were attributed to a malfunction in the DO control system (Parker, 2001). This time period was excluded from the calculations of ammonia oxidation rate. During the short time period this reactor was operated at a DO of 0.5 mg/L (December 28, 2000 to January 10, 2001), with the exception of the above mentioned anomaly, complete nitrification failure occurred (Figure 4-15A).

During operation at the low DO level, SRT was found to have a statistically significant impact on ammonia oxidation rate at a 95% confidence interval based on multiple linear regression analysis. As expected, the impact of DO was found to decrease as SRT increased.

The results of the 20°C study are similar to those reported in the literature. Hanaki et al. (1990) observed complete nitrification in laboratory CSTRs treating a synthetic waste with influent ammonia levels of 80 mg/L when operated at an SRT of 3.8 days. When the SRT was reduced to 1.5 days, ammonia oxidation efficiency decreased to 60%. McClintock et al. (1993) also reported decreased nitrification performance at an SRT of 1.5 days in their study using a pilot-scale activated sludge system treating domestic wastewater. The influent ammonia levels ranged from 16-30 mg/L, which are comparable to the levels measured in this study. McClintock et al. (1993) observed complete nitrification at SRTs greater than or equal to 2.7 days, while operation at an SRT of 1.5 days resulted in only 79% nitrification. Stenstrom and Poduska (1980) also reported that nitrification could be achieved at low DO concentrations when the SRT was high, but higher DO concentrations were required for low SRT values. The results of the current study support that conclusion with nitrification in the 5-day and 2-day SRT reactors being affected by low DO to a much greater extent than in the 20- and 10-day reactors.

15°C Operation

Figures 4-12B through 4-15B show the influent and effluent nitrogen concentrations at each DO operational phase during the 15°C study for the 20-, 10-, 5-, and 2-day SRT reactors, respectively. As shown in these figures, the influent ammonia concentration fluctuated during this treatment study more so than during the 20°C and 10°C studies. Average ammonia concentrations and ammonia oxidation rates and efficiencies are listed in Table 4-18. Comparison of Tables 4-17 and 4-18 shows that the temperature drop from 20°C to 15°C did not appear to negatively impact ammonia oxidation rates in the 20- and 10-day SRT reactors, however, the average ammonia oxidation rates in the 5-day and 2-day reactors were significantly lower at 15°C than at 20°C.

Efficient ammonia removal occurred in the 20-day SRT reactor throughout the high and intermediate DO operating periods at 15°C (Figure 4-12B). Ammonia was present in the effluent from this reactor on only two occasions, both of which were associated with large increases in influent ammonia level. Following the decrease in DO concentration to 0.2 mg/L on August 24, 2001, ammonia was discharged from the 20-day SRT reactor several times, however, the average rate of ammonia oxidation remained high during this time period. The average ammonia oxidation rate in the 20-day SRT reactor appeared to be unaffected by changes in DO concentration (Table 4-18). The ammonia oxidation rate was found to increase in all reactors during the intermediate DO level, which corresponded to an increase in the influent ammonia level.

Ammonia removal in the 10-day SRT reactor was similar to that of the 20-day reactor during operation at the high and intermediate DO levels, however, there were four episodes in which effluent ammonia was discharged from this reactor in response to fluctuations in influent ammonia concentration (Figure 4-13B). The recovery time for the 20-day SRT reactor following a spike in the influent ammonia level was generally only 1 day, while the it was generally several days for the 10-day SRT. Once the DO level in the reactors was decreased to a concentration of 0.2 mg/L, ammonia removal was inconsistent in this reactor. The average ammonia oxidation rates in the 10-day SRT reactor were similar to those observed in the 20-day SRT reactor during the high and

Table 4-18. Average Ammonia Oxidation During Operation at 15°C

DO Level	Parameter	20 day	10 day	5 day	2 day	Influent
High	Avg. NH_4^+ (mg N /L)	0.2 (±1.1)	0.4 (±1.2)	6 (±5)	12 (±6)	17 (±5)
	NH_4^+Oxidation Rate (mg N/L/day)	43 (±17)	40 (±14)	23 (±10)	7 (±3)	n/a
	NH_4^+ Oxidation Efficiency (%)	99 (±3)%	97 (±8)%	61 (±28)%	22 (±17)%	n/a
Intermediate	Avg. NH_4^+ (mg N /L)	0.0 (±0.0)	0.2 (±0.9)	6 (±6)	17 (±5)	24 (±5)
	NH_4^+Oxidation Rate (mg N/L/day)	64 (±16)	62 (±16)	41 (±21)	10 (±8)	n/a
	NH_4^+ Oxidation Efficiency (%)	100 (±0)%	98 (±11)%	65 (±32)%	16 (±12)%	n/a
Low	Avg. NH_4^+ (mg N /L)	0.2 (±0.9)	3 (±4)	11 (±4)	16 (±2)	17 (±2)
	NH_4^+Oxidation Rate (mg N/L/day)	47 (±8)	36 (±11)	10 (±9)	0.2 (±0.5)	n/a
	NH_4^+ Oxidation Efficiency (%)	99 (±6)%	82 (±23)%	24 (±22)%	0.5 (±1.1)%	n/a

intermediate DO levels, however, during the low DO level, a slight decrease in oxidation rate was noted.

Figure 4-14B shows that ammonia treatment performance at 15°C in the 5-day SRT system was significantly poorer than that of the higher SRT systems. The effluent ammonia concentration mimicked the influent concentration throughout all phases of the experiment, allowing for higher ammonia removal at lower influent concentrations. One exception to this occurred in the 5-day SRT reactor during the intermediate DO phase at 15°C. For approximately 26 days, ammonia oxidation was very high even at high ammonia loading. This time period corresponded to the passage of the ink-like material through the system previously discussed. The decrease in DO from 0.5 mg/L to 0.2 mg/L greatly impacted ammonia removal in the 5-day SRT reactor resulting in almost no ammonia oxidation during this time period (Figure 4-14B). At the high and intermediate DO levels, the ammonia oxidation rate in the 5-day SRT reactor was lower than the rates observed at SRTs of 20 and 10 days by approximately 20 mg N/L/day, and this discrepancy increased at the low DO level (Table 4-18).

Nitrification performance in the 2-day SRT reactor was poor throughout the 15°C, and failed completely at the low DO level. Average ammonia oxidation rates in this reactor were quite low during the high and intermediate DO levels (7 and 10 mg N/L/ day, respectively) and approached zero at the low DO level.

The multiple linear regression model developed for the measured 15°C ammonia oxidation rates fit the experimental data quite well, as indicated by a correlation coefficient of 0.85, compared to 0.56 for the 20°C data. Seventy-three percent of the observed variability in the ammonia oxidation rate was attributed to changes in SRT, DO, and influent ammonia concentration. All of these variables were found to significantly affect ammonia oxidation rates at a 95% confidence level. Analysis of the standardized partial regression coefficients indicated that the impact of SRT on ammonia oxidation rate was greater than that of DO by a factor of 2 and influent ammonia concentration by a factor of 3, and all three variables were found to be positively correlated. Certainly, in practice, the influent ammonia concentration would not be adjusted to increase ammonia oxidation, however, the SRT and DO levels are operational parameters that are frequently

manipulated to improve process performance. The results of this linear regression analysis show that both the DO and SRT could be adjusted at 15°C to increase ammonia oxidation (up to a point). This suggests that trade-offs between the two parameters could be managed to yield maximum performance at minimum cost.

A significant interaction between the DO level and SRT was observed in the model and additional analyses showed that the influence of SRT on ammonia oxidation rate increased as the DO level decreased. This indicated that at the low DO level an increase in SRT would yield a greater response than at the higher DO level. DO concentration was found not to have a significant effect at an SRT of 20 days, however, for SRTs less than or equal to 10 days, the impact of DO on ammonia oxidation rate was found to increase as SRT decreased.

10°C Operation

Influent and effluent nitrogen concentrations are shown in Figures 4-12C through 4-15C at each DO operational phase during the 10°C study for the 20-, 10-, 5-, and 2-day SRT reactors, respectively. When the temperature was dropped to 10°C, ammonia was detected in the effluent of the 20-day SRT system during the first week, but complete nitrification was regained thereafter as shown in Figure 4-12C. In contrast, complete nitrification was not achieved in the 10-day SRT reactor at any time during the 10°C study, and steady-state (with respect to ammonia oxidation) was not reached until approximately 28 days after the temperature was dropped to 10°C. Efficient nitrification was not achieved in the 5- and 2-day SRT reactors following the decrease in temperature from 15°C to 10°C, and a substantially higher amount of ammonia was discharged from these reactors at the low temperature (Table 4-19).

The average ammonia oxidation rates in the 20-day SRT reactor during this portion of the study were similar to those observed at the higher temperatures and DO was not shown to affect ammonia oxidation at this SRT. The average rate of ammonia oxidation incrementally decreased with decreasing SRT at all DO levels. In the 5-day SRT reactor, ammonia oxidation also decreased with decreasing DO. Nitrification failure was observed in the 2-day SRT reactor throughout the low temperature study.

Table 4-19. Average Ammonia Oxidation During Operation at 10°C

DO Level	Parameter	20 day	10 day	5 day	2 day	Influent
High	Avg. NH_4^+ (mg N /L)	0.2 (±0.8)	6 (±6)	14 (±5)	21 (±3)	25 (±2)
	NH_4^+Oxidation Rate (mg N/L/day)	66 (±8)	46 (±14)	21 (±11)	3 (±6)	n/a
	NH_4^+ Oxidation Efficiency (%)	99 (±3)%	74 (±23)%	37 (±19)%	5 (±9)%	n/a
Intermediate	Avg. NH_4^+ (mg N /L)	0.0 (±0.0)	10 (±2)	15 (±2)	21 (±2)	23 (±2)
	NH_4^+Oxidation Rate (mg N/L/day)	63 (±9)	32 (±4)	17 (±1)	0.6 (±0.4)	n/a
	NH_4^+ Oxidation Efficiency (%)	100 (±0)%	54 (±8)%	30 (±4)%	1.0 (±0.7)%	n/a
Low	Avg. NH_4^+ (mg N /L)	0.1 (±0.5)	6 (±3)	17 (±4)	20 (±3)	21 (±4)
	NH_4^+Oxidation Rate (mg N/L/day)	55 (±8)	36 (±4)	8 (±5)	0.2 (±0.3)	n/a
	NH_4^+ Oxidation Efficiency (%)	99 (±6)%	69 (±11)%	14 (±9)%	0.5 (±0.6)%	n/a

The multiple linear regression model developed for 10°C ammonia oxidation rate data described the measured values very well (R = 0.981) and showed that 96.2% of the observed variability in this parameter could be explained by changes in SRT, DO, influent ammonia, and the combined effects of SRT and DO. Both SRT and DO were found to significantly impact the ammonia oxidation rate, with SRT yielding the largest relative influence. A significant interaction between the DO and SRT was observed in the model, and in contrast to the 15°C data, the influence of SRT on ammonia oxidation rate was found to decrease slightly as the DO decreased. This may suggest that the negative impact of low DO on ammonia oxidation rate is compounded by the low temperature and cannot be counteracted by SRT as effectively as at the higher temperature.

Comparison of Data from All Three Temperatures

Linear regression analysis performed on all of the data from the 20°C, 15°C, and 10°C operating periods showed that 62.3% of the observed variability in ammonia oxidation rate could be explained by changes in the SRT, temperature, DO, and influent ammonia. All four of these variables were found to significantly affect ammonia oxidation rate at a 95% confidence interval. Comparison of the magnitude of the partial regression coefficients indicated that SRT had the largest impact on ammonia oxidation rate, nearly three times that of temperature, and four times that of the influent ammonia and DO concentrations. While the temperature and influent ammonia concentration generally cannot be controlled in full-scale WWTPs, the SRT and DO can be adjusted to compensate for low temperatures. These results indicated that small improvements to ammonia oxidation rate could be achieved by increasing the DO level, however, increasing the SRT would result in a much greater impact on nitrification performance.

These findings of this study are supported by reports in the literature. Cheremisinoff (1996) concluded that SRT was the single most important factor in determining whether or not a wastewater treatment system will support nitrification. Reports by Hanaki et al. (1990) and McClintock et al. (1993) provide evidence to support this statement as discussed previously. Multiple linear regression analyses performed in the current study showed SRT to have the greatest impact on ammonia oxidation rate at

20°C, 15°C, and 10°C, as well as when all three temperatures were considered. The results of this study are also consistent with the finding that nitrification can be achieved at low DO concentrations when the SRT is high, but higher DO concentrations were required for low SRT values (Stenstrom and Poduska, 1980). Under all temperatures in this study, ammonia oxidation in the 5-day and 2-day SRT reactors was affected by low DO to a much greater extent than the 20- and 10-day reactors.

Several researchers have demonstrated the negative impact of decreased temperature on nitrification rates and the necessity of increasing the SRT to compensate for these effects. Wild et al. (1971) concluded that it might be necessary to increase the SRT by up to 5 to accomplish complete nitrification at colder temperatures. McClintock et al. (1993) observed complete nitrification at an SRT of 15 days and temperatures of 20°, 15°, and 10°C, with ammonia oxidation rates of 64, 80, and 68 mg N/L/day, respectively. In contrast, at an SRT of 5 days complete nitrification was observed at 20°C and 15°C, while at 10°C, only 65% conversion of ammonia-N to nitrate-N was observed. The ammonia oxidation rates measured for the 5-day SRT reactor by McClintock et al. (1993) were 80, 78, and 45 mg N/L/day at temperatures of 20°, 15°, and 10°C, respectively. Ydestebo et al. (2000) found that in order to maintain efficient nitrification it was necessary to increase the aerobic SRT in their BNR system from 4 days at 15°C to 14 days at 6°C. In the current study, complete ammonia oxidation occurred at an SRT of 5 days at 20°C at the high and intermediate DO levels, while at 15°C, an SRT greater than 5 days was required. When the temperature was dropped to 10°C, an SRT of greater than 10 days was required to achieve high rates of ammonia oxidation. Thus, the results of this study agree with the literature finding that while the rate of nitrification slows as temperature decreases, the effects can be overcome, to a considerable degree, by increasing the SRT in the activated sludge system.

4.4.2 *Nitrosomonas oligotropha*-type AOB Concentration

Concentrations of *N. oligotropha*-type AOB were calculated from real-time PCR data assuming that *N. oligotropha*-type AOB have 2 copies of the *amo*A gene per cell

(McTavish et al.,1993).

20°C Operation

Table 4-20 lists the average *N. oligotropha*-type AOB concentrations at each SRT and DO level for the 20°C study, which are somewhat lower than those reported in the literature. Harms et al. (2003) and Dionisi et al. (2002a) measured the cell density of *N. oligotropha*-type AOB in twelve monthly mixed liquor samples taken from the full-scale municipal WWTP from which the influent waste for this study was collected. The average concentration of in this plant was reported to be 7.5 (±6.0) x 10^9 cells/L by Harms et al. (2003) using the same real-time PCR assay used in the current study. Dionisi et al. (2002a) used a cPCR assay and reported lower values of 4.3 (±0.6) x 10^7 to 4.1 (±1.3) x 10^8 *N. oligotropha*-type AOB cells/L. Daims et al. (2001) measured an average AOB cell density of 9.8 (±1.9) x 10^{10} cells/L in a separate stage nitrifying municipal WWTP using FISH. Lee et al. (2002) reported 1.18 x 10^{11} AOB cells/L measured by performing colony counts on samples taken from a bench-scale activated sludge reactor operated at 20°C, excess DO, an SRT of 10 days, and a C/N ratio of 12.5, which is comparable to the average value for the current study. Wagner et al. (1996) observed a similar average ammonia-oxidizer concentration of 6.6 (±0.3) x 10^{11} cells/L mixed liquor based on FISH measurements. However, this value was obtained at an industrial WWTP that receives sewage with ammonia concentrations 2 orders of magnitude higher than those measured in this study.

Table 4-20. Average *N. oligotropha*-type AOB Concentrations (cells/L) During Operation at 20°C

DO Level	High	Intermediate	Low
20-Day SRT	3.9 (±4.6) x 10^9	1.3 (±2.1) x 10^9	2.4 (±2.0) x 10^9
10-Day SRT	1.8 (±1.1) x 10^9	5.0 (±1.1) x 10^8	7.4 (±6.7) x 10^8
5-Day SRT	2.5 (±2.3) x 10^8	2.5 (±3.0) x 10^8	5.7 (±8.1) x 10^8
2-Day SRT	7.6 (±3.9) x 10^8	3.7 (±2.9) x 10^8	1.4 (±0.3) x 10^8

DO level did not appear to have a significant effect on the *N. oligotropha*-type AOB population with the exception of the 2-day SRT reactor. Multiple linear regression analyses performed on the data from each SRT individually showed that DO had a statistically significant impact on AOB cell numbers in the 2-day reactor, but not in the 20-, 10-, and 5-day SRT reactors at a 95% confidence interval. This can be seen more clearly in Figure 4-16 which shows a comparison of the trends in ammonia oxidation rate (for the dates when molecular sampling was performed) and *N. oligotropha*-type AOB concentration as a function of SRT and DO at 20°C. As shown in this figure, the rate of ammonia oxidation clearly slows in all four SRT reactors at the lowest DO level; however, this trend was not reflected in the *N. oligotropha*-type AOB concentration in the 20-, 10-, and 5-day SRT reactors. The trends in *N. oligotropha*-type AOB concentration do mirror the trends in ammonia oxidation rate in the 2-day SRT reactor which shows a significant drop in nitrification performance at each DO level.

The multiple linear regression model developed for the 20°C *N. oligotropha*-type AOB concentrations did not describe the data very well (R = 0.59) and showed that only 35% of the variability in the *N. oligotropha*-type AOB cell density could be attributed to changes in the SRT, DO, influent ammonia concentration and the interaction between SRT and DO. SRT, DO, and influent ammonia concentration were found to significantly affect ammonia oxidation rate at a 95% confidence level. The magnitude of the standardized partial regression coefficients revealed that SRT had the largest relative effect on the AOB concentration, followed by the DO, and then influent ammonia concentration.

15°C Operation

Average *N. oligotropha*-type AOB concentrations are shown in Table 4-21 for the 15°C study. Comparison of the data in Tables 4-20 and 4-21 revealed that *N. oligotropha*-type AOB concentrations decreased when the temperature was lowered from 20°C to 15°C. This was true for all SRTs and DO levels with the exception of the 5-day SRT reactor at the high and intermediate DO levels. The other SRT reactors show a decrease of 1 to 10 fold in cell numbers. Multiple linear regression analyses performed on

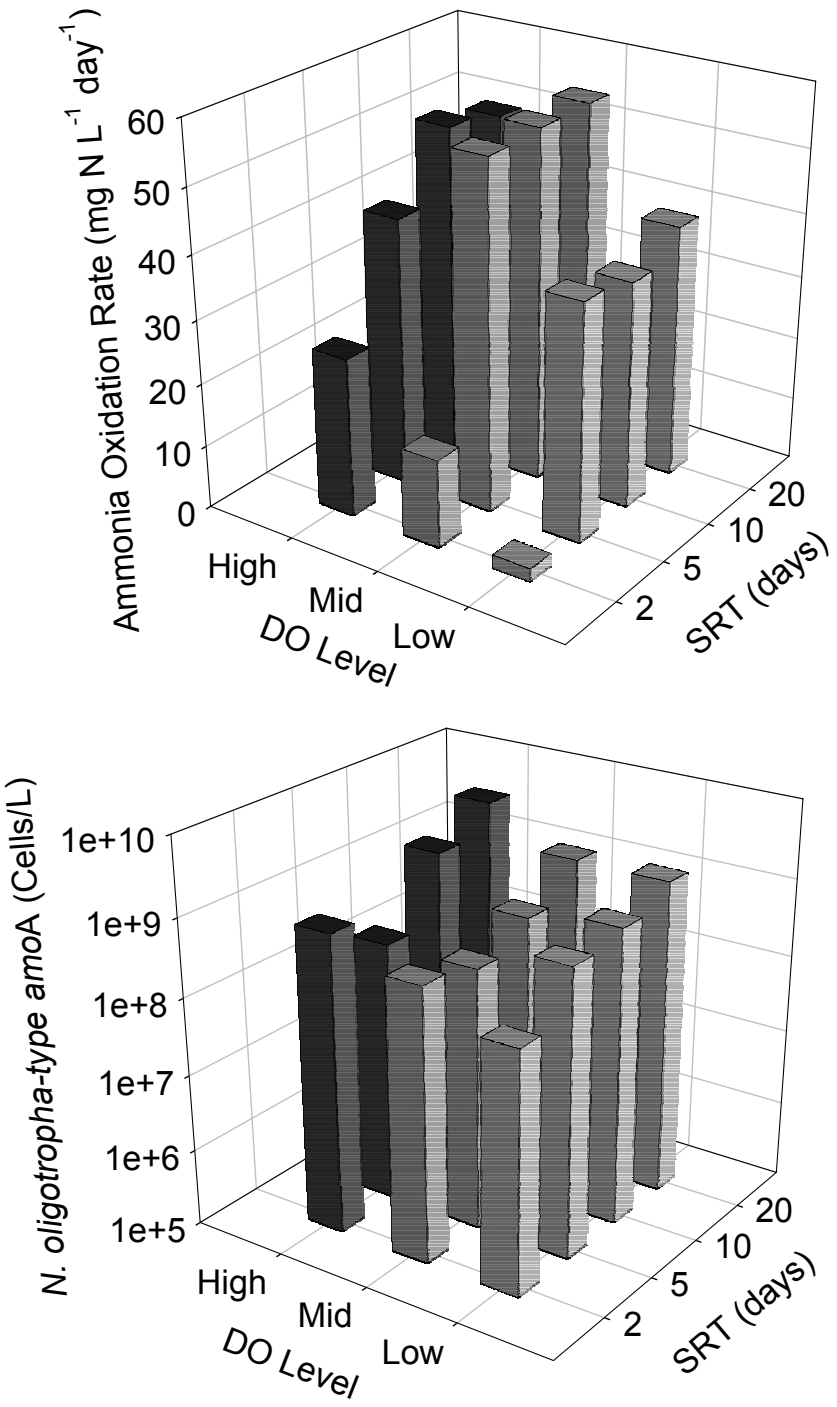

Figure 4-16. Comparison of Trends in Ammonia Oxidation Rate and *N. oligotropha*-type AOB Concentration at Varying SRT and DO Levels at 20°C

Table 4-21. Average *N. oligotropha*-type AOB Concentrations (cells/L) During Operation at 15°C

DO Level	High	Intermediate	Low
20-Day SRT	6.9 (±3.7) x 10^8	4.7 (±1.7) x 10^8	4.1 (±1.7) x 10^8
10-Day SRT	4.1 (±2.2) x 10^8	1.8 (±0.9) x 10^8	4.6 (±2.0) x 10^8
5-Day SRT	6.9 (±6.2) x 10^8	6.2 (±2.6) x 10^8	2.8 (±1.2) x 10^8
2-Day SRT	4.1 (±4.0) x 10^8	3.2 (±1.8) x 10^8	1.4 (±0.8) x 10^7

data taken during operation at 20°C and 15°C for each SRT individually, showed that the effect of the change in temperature significantly impacted the *N. oligotropha*-type AOB concentrations at a 95% confidence interval for the 20-, 10-, and 2-day SRT reactors, but did not significantly affect the 5-day SRT reactor. During operation at the high and intermediate DO levels at 15°C no clear trend was observed in the *N. oligotropha*-type AOB concentration with respect to SRT. At the low DO level, SRT was found to significantly impact the cell density of AOB at a 95% confidence interval according to multiple linear regression analysis. Average *N. oligotropha*-type AOB concentration did decrease with decreasing DO level, except in the 10-day SRT reactor at the low DO level. Inspection of Figure 4-17 revealed that the trends in ammonia oxidation rates were only mirrored by the *N. oligotropha*-type AOB concentrations in the 5- and 2-day SRT reactors.

When the 15°C *N. oligotropha*-type AOB data was described by a multiple linear regression model, only 23% of the observed variability in measured AOB concentrations could be explained by changes in the SRT, DO, influent ammonia concentration and the combined effects of SRT and DO. SRT and DO contributed to the model in a statistically significant manner and again SRT was found to have a larger relative effect on the AOB concentration than the DO.

10°C Operation

The average *N. oligotropha*-type AOB are listed in Table 4-22 for the 10°C study. Inspection of the data in Tables 4-21 and 4-22 shows, again, that as temperature

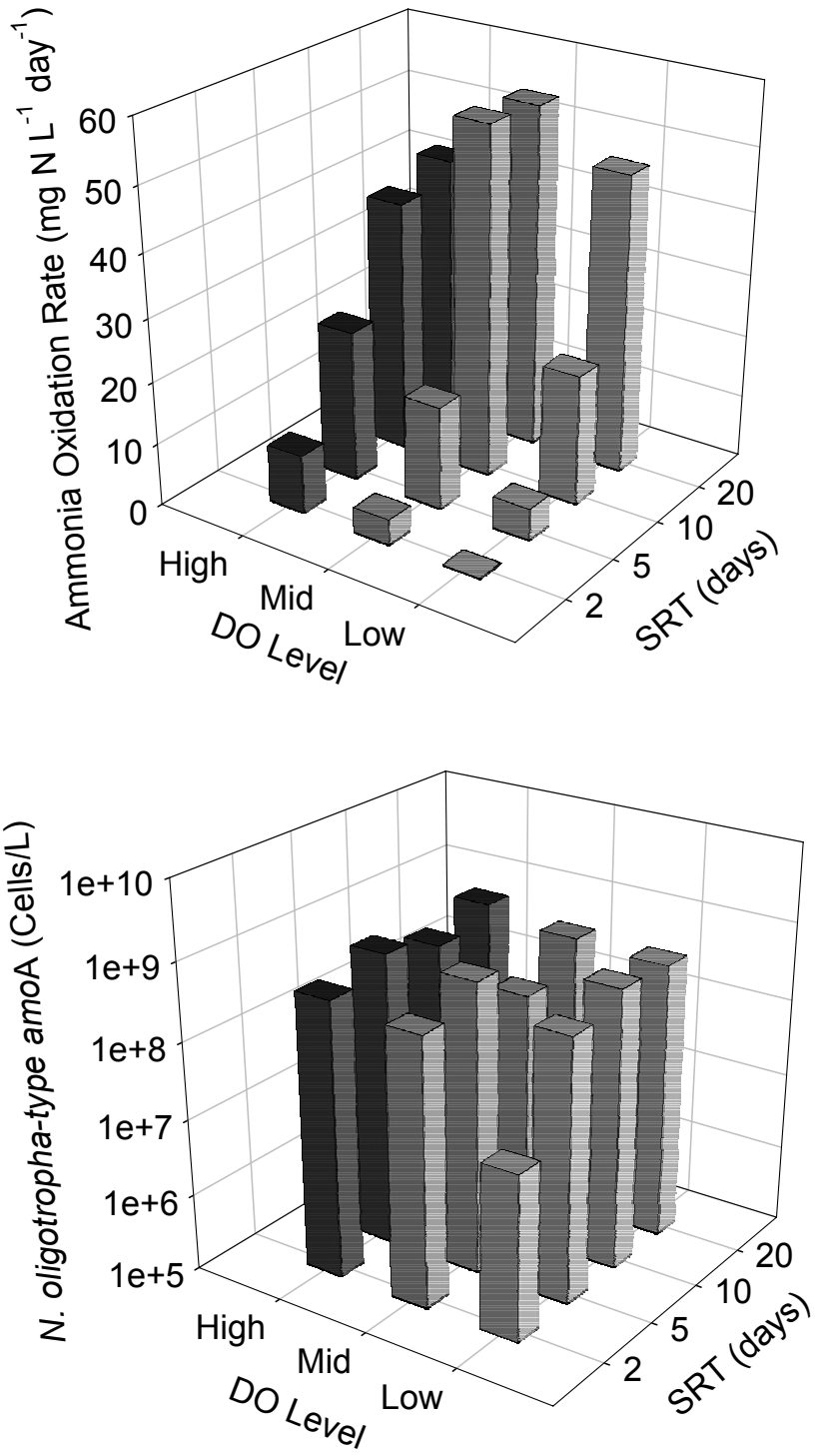

Figure 4-17. Comparison of Trends in Ammonia Oxidation Rate and *N. oligotropha*-type AOB Concentration at Varying SRT and DO Levels at 15°C

Table 4-22. Average *N. oligotropha*-type AOB Concentrations (cells/L) During Operation at 10°C

DO Level	High	Intermediate	Low
20-Day SRT	4.1 (±1.8) x 10^8	1.2 (±2.2) x 10^8	7.8 (±7.9) x 10^7
10-Day SRT	9.1 (±5.2) x 10^7	1.9 (±1.5) x 10^8	2.5 (±0.9) x 10^9
5-Day SRT	3.9 (±2.3) x 10^7	7.8 (±2.9) x 10^7	1.8 (±0.8) x 10^8
2-Day SRT	1.3 (±1.2) x 10^{6*}	2.3 (±2.7) x 10^{6*}	2.5 (±2.0) x 10^{6*}

*Two of the five samples for each of these operating periods were the detection limit of the real-time PCR assay of 5.0 x 10^5 cells/L.

decreased the concentration of *N. oligotropha*-type AOB also decreased. This can be seen in all SRT reactors at all DO levels with the exception of the 10-day SRT reactor at the intermediate and low DO levels. Multiple linear regression analyses performed on data obtained during operation at 15°C and 10°C data for each SRT individually showed that the temperature drop significantly affected AOB cell densities in the 20-, 5-, and 2-day SRT reactors at a 95% confidence level, but was not found to be the case for the 10-day SRT reactor. In general, the *N. oligotropha*-type AOB concentration decreased with decreasing SRT, with the exception of the 20-day SRT reactor at the low DO level. In the 20-day SRT, the concentration of *N. oligotropha*-type AOB, decreased with decreasing DO, while the opposite trend is observed in the 10-, 5-, and 2-day SRT reactors. These trends can be seen more clearly in Figure 4-18. This plot shows that a slight decrease in ammonia oxidation rate occurred in the 20-day SRT reactor, which corresponded to the decrease in *N. oligotropha*-type AOB level in this reactor. Interestingly, ammonia oxidation rates in the 10-day SRT reactor actually increased when the DO level was lowered and the *N. oligotropha*-type AOB levels obtained from real-time PCR do reflect this trend. The 2-day SRT reactor was at complete nitrification failure throughout the course of the 10°C treatment study and this was reflected in a fairly stable *N. oligotropha*-type AOB concentration of approximately 2 x 10^6 cells/L, which was over two orders of magnitude lower than the concentration observed when nitrification was occurring in this reactor. Figure 4-18 also shows that ammonia oxidation rates followed the same general trend as the *N. oligotropha*-type AOB concentration with the rate

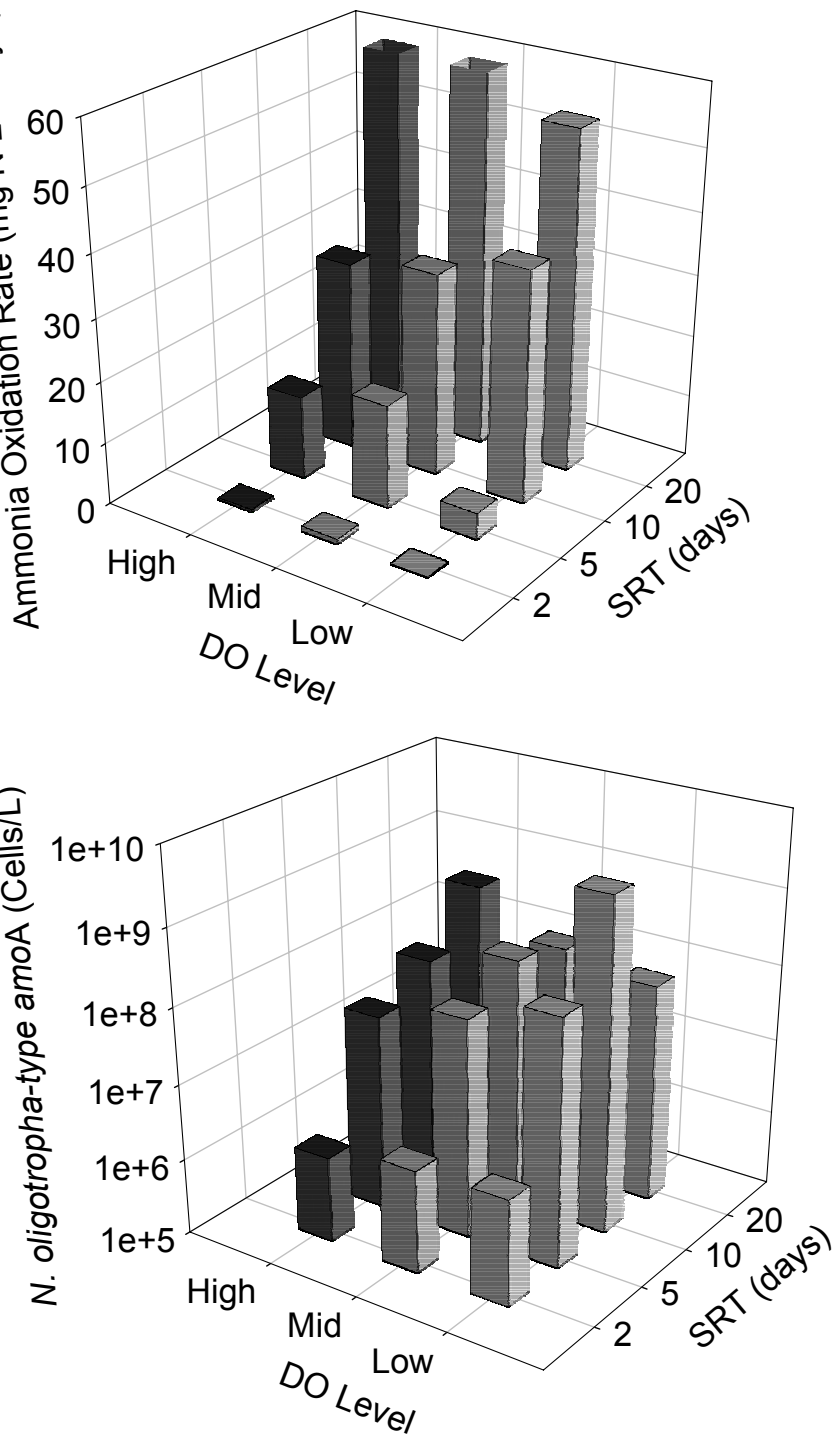

Figure 4-18. Comparison of Trends in Ammonia Oxidation Rate and *N. oligotropha*-type AOB Concentration at Varying SRT and DO Levels at 10°C

decreasing as SRT decreases and no consistent correlation between oxidation rate and DO level.

According to multiple linear regression analysis performed on the measured *N. oligotropha*-type AOB concentrations during 10°C operation, only 24% of the variability observed in *N. oligotropha*-type AOB concentration could be attributed to changes in the SRT, DO, and influent ammonia concentration. Of the controlled variables, only the SRT was found to significantly affect the *N. oligotropha*-type AOB cell density at a 95% confidence level.

Comparison of Data from All Three Temperatures

When data from all operational conditions were included in the linear regression model, only 18% of the observed variability in *N. oligotropha*-type AOB concentration could be explained by changes in the SRT, temperature, DO, and influent ammonia. Only SRT and temperature were found to significantly impact the concentration of *N. oligotropha*-type AOB, with little difference between the relative effects of the two parameters.

Table 4-23 lists the correlation coefficients and R^2 values obtained from the linear regression analyses performed on the ammonia oxidation rate and *N. oligotropha*-type AOB data when all variables and compound effects of variables were included in the analyses. This data shows that multiple linear regression models could better describe ammonia oxidation rates and more of the variability in measured values could be attributed to controlled parameters than for the *N. oligotropha*-type AOB concentrations. A likely explanation for this is that the real-time PCR assay only measured a subset of the

Table 4-23. Summary of Linear Regression Analyses for Ammonia Oxidation Rate and *N. oligotropha*-type AOB Concentrations

	Ammonia Oxidation Rate		Log *N. oligotropha*-type AOB	
Temperature	R	R^2	R	R^2
All	0.850	0.722	0.678	0.460
20°C	0.563	0.317	0.590	0.349
15°C	0.854	0.730	0.480	0.230
10°C	0.981	0.962	0.533	0.283

population and population shifts could occur due to changes in operating and environmental conditions. Therefore, organisms that are not being measured could significantly contribute to the removal of substrate.

4.4.3 Comparison of Ammonia Oxidation and AOB Concentrations

Attempts were made to compare the percentage of AOB measured in the reactors using real-time PCR for the *N. oligotropha*-type *amo*A gene and theoretical values estimated from design equations using typical kinetic parameters. The percentages of AOB measured in the reactors using real-time PCR were computed by dividing the *N. oligotropha*-type AOB concentration (cells/L) by the total eubacterial 16S concentration (cells/L) for the steady-state samples noted in Tables 4-4, 4-5, and 4-6. The theoretical values were calculated using the approach outlined in Rittmann and McCarty (2001). For the theoretical approach, the volatile suspended solids (VSS) production rates for all types of biomass (heterotrophs and ammonia-oxidizers) were computed according the following equation.

$$\frac{\Delta X_v}{\Delta t} = Q\left(S^o - S\right)Y\frac{1+\left(1-f_d\right)b\theta_x}{1+b\theta_x} \qquad (4\text{-}2)$$

where: $\frac{\Delta X_v}{\Delta t}$ = volatile suspended solids production rate (mg VSS/day)
Q = hydraulic flow rate (L/day)
S^o = influent substrate concentration (mg/L)
S = effluent substrate concentration (mg/L)
Y = true yield (mg/mg)
f_d = biodegradable fraction (unitless)
b = endogenous decay coefficient
θ_x = solids retention time (days)

The percentage of AOB was then estimated by taking the ratio of the VSS production rate for ammonia-oxidizers to the total biomass produced. A sample calculation is provided in Appendix B. Average influent and effluent parameters taken during steady-state operating periods corresponding to the times when molecular

sampling was performed were used in the calculations and are listed in Table 4-24 and Table 4-25, respectively. BOD values were estimated from COD values according to the following equation (Grady et al. 1999):

$$COD_T = 2.1(BOD_5) \quad (4\text{-}3)$$

where: COD_T = total COD (mg/L)
BOD_5 = five day biological oxygen demand (mg/L)

Typical kinetic parameters used in the calculations were taken from Rittmann and McCarty (2001) and are summarized in Tables 4-26 and 4-27 for heterotrophs and ammonia-oxidizers, respectively, as a function of temperature. Table 4-28 provides a comparison of the percentage of AOB measured in the reactors using real-time PCR for the *N. oligotropha*-type *amo*A gene and theoretical values estimated from design equations using typical kinetic parameters. The values measured using PCR are much lower than the theoretically predicted values. The extremely low percentage of ammonia oxidizers measured in this study suggests that AOB other than *N. oligotropha*-type were dominant in the bench-scale system. *N. oligotropha* was the only AOB identified in mixed liquor samples from the full-scale municipal WWTP and bench-scale reactors at the beginning of this study. However, since multiple AOB exist (at least 15 strains) (Purkhold et al., 2000), additional work is necessary to identify all of the major AOB species present in the reactors.

In addition to the measured percentages of AOB in the current study being much lower than the calculated values, they are also significantly lower than those reported in the literature. You et al. (2003) reported that *Nitrosospira*, which was identified as the sole ammonia-oxidizer in an A20 pilot plant BNR system, accounted for 4.1% of the total biomass measured using a cloning-denaturing gradient gel electrophoresis (DGGE) method. The A20 system, which contains anaerobic, anoxic, and aerobic phases to carry out carbon, nitrogen, and phosphorous removal, was operated at 20°C and an SRT of 10 days and used to treat synthetic wastewater with an influent concentration COD of 300 mg/L and an influent total nitrogen concentration of 40 mg/L. In this same study, the

Table 4-24. Average Steady-state Influent Parameters During High DO Operation

Temperature	SRT (days)	20	10	5	2
20ºC	COD (mg COD/L)	215	220	185	236
	BOD (mg BOD/L)	102	105	88	112
	NH^+_4-N (mg NH^+_4-N/L)	19	21	19	21
15ºC	COD (mg COD/L)	141	184	184	191
	BOD (mg BOD/L)	67	88	88	91
	NH^+_4-N (mg NH^+_4-N/L)	16	18	18	16
10ºC	COD (mg COD/L)	No steady-state data	174	174	174
	BOD (mg BOD/L)	No steady-state data	83	83	83
	NH^+_4-N (mg NH^+_4-N/L)	No steady-state data	27	27	27

Table 4-25. Average Steady-state Effluent Parameters During High DO Operation

Temperature	SRT (days)	20	10	5	2
20ºC	COD (mg COD/L)	27	23	29	33
	BOD (mg BOD/L)	13	11	14	16
	NH^+_4-N (mg NH^+_4-N/L)	0	0	0	8.3
	NO^-_2-N (mg NH^+_4-N/L)	0	0	0	1.3
15ºC	COD (mg COD/L)	26	30	33	38
	BOD (mg BOD/L)	12	14	16	18
	NH^+_4-N (mg NH^+_4-N/L)	0	0	5	11
	NO^-_2-N (mg NH^+_4-N/L)	0.21	0.34	0.35	0.39
10ºC	COD (mg COD/L)	No steady-state data	35	41	43
	BOD (mg BOD/L)	No steady-state data	17	20	20
	NH^+_4-N (mg NH^+_4-N/L)	No steady-state data	15	20	24
	NO^-_2-N (mg NH^+_4-N/L)	No steady-state data	0.4	0.5	0.01

Table 4-26. Typical Kinetic Parameters for Heterotrophs (Adapted from Rittmann and McCarty, 2001)

Parameter	20°C	15°C	10°C
Y (mg VSS/mg BOD)	0.45	0.45	0.45
$\hat{q}$ (mg BOD/mg VSS-d)	20	14.3	10.2
K (mg BOD/L)	10	10	10
b ($days^{-1}$)	0.15	0.11	0.076

Table 4-27. Typical Kinetic Parameters for Ammonia-Oxidizers (Adapted from Rittmann and McCarty, 2001)

Parameter	20°C	15°C	10°C
Y (mg VSS/mg NH^+_4-N)	0.33	0.33	0.33
$\hat{q}_n$ (mg NH^+_4-N/mg VSS-d)	2.3	1.7	1.3
K_n (mg NH^+_4-N/L)	1.0	0.57	0.32
b ($days^{-1}$)	0.11	0.082	0.060

Table 4-28. Comparison of %AOB Determined From Theoretical Calculations and Real-time PCR

	20°C		15°C		10°C	
SRT (days)	Theoretical	Measured	Theoretical	Measured	Theoretical	Measured
20	13.0%	0.3 (±0.4)%	16.7%	0.12 (±0.02)%	No steady-state data available	
10	13.1%	0.3 (±0.2)%	12.2%	0.1 (±0.04)%	10.3%	0.01 (±0.01)%
5	14.0%	0.07 (±0.09)%	9.8%	0.3 (±0.04)%	5.3%	0.01 (±0.001)%
2	6.0%	0.7 (±0.3)%	2.0%	0.3 (±0.2)%	Nitrification Failure	0.0004 (±0.0004)%

researchers reported a percentage of AOB of 5.2 (±3.8)% measured with FISH. McClintock et al. (1993) calculated 3.4% to 7.5% AOB in a pilot scale activated sludge system treating municipal wastewater operated at SRTs of 1.5 to 15 days on the basis of kinetic values found in the literature.

It is not surprising that a strong correlation does not exist between the measured values of ammonia oxidation rate and *N. oligotropha*-type AOB cells (Figure 4-19), since it seems likely that the *N. oligotropha*-type organisms measured in these reactors were not the dominant AOB present. As discussed in the preceding section, there were only rare instances when the same trends were observed in both the ammonia oxidation rate and *N. oligotropha*-type AOB cell density. Table 4-29 lists the correlation coefficients obtained between the logarithm of the *N. oligotropha*-type AOB concentrations and the ammonia oxidation rates for each temperature and DO level. While there were a few incidences when the correlation coefficient exceeded 0.5, such as during operation at the high DO level at 10°C, overall the *N. oligotropha*-type AOB concentration and ammonia oxidation rate were not highly correlated.

Specific ammonia oxidation rates were computed by dividing the measured oxidation rate by the measured concentration of *N. oligotropha*-type AOB and performing appropriate unit conversions for the steady-state samples shown in Tables 4-4, 4-5, and 4-6. These resulting ammonia oxidation rates are shown in Figure 4-20A, B, and C for the high, intermediate and low DO levels, respectively. The specific ammonia oxidation rates were, in general, much higher than the reported rates of 0.0018 to 0.023 pmol/cell/hr for pure cultures (Belser, 1979). The high specific ammonia oxidation rates in this study are reflective of the low reported concentrations of AOB. Figures 4-20A and B suggested that the specific ammonia oxidation rate tended to increase with increasing ammonia concentration during operation at the high and intermediate DO levels. Figure 4-20C shows much lower specific ammonia oxidation rates were observed at the low DO level than at the higher DO levels with no observable difference with varying ammonia concentrations. However, due to the unrealistically high specific ammonia oxidation rates measured in this study it is difficult to draw conclusions from this information.

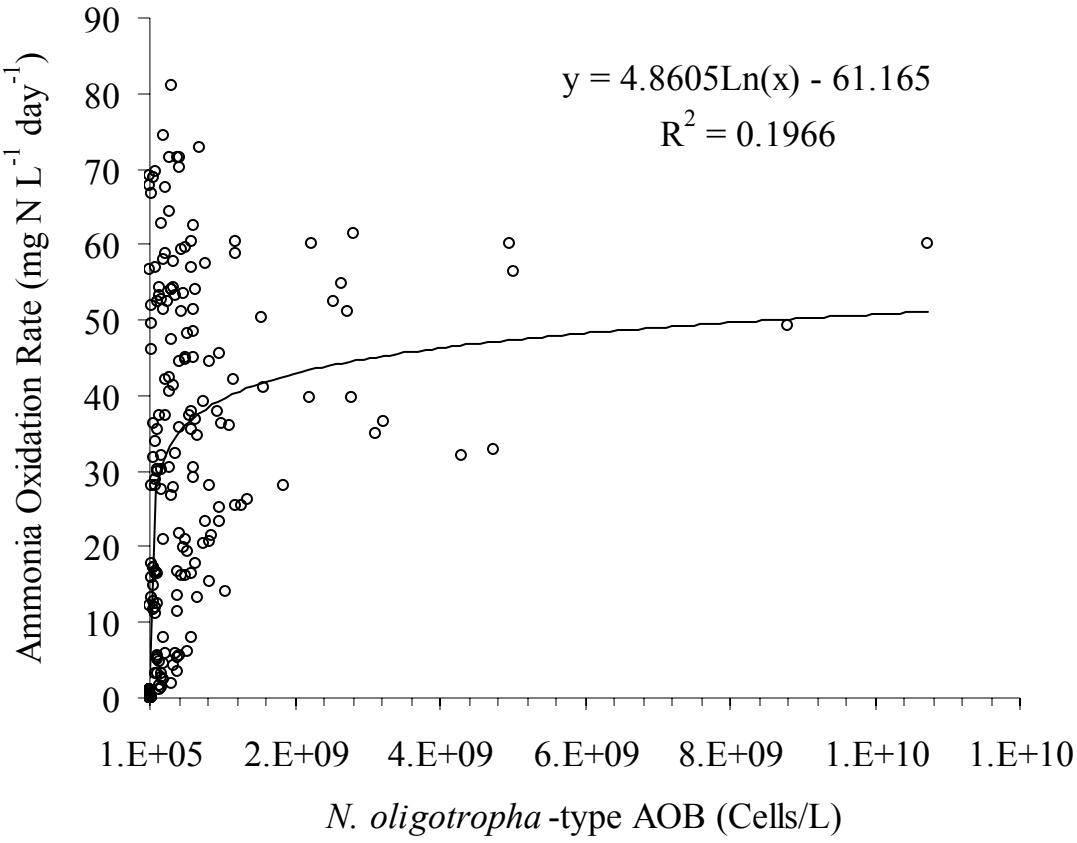

Figure 4-19. Correlation between Ammonia Oxidation Rate and *N. oligotropha*-type AOB Concentration (Includes Data From All Operational Conditions)

Table 4-29. Pearson Correlation Coefficients Between *N. oligotropha*-type AOB Concentrations and Ammonia Oxidation Rates

	DO Level		
Temperature (°C)	High	Intermediate	Low
20	0.32	0.11	0.67*
15	0.42	0.17	0.60
10	0.84	0.41	0.43

* Data only includes samples taken during operation at 0.5 mg/L DO

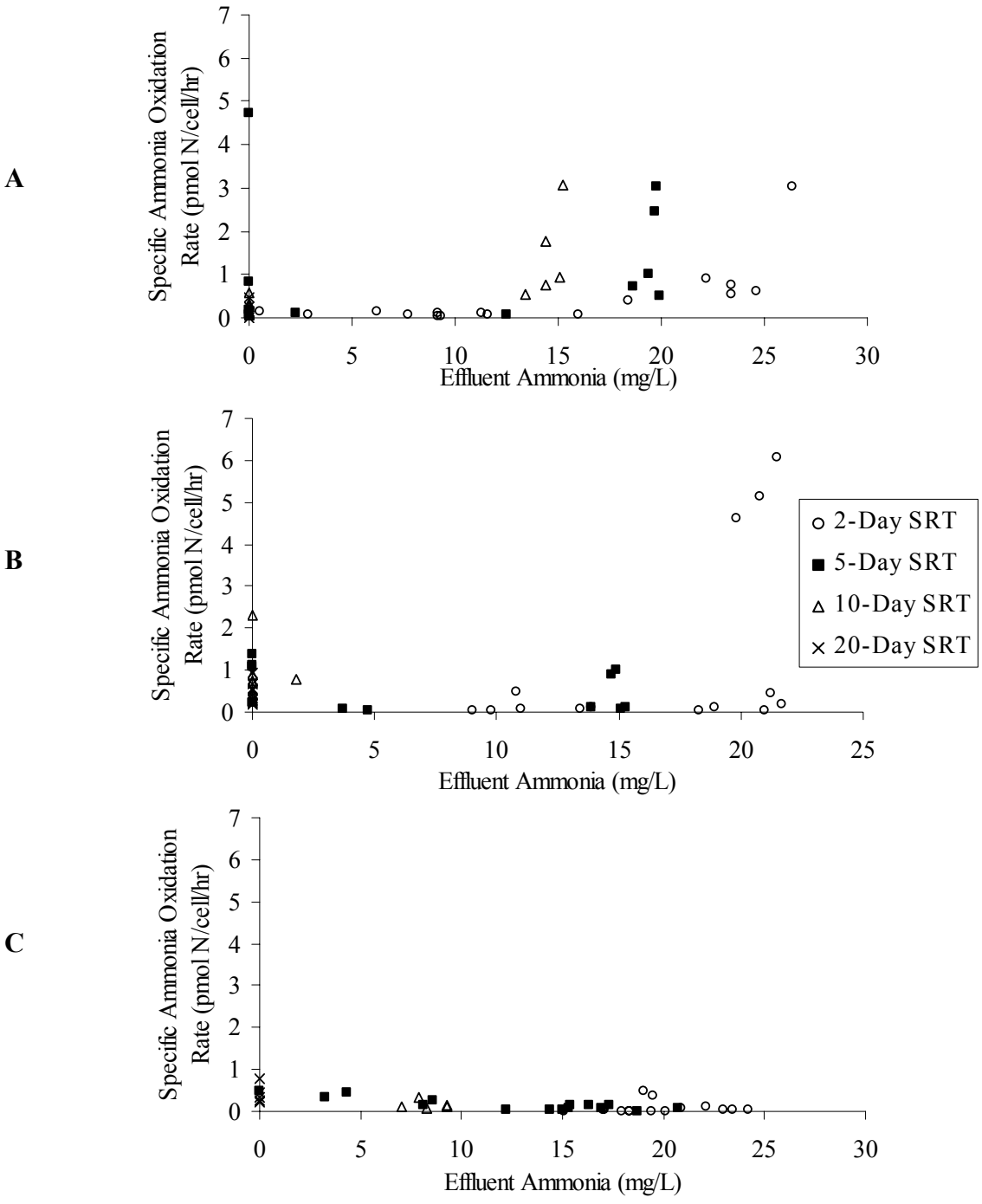

Figure 4-20. Steady-state Specific Ammonia Oxidation Rates as a Function of Effluent Ammonia Concentration (A) High DO, (B) Intermediate DO, (C) Low DO

4.4.4 Nitrite Oxidation

20°C Operation

High rates of nitrite oxidation were consistently achieved in the 20-, 10-, and 5-day SRT reactors during operation at the high and intermediate DO levels at 20°C (Figures 4-12A, 4-13A, 4-14A and Table 4-30). The presence of effluent nitrate-N concentrations comparable to influent ammonia-N levels and the lack of nitrite in the effluent of the 20- and 10-day SRT reactors indicated that complete nitrite oxidation occurred in these reactors throughout this time period. In fact, the average percent conversion of the available nitrite during operation at the high and intermediate DO levels was 99% (Table 4-30). The concentration of available nitrite was computed as the sum of the reactor effluent nitrite and nitrate concentrations. While effluent nitrite averaged 0.3 mg/L in the 5-day SRT reactor during the high and intermediate DO periods of operation at 20°C, the average nitrite oxidation rates observed were roughly equivalent to those measured at SRTs of 20- and 10-days (Table 4-30). As with the ammonia oxidation rate at 20°C, when the nitrite oxidation rates measured during operation at the high and intermediate DO levels in the 20-, 10-, and 5-day SRT reactors were included in a multiple regression analysis, only the concentration of available nitrite was found to significantly affect nitrite oxidation rates at a 95% confidence level. This result suggests that at an operating temperature of 20°C, increasing the DO concentration above 1.0 mg/L or the SRT above 5 days does not enhance nitrification performance.

Nitrite oxidation efficiency in the 20-day SRT reactor remained high during operation at a DO concentration of 0.5 mg/L, but was initially impacted by the change in DO level from 0.5 to 0.2 mg/L on November 29, 2000. Complete nitrite oxidation was eventually recovered in this reactor (Figure 4-12A), and the average nitrite oxidation rate during the low DO operating period was consistent with the average nitrite oxidation rates measured at the high and intermediate DO operating periods. Although the walls of the reactors were scrubbed on a daily basis to inhibit attached growth, biofilm development cannot be completely discounted as a contributing factor in nitrification at DO levels of 0.2 mg/L. Nitrite oxidation efficiency also remained high in the 10-day SRT

Table 4-30. Average Nitrite Concentrations and Nitrite Oxidation Rates During Operation at 20°C

DO Level	Parameter	20 day	10 day	5 day	2 day
High	Avg. NO_2^- (mg N /L)	0.1 (± 0.5)	0.1 (± 0.5)	0.3 (± 0.6)	1.2 (± 0.6)
	NO_2^- Oxidation Rate (mg N/L/day)	48 (± 11)	48 (± 10)	47 (± 11)	23 (± 9)
	NO_2^- Oxidation Efficiency (%)	99 (± 7)	99 (± 7)	98 (± 7)	86 (± 8)
Intermediate	Avg. NO_2^- (mg N /L)	0.0 (± 0.0)	0.0 (± 0.0)	0.3 (± 0.3)	1.1 (± 0.4)
	NO_2^- Oxidation Rate (mg N/L/day)	53 (± 8)	53 (± 8)	51 (± 7)	12 (± 5)
	NO_2^- Oxidation Efficiency (%)	100 (± 0)	100 (± 0)	99 (± 1)	80 (± 7)
Low	Avg. NO_2^- (mg N /L)	0.1 (± 0.2)	0.2 (± 0.3)	3.9 (± 3.8)	0.3 (± 0.1)
	NO_2^- Oxidation Rate (mg N/L/day)	48 (± 11)	42 (± 12)	17 (± 14)	1.1 (± 0.6)
	NO_2^- Oxidation Efficiency (%)	99 (± 2)	98 (± 3)	61 (± 25)	52 (± 8)

reactor during operation at a DO concentration of 0.5 mg/L. However, in contrast to the 20-day SRT reactor, complete nitrification was not achieved in the 10-day SRT reactor during operation at 0.2 mg/L (Figure 4-13A).

Nitrite oxidation in the 5-day SRT reactor was strongly impacted by the decrease in DO to the low level (Figure 4-14A), and a large decline in average nitrite oxidation rate was noted during this operating period. The decrease in nitrite oxidation rate resulted not only from a decline in available nitrite due to incomplete ammonia oxidation (Table 4-17) but also from a decline in nitrite oxidation efficiency (Table 4-30). Although ammonia oxidation has been reported to be the rate-limiting step in nitrification, Figure 4-14A indicates a build-up of nitrite in the effluent of the 5-day SRT reactor during 0.5 mg/L DO operation. It was reported by Laanbroek et al. (1994) that ammonia-oxidizers had a higher affinity for oxygen (i.e. a lower half-saturation constant) than nitrite-oxidizers, therefore, NOB may have difficulty competing with AOB for available oxygen. A downward trend in effluent nitrite over time suggests that the nitrite-oxidizers began to acclimate to the low DO conditions.

Multiple linear regression analyses were performed individually for each SRT with nitrite oxidation rates measured during the intermediate and low DO level operating periods at 20ºC. For the 2-day SRT reactor, both DO level and available nitrite concentration significantly impacted oxidation rate at a 95% confidence interval, with nitrite concentration yielding 10 times as much influence as the DO concentration. For the 5-day SRT reactor, only the DO concentration significantly impacted the nitrite oxidation rate, which is supported by the fact that a nitrite build-up occurred. This indicates that for a time, nitrite oxidation controlled the rate of nitrification in this reactor, which was not observed at the other SRTs. According to multiple linear regression analysis of the 10-day SRT data, both DO and available nitrite concentration significantly impacted the oxidation rate, with the available nitrite concentration having nearly 30 times the impact of DO concentration. For the 20-day SRT reactor, only the amount of available nitrite significantly impacted the nitrite oxidation rate under these operating conditions.

The nitrogen speciation data for the 2-day SRT reactor, shown in Figure 4-15A for the 20°C study, were much different than that of the other reactors at this temperature even under excess DO conditions. During the high and intermediate DO operating periods, significant ammonia and nitrite concentrations were regularly measured in the effluent of the 2-day SRT reactor and the average nitrite oxidation rates were much lower than those measured at higher SRTs. At the high DO level, the average nitrite oxidation rate was approximately 50% lower than observed for the 20-, 10-, and 5-day SRTs, however, the percentage of available nitrite oxidized was only 12% lower than the higher SRTs. Similarly, at the intermediate DO level, the average nitrite oxidation rate and efficiency were 75% and 18% lower than at the higher SRTs, respectively. This data suggests that the decline in nitrite oxidation rate was caused in large part by the lowered amount of available nitrite. Operation of the 2-day SRT reactor at the low DO level resulted in near complete nitrification failure. Data from January 2nd-10th clearly shows that ammonia oxidation had essentially ceased. For these dates, only trace amounts of nitrate and nitrite (averaging 0.4 and 0.4 mg/L respectively) could be measured in the effluent. This data again shows much higher nitrite oxidation efficiency than ammonia oxidation efficiency (52% vs. 3%, respectively) supporting the theory that ammonia oxidation is the rate-limiting step. Multiple linear regression analysis of the 2-day SRT reactor suggested that the concentration of available nitrite controlled the nitrite oxidation rate rather than the DO concentration at this SRT.

15°C Operation

Table 4-31 provides a tabulation of the average effluent nitrite concentrations and nitrite oxidation rates and efficiencies measured during each DO level in each reactor during the 15°C study. Comparison of Tables 4-30 and 4-31 shows that the average nitrite oxidation rates in the 20-day SRT reactor were similar, suggesting that temperature did not significantly impact nitrification under these conditions. Nitrite oxidation rates in the 20-day SRT also did not appear to be negatively impacted by decreasing DO at this temperature. Nitrification was initially disrupted in the 20-day SRT reactor when the DO concentration was dropped to 0.2 mg/L, however, complete nitrification was eventually

Table 4-31. Average Nitrite Concentrations and Nitrite Oxidation Rates During Operation at 15°C

DO Level	Parameter	20 day	10 day	5 day	2 day
High	Avg. NO_2^- (mg N /L)	0.2 (± 0.3)	0.3 (± 0.4)	0.6 (± 0.3)	0.4 (± 0.1)
	NO_2^- Oxidation Rate (mg N/L/day)	43 (± 17)	39 (± 14)	21 (± 10)	6 (± 3)
	NO_2^- Oxidation Efficiency (%)	99 (± 4)	98 (± 1)	93 (± 5)	81 (± 12)
Intermediate	Avg. NO_2^- (mg N /L)	0.1 (± 0.1)	0.3 (± 0.5)	0.9 (± 0.5)	0.6 (± 0.3)
	NO_2^- Oxidation Rate (mg N/L/day)	64 (± 16)	62 (± 16)	38 (± 20)	8 (± 8)
	NO_2^- Oxidation Efficiency (%)	99 (± 1)	98 (± 3)	92 (± 5)	78 (± 12)
Low	Avg. NO_2^- (mg N /L)	0.2 (± 0.1)	0.2 (± 0.2)	0.4 (± 0.2)	0.0 (± 0.1)
	NO_2^- Oxidation Rate (mg N/L/day)	47 (± 8)	35 (± 11)	9 (± 9)	0.1 (± 0.4)
	NO_2^- Oxidation Efficiency (%)	99 (± 1)	98 (± 1)	86 (± 9)	73 (± 38)

restored in this reactor (Figure 4-12B). Multiple linear regression of the measured nitrite oxidation rates in the 20-day SRT reactor at 15°C showed that only available nitrite concentration significantly impacted the rate of nitrite oxidation at this SRT.

Nitrite oxidation efficiency in the 10-day SRT reactor was similar to that observed in the 20-day SRT reactor during the high and intermediate DO levels, however, there were a few more instances where effluent ammonia and nitrite were measured in the 10-day SRT reactor (Figure 4-13B). A decrease in average nitrite oxidation rate was observed at the low DO level, however the percentage of available nitrite oxidized remained at 98% (Table 4-31), suggesting the decline in oxidation rate is the result of incomplete ammonia oxidation (Table 4-18). Multiple linear regression analysis of the 10-day SRT data showed that only the concentration of available nitrite significantly affected nitrite oxidation rates at a 95% confidence level. Nitrite oxidation rates in the 5-day SRT reactor were significantly lower at 15°C than at 20°C and were drastically reduced at the low DO level. In spite of the fact that the oxidation rates were lower, the percent nitrite oxidation efficiency remained greater than 85% in the 5-day SRT reactor throughout operation at 15°C, suggesting that the reduction in rate was primarily due to the decrease in available nitrite. As shown in Figure 4-15B, the 2-day SRT reactor failed to achieve efficient nitrification during any phase of this experiment and nitrification failed completely during the low DO phase at 15°C. Even so, in excess of 70% of the available nitrite was converted to nitrate during 15°C operation, suggesting that nitrification was limited by the ammonia oxidation step. According to multiple linear regression analyses, only available nitrite concentration was found to significantly impact the nitrite oxidation rate at a 95% confidence level at SRTs of both 5 and 2 days.

The multiple linear regression model developed for the 15°C nitrite oxidation rate data described the measured rates very well (R=1.0) and indicated that 99.9% of the observed variability in nitrite oxidation rate could be attributed to changes in concentration of available nitrite, SRT and DO level. All of the independent variables included in the model significantly affected the nitrite oxidation rate, with available nitrite concentration exerting nearly three times as much influence on the nitrite oxidation rate as SRT and nearly four times the influence of DO concentration.

10°C Operation

Efficient nitrite oxidation occurred in the 20-day SRT reactor throughout all phases of the 10°C experiment (Figure 4-12C) suggesting that the temperature drop and changes in DO did not significantly impact nitrification at this SRT. In contrast, nitrite oxidation in the 10-day SRT reactor was severely impacted by the decrease in temperature. Figure 4-13C shows a build-up of nitrite in the effluent following the temperature change, similar to the build-up observed in the 5-day SRT reactor during operation at the low DO level at 20°C (Figure 4-14A). Randall and Buth (1984) noted a similar phenomenon in laboratory- and full-scale activated sludge systems and suggested that although the maximum possible rate of nitrate formation may be substantially greater than the maximum rate of nitrite formation at 20°C, there exists a lower critical temperature below which the rate of nitrite formation will exceed that of nitrate, resulting in a build-up of nitrite. In their experiments, the critical temperatures for a laboratory-scale and a full-scale reactor were 14° and 12°C, respectively. Below the critical temperature, the rate of nitrate formation controlled the overall nitrification rate. In the current study, the critical temperature for the 10-day SRT reactor appears to be between 15°C and 10°C. After an extended transition period, the effluent nitrite levels decreased until this substance was no longer consistently detected in the 10-day SRT reactor effluent and a corresponding increase in the average conversion efficiency of nitrite to nitrate was observed. These results suggest that the nitrite-oxidizers were able to acclimate to the low temperature conditions. The ammonia-oxidizers did not appear to fully acclimate to the low temperature as evidenced by the significant amount of ammonia-N measured in the effluent of this reactor throughout the remainder of the 10°C study (Figure 4-13C). Even though nitrite was no longer routinely present in the effluent from the 10-day SRT reactor after the acclimation period, nitrite oxidation rates remained suppressed during the intermediate and low DO portions of the study (Table 4-32) because of the simultaneous decline in ammonia oxidation rate.

Figure 4-14C shows that nitrification was inhibited in the 5-day SRT reactor when operated at a temperature of 10°C. Nitrification performance decreased with decreasing

Table 4-32. Average Nitrite Concentrations and Nitrite Oxidation Rates During Operation at 10°C

DO Level	Parameter	20 day	10 day	5 day	2 day
High	Avg. NO_2^- (mg N /L)	0.2 (± 0.1)	2.4 (± 3.0)	0.6 (± 0.3)	0.1 (± 0.1)
	NO_2^- Oxidation Rate (mg N/L/day)	66 (± 7)	40 (± 14)	20 (± 10)	3 (± 6)
	NO_2^- Oxidation Efficiency (%)	99 (± 0)	87 (± 16)	92 (± 2)	90 (± 14)
Intermediate	Avg. NO_2^- (mg N /L)	0.5 (± 1.2)	0.5 (± 0.1)	0.5 (± 0.0)	0.1 (± 0.1)
	NO_2^- Oxidation Rate (mg N/L/day)	62 (± 11)	30 (± 4)	15 (± 1)	0.3 (± 0.2)
	NO_2^- Oxidation Efficiency (%)	97 (± 7)	96 (± 1)	91 (± 0)	73 (± 28)
Low	Avg. NO_2^- (mg N /L)	0.1 (± 0.1)	0.3 (± 0.1)	0.3 (± 0.1)	0.0 (± 0.1)
	NO_2^- Oxidation Rate (mg N/L/day)	55 (± 8)	35 (± 4)	7 (± 5)	0.1 (± 0.1)
	NO_2^- Oxidation Efficiency (%)	100 (± 1)	98 (± 1)	88 (± 7)	76 (± 34)

DO level and complete nitrification failure in the 5-day SRT system was documented during the final days of the low DO phase at 10°C (as evidenced by the very low effluent nitrite and nitrate concentrations). While the average nitrite oxidation rate decreased from 20 mg N/L/day to 7 mg/L/day from the high to low DO levels, the nitrite oxidation efficiency only decreased from 92% to 88%. As shown in Figure 4-15C, the 2-day SRT reactor remained at a state of complete failure throughout the duration of the 10°C experiment. Even so, greater than 75% of the available nitrite was converted to nitrite, suggesting once again that incomplete ammonia oxidation was responsible for the decrease in nitrite oxidation rate.

Multiple linear regression analysis of the 10°C data showed that available nitrite concentration and SRT significantly impacted the nitrite oxidation rate at a 95% confidence level, with the available nitrite concentration yielding more than 20 times more influence on the rate than SRT. Further analysis revealed that at the high DO level, only the available nitrite concentration influenced the nitrite oxidation rate, whereas at the intermediate and low DO levels both available nitrite and SRT were significant.

Comparison of Data from All Three Temperatures

When all operational conditions were included in the linear regression model, 94% of the observed variability in nitrite oxidation rate could be explained by changes in SRT, temperature, DO concentration, and available nitrite concentration, and of the four variables, only temperature did not significantly impact nitrite oxidation at a 95% confidence level. The relative impact of available nitrite concentration on nitrite oxidation was found to be five times greater than that of SRT, and more than fifteen times greater than that of the DO.

In general, the percent of nitrite oxidized was lower for the 5- and 2-day SRTs than for the 20- and 10-day SRTs, and for the lower SRTs, the percent nitrite oxidized decreased with decreasing DO. However, the data suggests that nitrite oxidation rate was controlled by the amount of nitrite available, which was controlled by the ammonia oxidation rate. Since ammonia oxidation was found to be the rate-limiting step, the

impact of SRT, DO, and temperature on the ammonia oxidation rate indirectly affected the nitrite oxidation rate.

4.4.5 *Nitrospira* spp. NOB Concentration

Real-time PCR measurements for *Nitrospira spp.* 16S rDNA were made on samples collected from reactors operating at 20°C, 15°C and 10°C. Since the number of *Nitrospira* 16S rDNA copies per cell is unknown, it was assumed to be one based on the average copies of 16S rDNA per cell in other nitrifying bacteria, such as *Nitrosomonas* and *Nitrobacter* (Navarro *et al*., 1992; Klappenbach *et al*., 2001).

20°C Operation

Table 4-33 presents the average *Nitrospira* concentrations in each of the reactors for the 20°C study period. In contrast to the measured AOB cell densities, the NOB concentrations listed in Table 4-33 are very similar to those reported in the literature. Yuan and Blackall (2002) reported *Nitrospira* concentrations of approximately 3×10^9 *Nitrospira* cells/L in lab-scale activated sludge reactors treating municipal wastewater, using a real-time PCR assay targeting *Nitrospira* 16S rDNA. Hall et al. (2002) applied the same real-time PCR *Nitrospira* assay to samples from five full-scale municipal WWTPs and measured *Nitrospira* cell densities of 2.9×10^6, 4.1×10^{10}, 1.8×10^{12}, 1.2×10^7, and 2.3×10^{13} cells/L mixed liquor for the WWTPs achieving 48.1%, 98.8%, 99.3%, 99.7%, and 99.8% nitrification, respectively. Ammonia in the influent for all plants ranged from 21-42 mg/L. Harms et al. (2003) observed an average *Nitrospira* concentration of $3.7 (\pm 3.5) \times 10^{10}$ cells/L for 12 monthly mixed liquor samples from the

Table 4-33. Average *Nitrospira* Concentrations (cells/L) During Operation at 20°C

DO Level	High	Intermediate	Low
20-Day SRT	$1.9 (\pm 0.7) \times 10^{10}$	$1.0 (\pm 0.4) \times 10^{10}$	$1.3 (\pm 0.7) \times 10^{10}$
10-Day SRT	$2.9 (\pm 1.0) \times 10^{10}$	$2.3 (\pm 0.9) \times 10^{10}$	$2.5 (\pm 1.9) \times 10^{10}$
5-Day SRT	$1.3 (\pm 0.8) \times 10^{10}$	$1.3 (\pm 0.4) \times 10^{10}$	$7.2 (\pm 9.1) \times 10^{9}$
2-Day SRT	$2.3 (\pm 1.7) \times 10^{9}$	$5.3 (\pm 7.5) \times 10^{8}$	$1.9 (\pm 0.2) \times 10^{8}$

full-scale municipal WWTP used to seed the reactors measured with the same real-time PCR assay used in the current study. Dionisi et al (2002a) reported *Nitrospira* cell densities of 5.8 (± 0.98) x 10^9 to 5.5 (± 0.2) x 10^{10} cells/L for the same samples using a cPCR assay. Lee et al. (2002) obtained similar results using direct counts of colony forming units in a 10-day SRT bench-scale activated sludge reactor operated at 20°C and excess DO. Lee et al. (2002) measured 5.44 x 10^{10} NOB cells/L when the reactor was operated at a carbon/nitrogen ratio of 12.5, which is comparable to the ratio observed in the current study.

Nitrospira levels remained fairly constant during 20°C operation in the 20- and 10-day SRT reactors at all DO levels and in the 5-day SRT reactor at the high and intermediate DO levels. The average *Nitrospira* concentration in the 5-day SRT reactor decreased by almost one-half at the low DO level. The *Nitrospira* concentration in the 2-day reactor decreased with decreasing DO and was significantly lower than levels measured in the other SRT reactors at this temperature. Multiple linear regression analyses performed on data from each SRT at 20°C confirm these findings, with DO concentration significantly impacting the NOB concentration in the 2- and 5-day SRT reactors, but not in the 20- and 10-day SRT reactors. This relationship can be seen more clearly in Figure 4-21 which shows a comparison of the trends in nitrite oxidation efficiency (described previously) and *Nitrospira* concentration as a function of SRT and DO at 20°C. At the high DO level, nitrite oxidation rates were similar in the 20- and 10-day SRT reactors and decreased incrementally as the SRT decreased below 10 days. This trend was mirrored in the *Nitrospira* cell densities. At the intermediate DO level, nearly identical average nitrite oxidation rates were observed in the 20-, 10-, and 5-day SRT reactors, whereas at an SRT of 2 days, a much lower average nitrite oxidation rate was observed. This behavior was also reflected in the average *Nitrospira* concentrations. At the low DO level, nitrite oxidation decrease incrementally with SRT, which is also observed in the cell numbers of *Nitrospira* except at an SRT of 10 days. Multiple linear regression analysis of the low DO level data showed that both SRT and available nitrite concentration exerted a significant impact on the NOB concentrations at a 95%

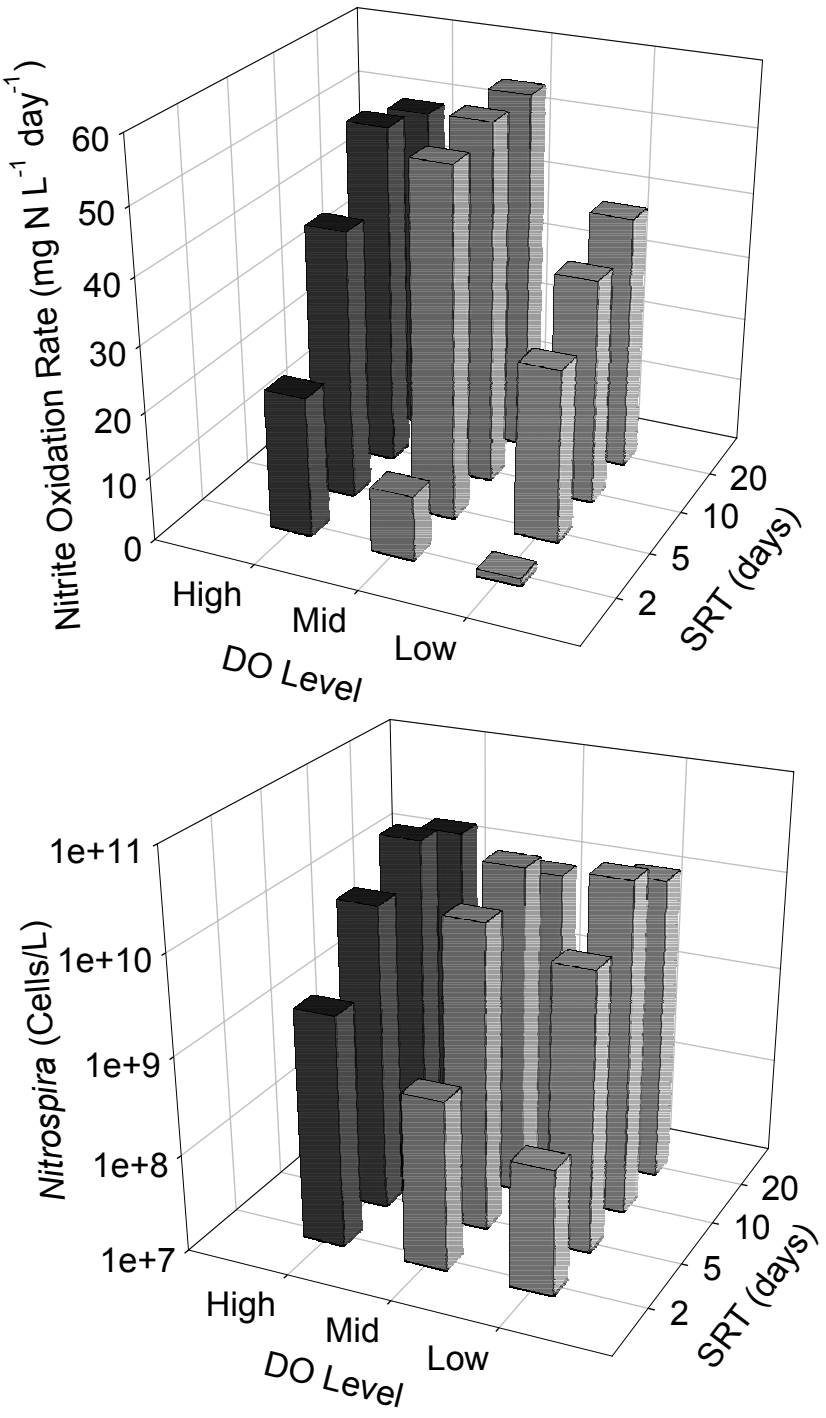

Figure 4-21. Comparison of Trends at 20°C in Nitrite Oxidation Rate and *Nitrospira* Concentration at Varying SRT and DO Levels

confidence interval. A decline in nitrite oxidation rate was observed in all SRT reactors at the low DO level and nitrite oxidation rates decreased incrementally in the 2-day SRT reactor each time the DO level was lowered. The trends observed in nitrite oxidation rate with respect to DO level in the 5- and 2-day SRT reactors were mirrored in the trends in *Nitrospira* concentration in these reactors. However, the decrease in nitrite oxidation rate at the low DO level in the 20- and 10- day SRT reactors was not reflected in the *Nitrospira* concentration, which may be due to the fact that although a decrease in rate was observed, a decline in nitrite oxidation efficiency did not occur under these conditions (Table 4-30). Multiple linear regression analysis performed on all of the NOB cell densities measured during 20°C operation indicated that both SRT and the available nitrite concentration significantly impacted the concentration of *Nitrospira* at a 95% confidence level, with the available nitrite concentration yielding 1.8 times more influence than SRT.

15°C Operation

Average *Nitrospira* concentrations in each of the reactors during the 15°C study period are shown in Table 4-34. Comparison of Tables 4-33 and 4-34 show that the *Nitrospira* concentrations in the 20- and 10-day SRT reactors were similar at temperatures of 20°C to 15°C. In contrast, the decrease in temperature yielded a decline in *Nitrospira* levels in the 5-day SRT reactor and regression analysis supported this observation with temperature having a significant impact on *Nitrospira* concentration at a 95% confidence interval. The impact of temperature on NOB concentration in the 2-day SRT reactor was inconclusive.

Table 4-34. Average *Nitrospira* Concentrations (cells/L) During Operation at 15°C

DO Level	High	Intermediate	Low
20-Day SRT	$1.2 (\pm 1.2) \times 10^{10}$	$3.1 (\pm 1.0) \times 10^{10}$	$1.2 (\pm 0.2) \times 10^{11}$
10-Day SRT	$1.8 (\pm 0.7) \times 10^{10}$	$2.6 (\pm 0.7) \times 10^{10}$	$8.4 (\pm 1.4) \times 10^{10}$
5-Day SRT	$4.3 (\pm 3.2) \times 10^{9}$	$4.5 (\pm 2.4) \times 10^{9}$	$2.7 (\pm 0.5) \times 10^{9}$
2-Day SRT	$6.7 (\pm 3.1) \times 10^{8}$	$8.1 (\pm 2.1) \times 10^{8}$	$1.8 (\pm 0.9) \times 10^{9}$

As shown in Table 4-34 and Figure 4-22, *Nitrospira* concentrations at 15°C decreased with decreasing SRT. The *Nitrospira* concentration actually increased in the 20-, 10- and 2-day SRT reactors when the DO levels were lowered. In the 5-day SRT reactor, the *Nitrospira* concentration was relatively unchanged for all DO levels. Multiple linear regression analysis showed that the DO significantly impacted the *Nitrospira* cell densities at a 95% confidence level in the 20-, and 10- day SRT reactors and that the two parameters were negatively correlated. However, in the 5-day SRT reactor only influent available nitrite concentration significantly influenced the *Nitrospira* concentrations. Linear regression results for the 2-day SRT reactor were inconclusive. Inspection of Figure 4-22 shows that the 20-day SRT achieved high rates of nitrite oxidation throughout the 15°C study, while in the 10-day SRT reactor a significant decline in nitrite oxidation rate occurred at the low DO level. The 5- and 2-day SRT reactors showed incremental decreases in nitrite oxidation rate with decreasing DO level. However, these trends were not clearly reflected in *Nitrospira* concentrations.

When the 15°C *Nitrospira* data was described by a linear regression, 67% of the observed variability in measured NOB concentrations could be explained by changes in the SRT, DO, and available nitrite concentration. All three variables were found to significantly impact the *Nitrospira* concentration at a 95% confidence level. DO concentration was found to be negatively correlated with NOB cell density, while SRT and available nitrite concentration were positively correlated and the relative impact of available nitrite was greater than the impact of DO concentration and SRT by a factor of 1.2.

10°C Operation

Inspection of the data in Table 4-35 shows, again, that as the temperature was decreased the concentration of *Nitrospira* in 20- and 10-day SRT reactors remained fairly stable. This was not true for the 5- and 2-day SRT reactors in which the *Nitrospira* concentration decreased with decreasing temperature, an observation that was supported by the results of regression analysis. Again, *Nitrospira* concentration decreased with decreasing SRT. There also appeared to be no clear correlation between the *Nitrospira*

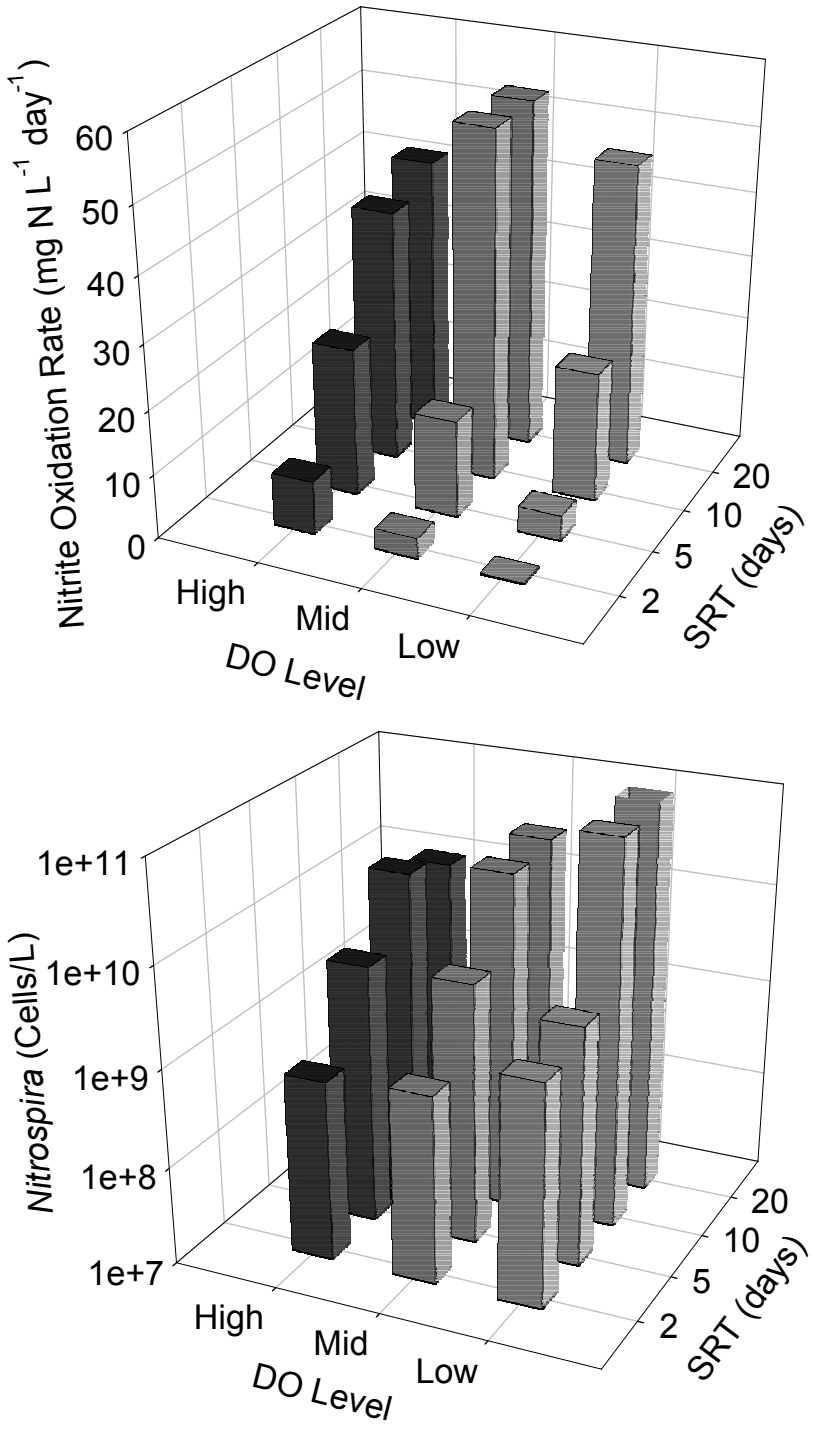

Figure 4-22. Comparison of Trends at 15°C in Nitrite Oxidation Rate and Nitrospira Concentration at Varying SRT and DO Levels

Table 4-35. Average *Nitrospira* Concentrations (cells/L) During Operation at 10°C

DO Level	High	Intermediate	Low
20-Day SRT	9.7 (±1.9) x 10^{10}	4.3 (±0.9) x 10^{10}	5.3 (±0.9) x 10^{10}
10-Day SRT	2.0 (±0.5) x 10^{10}	3.4 (±0.3) x 10^{10}	2.5 (±0.7) x 10^{10}
5-Day SRT	1.7 (±0.9) x 10^{9}	7.2 (±2.3) x 10^{8}	1.2 (±0.4) x 10^{9}
2-Day SRT	4.1 (±2.3) x 10^{8}	2.6 (±0.6) x 10^{8}	3.9 (±1.9) x 10^{8}

concentration and DO level in these reactors when operated at 10°C. These relationships can be seen more clearly in Figure 4-23. These plots show that the 20-day SRT reactor achieved high rates of nitrite oxidation throughout the study period. Again, nitrification performance in the 10-day SRT reactor actually improved when the DO level was lowered. The nitrite oxidation rate in the 5-day SRT reactor decreased significantly at the low DO level. The 2-day SRT reactor was at complete nitrification failure throughout the course of the 10°C treatment. The trends in nitrite oxidation rate were reflected in the *Nitrospira* levels found in these reactors with the exception of the 5-day SRT reactor. Multiple linear regression analysis performed on the measured *Nitrospira* concentrations data during 10°C operation indicated that only the available nitrite concentration significantly impacted the NOB cell density at a 95% confidence level.

Comparison of Data from All Three Temperatures

When data from all operational conditions were included in the linear regression model, approximately 66% of the observed variability in nitrite oxidation rate could be explained by changes in the SRT, temperature, DO, and available nitrite concentration and all four variables significantly impacted the *Nitrospira* concentration at a 95% confidence interval. The concentration of available nitrite and SRT were positively correlated with *Nitrospira* concentration and yielded similar influence, while temperature and DO were negatively correlated with *Nitrospira* concentration and yielded slightly less influence than available nitrite concentration and SRT.

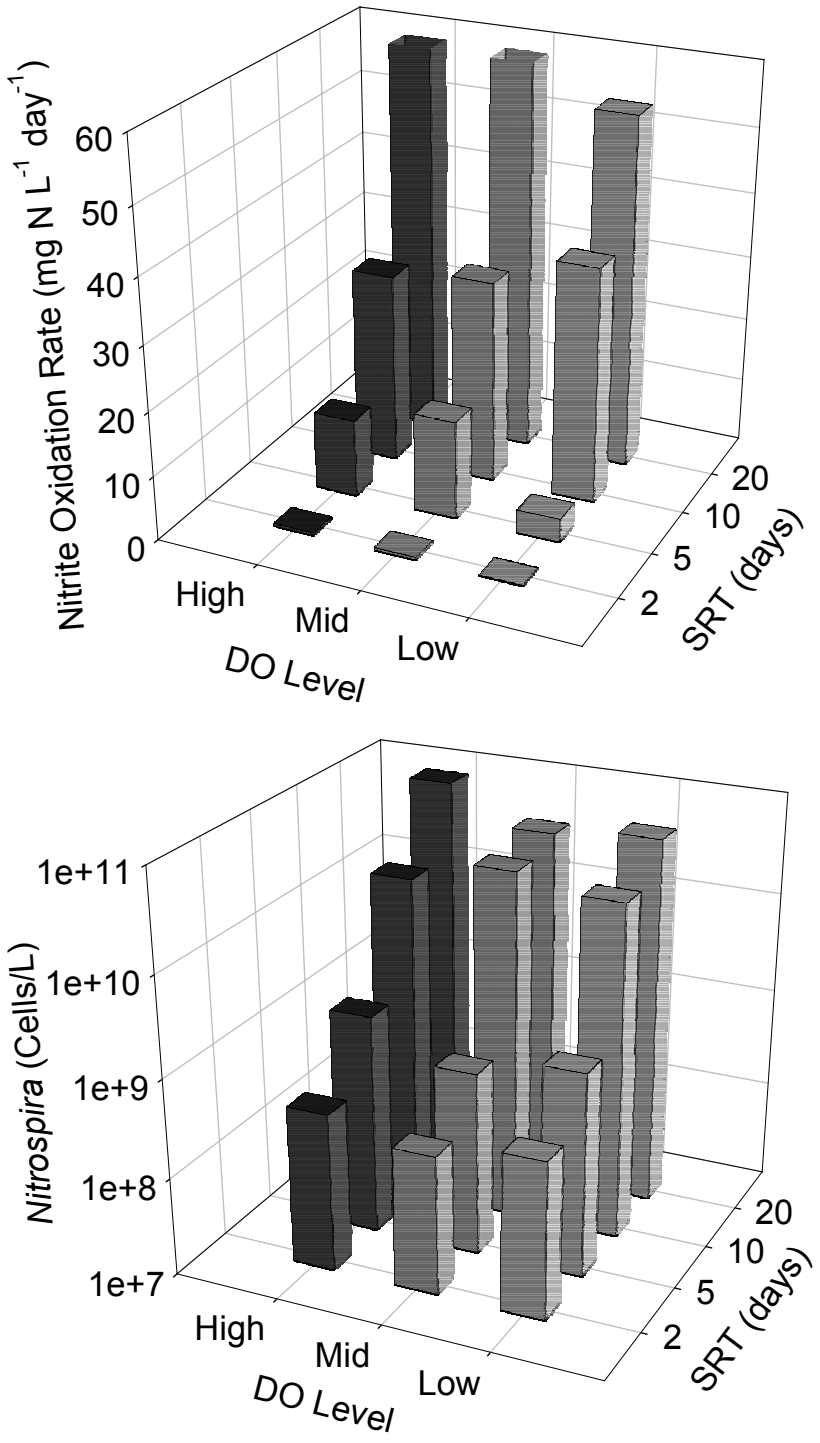

Figure 4-23. Comparison of Trends at 10°C in Nitrite Oxidation Rate and *Nitrospira* Concentration at Varying SRT and DO Levels

Table 4-36 lists the correlation coefficients and R^2 values obtained from the linear regression analyses performed on the nitrite oxidation rate and *Nitrospira* data when all controlled variables and interaction terms were included in the analysis. While, the traditional measure of nitrite-oxidizers was modeled with slightly more accuracy than the molecular measure, the results are actually quite similar. This is a very different finding than that for ammonia oxidation and suggests that the *Nitrospira* assay is representative of the NOB population in the reactors.

4.4.6 Comparison of Nitrite Oxidation and NOB Concentrations

A comparison between the percentages of NOB measured in the reactors using real-time PCR for *Nitrospira* 16S rDNA and theoretical values estimated from design equations using typical kinetic parameters was also made. The percentages of NOB measured in the reactors using real-time PCR were computed by dividing the *Nitrospira* concentration (cells/L) by the total eubacterial 16S rDNA concentration (cells/L). The theoretical values were calculated by using the approach outlined previously for AOB. Steady-state VSS production rates for NOB were estimated using equation 4-2 and the typical kinetic parameters shown in Table 4-37 (Rittmann and McCarty 2001). Table 4-38 provides a comparison of the percentage of NOB measured in the reactors using real-time PCR for *Nitrospira* and theoretical values estimated from design equations using typical kinetic parameters. The values measured using PCR are quite similar to the theoretically predicted values and are in much better agreement than the AOB values.

Table 4-36. Summary of Linear Regression Analyses for Nitrite Oxidation Rate and *Nitrospira* Concentrations

	Nitrite Oxidation Rate		Log *Nitrospira* Concentration	
Temperature	R	R^2	R	R^2
All	0.971	0.942	0.823	0.677
20°C	0.900	0.810	0.788	0.621
15°C	1.000	0.999	0.834	0.695
10°C	1.000	1.000	0.916	0.840

Table 4-37. Typical Kinetic Parameters for Nitrite-Oxidizers (Adapted from Rittmann and McCarty, 2001)

Parameter	20°C	15°C	10°C
Y (mg VSS/mg NO^-_2-N)	0.083	0.083	0.083
$\hat{q}_n$ (mg NO^-_2-N/mg VSS-d)	9.8	7.3	5.5
K_n (mg NO^-_2-N/L)	1.3	0.62	0.30
b ($days^{-1}$)	0.11	0.082	0.060

Table 4-38. Comparison of %NOB Determined From Theoretical Calculations and Real-Time PCR

	20°C		15°C		10°C	
SRT (days)	Theoretical	Measured	Theoretical	Measured	Theoretical	Measured
20	3.2%	2.2 (±1.2)%	4.0%	4.6 (±0.3)%	No steady-state data available	
10	3.2%	5.6 (±3.9)%	2.9%	4.8 (±1.5)%	2.4%	2.1 (±1.1)%
5	3.4%	3.3 (±1.0)%	2.3%	1.4 (±0.4)%	1.1%	0.2 (±0.007)%
2	1.2%	1.5 (±1.0)%	0.4%	0.6 (±0.5)%	Nitrification Failure	0.1 (±0.1)%

The close agreement between measured and calculated values suggest that *Nitrospira spp.* were the dominant nitrite oxidizers in the bench-scale systems.

The values reported in Table 4-38 are also consistent with those reported in the literature. You et al. (2003) found that *Nitrospira* accounted for 2.1% of the total eubacterial population in a pilot plant A20 BNR system operated at 20°C and an SRT of 10 days, using a cloning-DGGE method. Analysis of the nitrifier abundance in this treatment system by FISH yielded similar results of 2.3 (±0.8)% nitrite-oxidizers in the activated sludge. Rittmann et al. (1999) conducted as study of full-scale WWTPs in the France and Netherlands and measured 4 to 8.5% nitrifiers (both AOB and NOB) in nitrifying plants, and 0.5-0.8% nitrifiers in plants in which no nitrification was measured. These values were determined by slot blot hybridization and FISH.

Figure 4-24 shows nitrite oxidation rate as a function of the *Nitrospira* concentration for all conditions studied. A strong logarithmic relationship exists between nitrite oxidation rate and NOB concentration. The Pearson correlation coefficient (R) for these two parameters was 0.78. A similar plot was obtained by Wong-Chong and Loehr (1975) for *Nitrobacter* concentration and nitrite oxidation rate in batch experiments using enriched acclimated nitrifying activated sludge cultures. The researchers observed a curve in the form of a Michaelis-Menten saturation plot. Figure 4-24 suggests that *Nitrospira* follow first order kinetics until nitrite becomes limiting, at which time the kinetics become zero order and the presence of additional organisms no longer produces an increase in nitrite oxidation rate.

The strength of the correlation between nitrite oxidation rates and *Nitrospira* concentration increased when the data from each temperature and DO level was considered separately. Table 4-39 shows the Pearson correlation coefficient between these two parameters for each set of conditions and shows that *Nitrospira* concetration tracked that nitrite oxidation rate quite well with R values greater than 0.86 in all cases. These values are much higher than those obtained for *N. oligotropha*-type AOB concentrations and ammonia oxidation rates.

Specific nitrite oxidation rates were computed by dividing the measured oxidation rate by the measured concentration of *Nitrospira spp.* NOB and performing appropriate

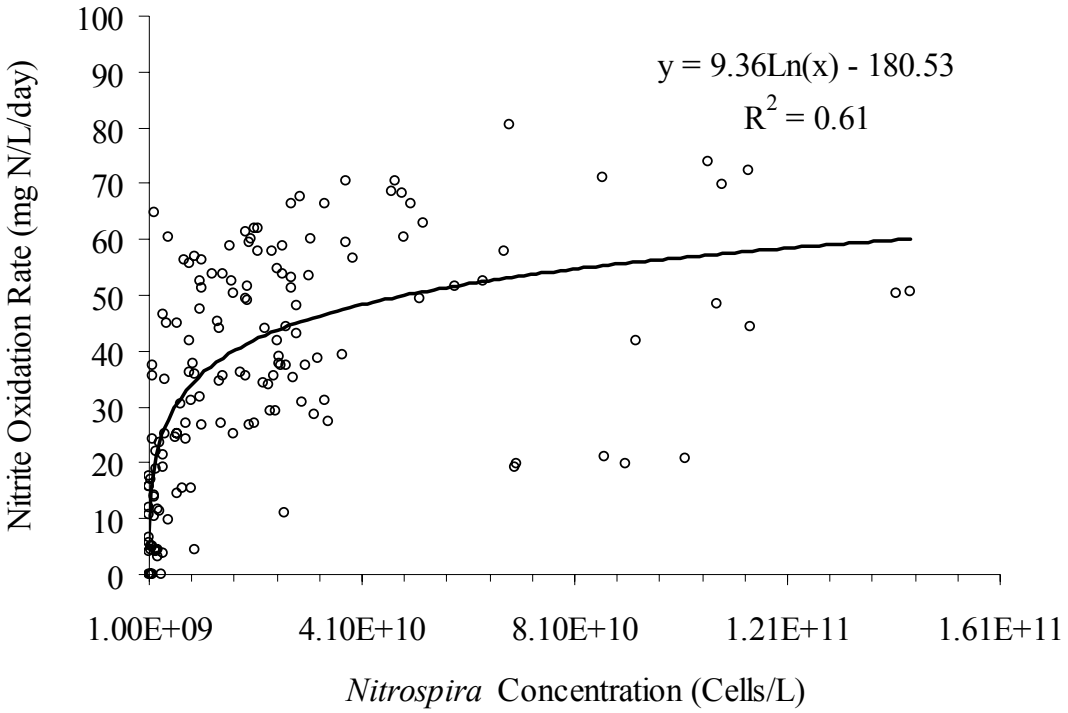

Figure 4-24. Correlation between Nitrite Oxidation Rate and *Nitrospira* Concentration (Includes Data From All Conditions Studied)

Table 4-39. Correlation Coefficients Between *Nitrospira* Concentrations and Nitrite Oxidation Rates

	DO Level		
Temperature (°C)	High	Intermediate	Low
20	0.86	0.93	0.86*
15	0.87	0.89	0.88
10	0.92	0.87	0.97

* Data only includes samples taken during operation at 0.5 mg/L DO

unit conversions for the steady-state samples shown in Tables 4-4, 4-5, and 4-6. The resulting nitrite oxidation rates are shown in Figure 4-25A, B, and C for the high, intermediate and low DO levels, respectively. The specific nitrite oxidation rates were in the range of reported rates of 0.009 to 0.042 pmol/cell/hr for pure cultures (Belser, 1979). Figures 4-25A and B and C suggested that the specific nitrite oxidation rate tended to increase with increasing nitrite concentration. Figure 4-25C shows much lower specific nitrite oxidation rates were observed at the low DO level in comparison to the intermediate and high DO levels (Figures 4-25A and B).

Interestingly, *Nitrospira* concentrations were also highly correlated with ammonia oxidation rates as shown in Figure 4-26 and Table 4-40. This result is logical since NOB are dependent upon the activity of AOB for the production of their growth substrate (nitrite-N). This finding suggests that *Nitrospira* cell densities may serve as an indicator for nitrification treatment performance, and the monitoring of AOB may not be necessary. Hall et al. (2002) obtained a similar finding for *Nitrospira* concentrations in samples from five full-scale municipal WWTPs. *Nitrospira* cell densities of 2.9×10^3, 4.1×10^7, 1.8×10^9, 1.2×10^4, and 2.3×10^{10} cells/mL mixed liquor were reported for the WWTPs achieving 48.1%, 98.8%, 99.3%, 99.7%, and 99.8% nitrification, respectively. Hall et al. (2002) noted that, on the surface, nitrification performance appeared to be correlated with *Nitrospira* cell numbers for the plants investigated.

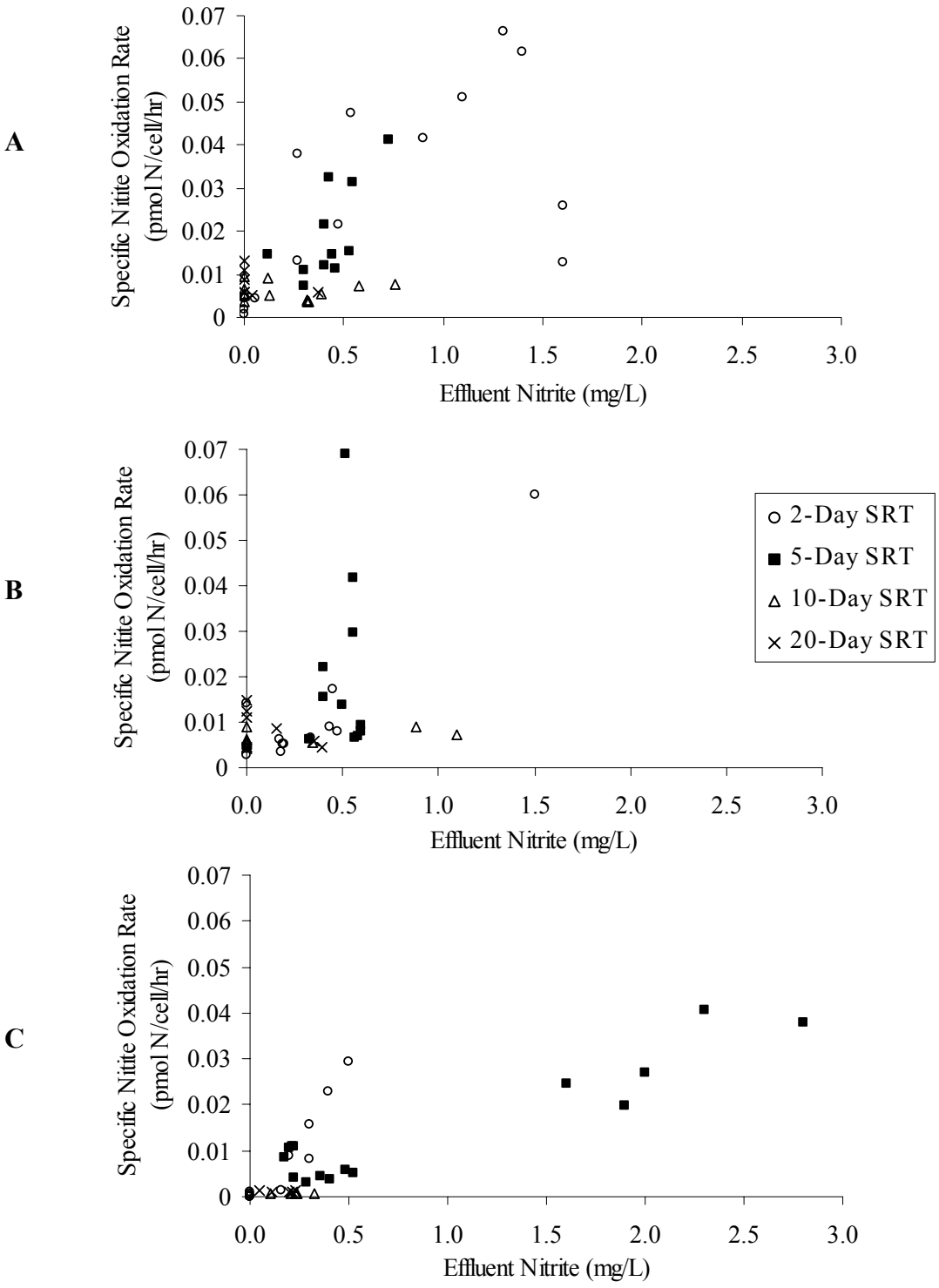

Figure 4-25. Steady-state Specific Nitrite Oxidation Rates as a Function of Effluent Nitrite Concentration (A) High DO, (B) Intermediate DO, (C) Low DO

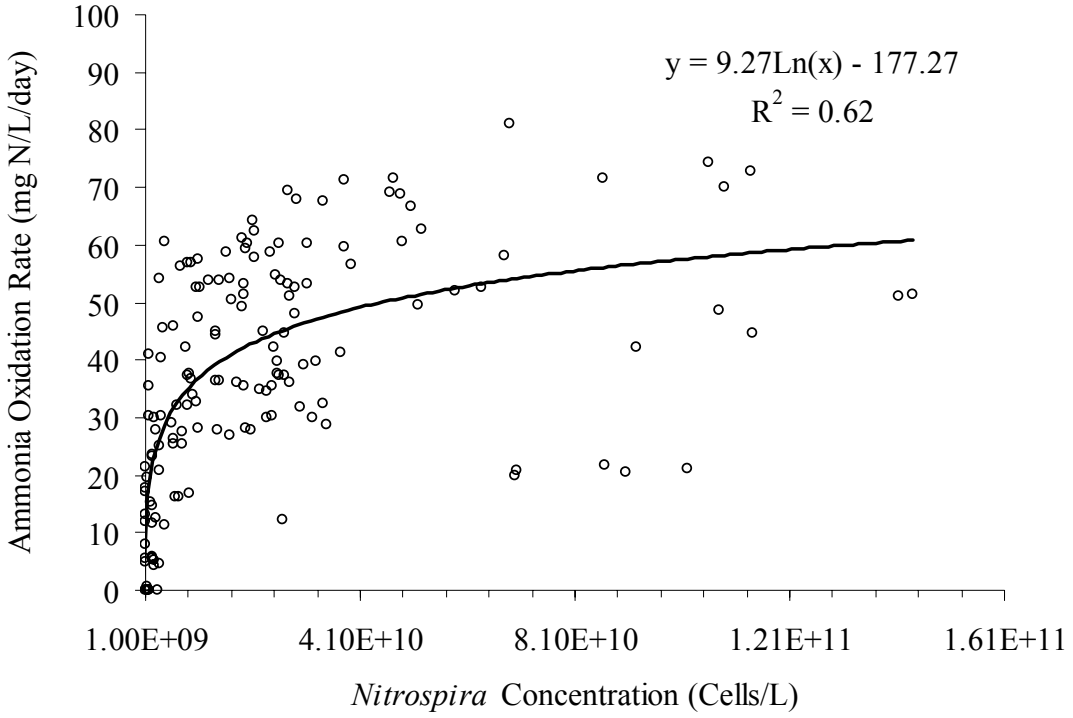

Figure 4-26. Correlation between Ammonia Oxidation Rate and *Nitrospira* Concentration (Includes Data From All Conditions Studied)

Table 4-40. Correlation Coefficients Between *Nitrospira* Concentrations and Ammonia Oxidation Rates

	DO Level		
Temperature (°C)	High	Intermediate	Low
20	0.84	0.93	0.88*
15	0.86	0.88	0.95
10	0.93	0.88	0.94

- Data only includes samples taken during operation at 0.5 mg/L DO

Chapter 5.0
Summary and Conclusions

The objective of this study was to assess the impact of changes in SRT, DO and temperature on treatment performance and microbial population densities. The following conclusions can be drawn from this study.

5.1 Evaluation of Carbon Treatment Performance and Total Biomass

5.1.1 COD Removal Efficiency

- Efficient COD removal occurred throughout all phases of the study and even operation at an SRT of 2 days, a temperature of 10°C and low DO level was adequate to meet the carbon treatment requirements of a full-scale municipal WWTP.
- COD removal efficiency was found to increase with increasing SRT.
- DO concentration and temperature were not found to impact COD removal efficiency, which has been attributed to the low $K_{S,O2}$ value associated with heterotrophic bacteria and the high biomass concentrations maintained in activated sludge.

5.1.2 MLVSS and Total Eubacterial Concentrations

- SRT was the controlling factor in determining the MLVSS concentration, while fluctuations from steady-state could be attributed to changes in influent COD rather than changes in temperature or DO level.
- SRT was found to be the prime determinant of total eubacterial concentration.

- At temperatures of 20°C and 10°C, no clear trend was observed in total eubacterial cell density in response to changes in DO, however, at a temperature of 15°C, the cell density did increase as the DO level decreased.
- The effect of temperature on the concentration of total eubacteria was ambiguous.
- Trends in total eubacterial cell density were generally similar to those observed in MLVSS for varying operational conditions.

5.2 Evaluation of Nitrification Performance

5.2.2 Ammonia Oxidation Rate and *N. oligotropha*-type AOB Concentration

- Consistent with the literature, the findings of this study show SRT to be the single most important factor in determining whether or not nitrification will occur in a treatment system. Efficient nitrification could occur at low temperatures and low DO levels for the higher SRT reactors, but the 5-day and 2-day SRT reactors were dramatically affected by changes in these parameters.
- SRT, DO, and temperature were all found to significantly affect ammonia oxidation rate. Based on multiple linear regression analysis, SRT was found to have the largest impact on ammonia oxidation rate, nearly three times that of temperature and four times that of DO concentration.
- The contribution of *N. oligotropha*-type AOB to the total eubacteria population determined by real-time PCR (≤0.7%) was much lower than expected based on theoretical calculations (2-17%). These findings suggest that *N. oligotropha* was not the dominant AOB species in the bench-scale reactors.
- Although, the concentration of *N. oligotropha*-type AOB in the mixed liquor was exceedingly low, the cell density decreased with decreasing temperature and SRT. However, no clear correlation between AOB cell concentration and DO level could be ascertained.

- Statistical analysis showed that SRT and temperature both significantly impacted the *N. oligotropha*-type AOB cell density with little difference between the relative effects of these two parameters.
- The concentration of *N. oligotropha*-type AOB and ammonia oxidation rate did not closely follow the same trends with respect to changes in SRT, temperature, and DO and were not found to be highly correlated.

5.2.3 Nitrite Oxidation Rate and *Nitrospira*-type NOB Concentration

- Trends in nitrite oxidation rate were very similar to those observed for ammonia oxidation rate.
- SRT, DO and available nitrite concentration were all found to significantly influence the nitrite oxidation rate. The relative impact of available nitrite concentration was more than five times greater than that of SRT and more than fifteen times that of DO.
- The percentages of *Nitrospira* with respect to total eubacteria measured in this study using real-time PCR ranged from 0.2 to 5.6% when nitrification was occurring. These numbers corresponded very well with the predicted values of 0.4 to 4.0% based on typical kinetic parameters suggesting good quantitative agreement between theoretical and measured *Nitrospira* concentrations.
- The concentration of available nitrite and SRT were positively correlated with *Nitrospira* concentration, while DO concentration and temperature were negatively correlated with NOB cell density.
- The concentration of *Nitrospira*-type NOB reflected changes in nitrite oxidation rate with respect to SRT, however, did not closely mirror changes in nitrite oxidation rate resulting from changes in DO and temperature.
- With the exception of two incidences when a temporary nitrite build-up occurred in two of the reactors following a change in environmental conditions, the

ammonia oxidation rate controlled the rate of nitrite oxidation and *Nitrospira* concentration in the reactors by limiting the amount of available nitrite. Thus, while SRT, temperature, and DO yielded some direct impacts on nitrite oxidation and *Nitrospira* concentration, these parameters exerted more influence indirectly through their effects on ammonia oxidation.

- A strong logarithmic relationship existed between *Nitrospira* cell density and nitrite oxidation rate under all experimental conditions, with a Pearson correlation coefficient of 0.78 between the two measures. When each temperature and DO level were considered separately, the strength of the correlation improved, with coefficients ranging from 0.86 to 0.93. Thus, the presence of additional organisms was found to increase nitrite oxidation rate to the point at which nitrite became limiting.
- A similar relationship was found between the concentration of *Nitrospira* and ammonia oxidation rate, with a correlation coefficient of 0.79 when all experimental conditions were considered and coefficients between 0.84 and 0.95 when each temperature and DO level were considered individually.

5.3 General Conclusions

The overall goal of this research was to evaluate the use of real-time PCR in quantifying specific microbial populations in nitrifying activated sludge. The real-time PCR assay for *Nitrospira* proved to be a useful tool in quantifying the nitrifying population in activated sludge. The concentration of *Nitrospira* measured with this assay was consistent with the NOB cell densities reported in other studies and the percentage of the total population comprised of *Nitrospira* agreed well with predicted values. In addition, *Nitrospira* concentration was found to be highly correlated with both nitrite and ammonia oxidation rates. The fact that this measure was so closely related to ammonia oxidation rate suggests that it may not be necessary to monitor both AOB and NOB, but rather only NOB. This would eliminate the need to characterize the AOB population,

which would be beneficial since the high number of AOB species and apparent frequency in population shifts make this a complicated task. This would also reduce the labor and cost associated with monitoring nitrifying organisms in a treatment system.

List of References

List of References

Åakra, A.; Utåker, J. B.; Nes, I. F. (2001) Comparative Phylogeny of the Ammonia Monooxygenase Subunit A and 16S rRNA Genes of Ammonia-Oxidizing Bacteria. *FEMS Microbiol. Lett.*, **205**, 237-242.

American Public Health Association (1998) *Standard methods for the Examination of Water and* Wastewater, 2nd ed.; American Public Health Association: New York, NY.

Andrews, J. H.; Harris, R. F. (1986) r and K-Selection and Microbial Ecology. *Adv. Microb. Ecol*. **9**, 99-147.

Antoniou, P.; Hamilton, J.; Koopman, B.; Jain, R.; Holloway, B.; Lyberatos, G.; Svoronos, S. A. (1990) Effect of temperature and pH on the effective maximum specific growth rate of nitrifying bacteria. *Water Res*., **24**, 97-101.

Applegate, B.; Matrubutham, U.; Sanseverino, J.; Sayler, G. (1995) Biodegradation Genes as Marker Genes in Microbial Ecosystems. In *Molecular Microbial Ecology Manual 6.1*; Kluwer Academic Publishers: Netherlands; Chapter 8, pp. 1-14.

Atlas, R. M.; Sayler, G.; Burlage, R.; Bej, A. (1992) Molecular Approaches for Environmental Monitoring of Microorganisms. *BioTechniques,* **12**, 706-716.

Bassler, H. A.; Flood, S. J.; Livak, K. J.; Marmaro, J.; Knorr, R.; Batt, C. A. (1995) Use of a Fluorogenic Probe in a PCR-Based Assay for the Detection of Listeria-Monocytogenes. *Appl. Environ. Microbiol*., **61**, 3724-3728.

Becker, S.; Fahrbach, M.; Böger, P.; Ernst, A. (2002) Quantitative Tracing, by Taq Nuclease Assays, of a Synechococcus ecotype in a highly diversified natural population. *Appl. Environ. Microbiol.*, **68**, 4486-4494.

Belser, L. W. (1979) Population Ecology of Nitrifying Bacteria. *Ann. Rev, Micobiol.*, **33**, 309-333.

Benefield, L. D.; Randall, C. W.; King, P. H. (1975) *Temperature Considerations in the Design and Control of Completely-Mixed Activated Sludge Plants*, paper presented at the 2nd Annual National Conference on Environmental Engineering Research, Development and Design, ASCE, University of Florida, Gainseville, Fla.

Benefield, L. D.; Randall, C. W. (1980) *Biological Process Design for Wastewater Treatment*; Prentice-Hall: Englewood Cliffs.

Biesterfeld, S.; Figueroa, L.; Hernandez, M; Russell, P. (2001) Quantification of Nitrifying Bacterial Populations in a Full-Scale Nitrifying Trickling Filter Using Fluorescent In situ Hybridization. *Water Environ. Res*., **73**, 329-338.

Biesterfeld, S.; Figueroa, L. (2002) Nitrifying Biofilm Development with Time: Activity Versus Phylogenetic Composition. *Water Environ. Res*., **74**, 470-479.

Bitton, G. (1999) *Wastewater Microbiology*, 2nd ed.; Wiley-Liss: New York.

Bjerrum, L.; Kjaer, T.; Ramsing, N. B. (2002) Enumerating Ammonia-Oxidizing Bacteria in Environmental Samples Using Competitive PCR. *Jour. Microbiol. Methods,* **51**, 227-239.

Bothe, H.; Jost, G.; Ward, B. B.; Witzel, K.-P. (2000) Molecular Analysis of Ammonia Oxidation and Denitrification in Natural Environments. *FEMS Microbiol. Rev*., **24**, 673-690.

Bowers, H. A.; Tengs, T.; Glasgow, H. B. Jr.; Burkholder, J. M.; Rublee, P. A.; Oldach, D. W. (2000) Development of Real-time PCR Assays for Rapid Detection of Pfiesteria piscicida and Related Dinoflagellates. *Appl. Environ. Microbiol*., **66**, 4641-4648.

Burrell, P. C.; Keller, J.; Blackall, L. L. (1998) Characterisation of the Bacterial Consortium Involved in Nitrite Oxidation in Activated Sludge. *Appl. Environ. Microbiol*., **64**, 1878-1883.

Characklis, W. G. and W. Gujer, *Temperature dependency of microbial reactions*. In Kinetics of Wastewater Treatment, S. H. Jenkins ed., Pergamon Press: Elmsford, NY, pp. 111-130, 1979.

Charley, R. C.; Hooper, D. G.; McLee, A. G. (1980) Nitrification Kinetics in Activated Sludge at Various Temperatures and Dissolved Oxygen Concentrations. *Water Res.*, **14**, 1387-1396.

Cheremisinoff, N. P. (1996) *Biotechnology for Waste and Wastewater Treatment*; Noyles: New Jersey.

Chuang, S.H.; Ouyang, C. F.; Yuang, H. C.; You, S. J. (1997) Effects of SRT and DO on Nutrient Removal in a Combined AS-Biofilm Process. *Wat. Sci. Tech*., **36**, 19-27.

Condon, D.; Liveris, D.; Squires, C.; Schwartz, I.; Squires, C. L. (1995) Ribosomal-RNA Operon Multiplicity in *Escherichia coli* and the Physiological Implications of RRN Inactivation. *J. Bacteriol*., **177**, 4152-4156.

Daims, H.; Purkhold, U; Bjerrum, L.; Arnold, E.; Wilderer, P. A.; Wagner M. (2001a) Nitrification in Sequencing Biofilm Batch Reactors: Lessons Learned from Molecular Approaches. *Wat. Sci. Tech*., **43**, 9-18.

Daims, H.; Nielsen, J. L.; Nielsen, P. H.; Schleifer, K. H.; Wagner, M. (2001b) In Situ Characterization of Nitrospira-like Nitrite Oxidizing Bacteria Active in Wastewater Treatment Plants. *Appl. Environ. Microbiol*., **67**, 5273-5284.

Daims, H.; Ramsing, N. B.; Schleifer, K-H.; Wagner, M. (2001c) Cultivation-Independent, Semiautomatic Determination of Absolute Bacterial Cell Numbers in Environmental Samples by Fluorescence In Situ Hybridization. *Appl. Environ. Microbiol*., **67**, 5810-5818.

Dancong, P.; Bernet, N.; Delgenes, J.-P.; Moletta, R. (2000) Effects of Oxygen Supply Methods on the Performance of a Sequencing Batch Reactor for High Ammonium Nitrification. *Water Environ. Res.*, **72**, 195-200.
Davis, M. L.; Cornwell, D. A. *Introduction to Environmental Engineering*, 3rd ed.; WCB/McGraw-Hill: Boston, 1998.

Dionisi, H. M.; Layton, A. C.; Harms, G.; Gregory, I. R.; Robinson, K. G.; Sayler, G. S. (2002a) Quantification of *Nitrosomonas oligotropha*-like Ammonia Oxidizing Bacteria and *Nitrospira* spp. from Full-scale Wastewater Treatment Plants by Competitive PCR. *Appl. Environ. Microbiol*., **68**, 245-253.

Dionisi, H. M.; Layton, A. C.; Robinson, K. G.; Brown, J. R.; Gregory, I. R.; Parker, J. J.; Sayler, G. S. (2002b) Quantification of *Nitrosomonas oligotropha* and *Nitrospira* spp. using Competitive Polymerase Chain Reaction in Bench-Scale Wastewater Treatment Reactors Operating at Different Solids Retention Times. *Water Environ. Res*., **74**, 462-469.

Eckenfelder, W. W., Jr. (1989) *Industrial Water Pollution Control*. 2nd ed. McGraw-Hill: New York.

Environmental Protection Agency (1975) Process *Design Manual for Nitrogen Control*. Office of Technology Transfer, Cincinatti, Ohio.

Erlich, H. A.; Gelfand, D.; Sninsky, J. J. (1991) Recent Advances in Polymerase Chain Reaction. *Science*, **252**, 1643-1651.

Ferris, M. J.; Muyzer, G.; Ward, D. M. (1996) Denaturing Gradient Gel Electrophoresis Profiles of 16S rRNA-Defined Populations Inhabiting a Hot Springs Microbial Mat Community. *Appl. Environ. Microbiol*., **62**, 340-346.

Furumai, H.; Rittmann, B. E. (1992) Advanced Modeling of Mixed Populations of Heterotrophs and Nitrifiers Considering the Formation and Exchange of Soluble Microbial Products. *Wat. Sci. Technol.*, **26**, 493-502.

Garrett, M. T.; Sawyer, C. N. (1951) *Kinetics of Removal of Soluble B.O.D. by Activated Sludge*. Proceedings, Seventh Industrial Waste Conference. Lafayette, IN: Purdue University.

Giulietti, A.; Overbergh, L.; Valckx, D.; Decallonne, B.; Bouillon, R.; Mathieu, C. (2001) An Overview of Real-time Quantitative PCR: Applications to Quantify Cytokine Gene Expression. *Methods*, **25**, 386-401

Grady, C. P. L., Jr.; Daigger G. T.; Lim, H. C. (1999) *Biological Wastewater Treatment*, 2nd ed.; Marcel Dekker: New York.

Grady, C. P. L.; Filipe, C. D. M. (2000) Ecological Engineering of Bioreactors for Wastewater Treatment. *Water Air Soil Pollut*., **123**, 117-132.

Gray, N. F. (1989) *Biology of Wastewater Treatment*; Oxford University: New York, NY.

Grüntzig, V.; Nold, S. C.; Zhou, J.; Tiedje, J. M. (2001) Pseudomonas stutzeri Nitrite Reductase Gene Abundance in Environmental Samples Measured by Real-time PCR. *Appl. Environ. Microbiol*., **67**, 760-768.

Hall, E.R.; Murphy, K. L. (1985) Sludge Age and Substrate Effects on Nitrification Kinetics. *Jour. Water Poll. Control Fed.*, **57**, 413-418.

Hall E. R.; Murphy K. L. (1980) Estimation of Nitrifying Biomass and Kinetics in Wastewater Treatment. W*ater Res.*, **14**, 297-304.

Hall, S. J.; Hugenholtz, P.; Slyambaiapitiya, N.; Keller, J.; Blackall, L.L. (2002) The Development and Use of Real-time PCR for the Quantification of Nitrifiers in Activated Slduge. *Water Sci. Technol*., **46**, 267-272.

Hanaki, K.; Wantawin, C.; Ohgaki, S. (1990) Nitrification at Low Levels of Dissolved Oxygen with and without Organic Loading in a Suspended-Growth Reactor. *Water Res*., **24**, 297-302.

Harms, G.; Layton, A. C., Dionisi, H. M., Gregory, I. R.; Garrett, V. M.; Hawkins, S. A.; Robinson, K. G.; Sayler, G. S. (2003) Real-time PCR Quantification of Nitrifying Bacteria in a Municipal Wastewater Treatment Plant. *Environ. Sci. Technol*., **37**, 343-351.

Hawkins, S. (2000) A Bench Scale Activated Sludge Study of Nitrification and Carbon Treatment Using Municipal Wastewater. M.S. Thesis, University of Tennessee at Knoxville.

Heid, C. A.; Stevens, J.; Livak K. J.; Williams P. M. (1996) Real Time Quantitative PCR. *Genome Res*., **6**, 986-994.

Henze, M.; Grady, C. P. L. Jr.; Gujer, W.; Marais, G. V. R.; Matsuo, T. (1987) A General Model for Single-Sludge Wastewater Treatment Systems. *Water Res*., **21**, 505-515.

Henze, M.; Harremoes, P.; Jansen, J. C.; Arvin, E. (1995) *Wastewater Treatment: Biological and Chemical Processes*; Springer-Verlag: Berlin Heidelberg.

Hermansson, A.; Lindgren, P. (2001) Quantification of Ammonia-Oxidizing Bacteria in Arable Soil by Real-time PCR. *Appl. Environ. Microbiol*., **67**, 972-976

Holland, P. M.; Abramson, R. D.; Watson, R.; Gefand, D.H. (1991) Detection of Specific Polymerase Chain Reaction Product by Utilizing the 5'→3' Exonuclease Activity of *Thermus aquaticus* DNA Polymerase. *Proc. Natl. Acad. Sci. USA*., **88**, 7276-7280.

Hovanec, T. A.; Delong, E. F. (1996) Comparative Analysis of Nitrifying Bacteria Associated with Freshwater and Marine Aquaria. *Appl. Environ. Microbiol*., **62**, 2888-2896.

Hovanec, T. A.; Taylor, L. T.; Blakis, A.; Delong, E. F. (1998) *Nitrospira*-like Bacteria Associated with Nitrite Oxidation in Freshwater Aquaria. *Appl. Environ. Microbiol*., **64**, 258-264.

Jenkins, D.; Richard, M. G.; Daigger, G. T. (1993) *Manual on the Causes and Control of Activated Sludge Bulking and Foaming*. 2nd ed. Lewis Publishers, Chelsea, MI.

Jianlong, W.; Hanchang, S.; Yi, Q. (2000) Wastewater Treatment in a Hybrid Biological Reactor (HBR): Effect of Organic Loading Rates. *Process Biochem*., **36**, 297-303.

Juretschko, S.; Timmermann, G.; Schmid, M.; Schleifer, K.; Pommerening-Roser, A.; Koops, H.; Wagner, M., (1998) Combined Molecular and Conventional Analyses of Nitrifying Bacterium Diversity in Activated Sludge: *Nitrosococcus mobilis* and *Nitrospira*-like Bacteria as Dominant Populations. *Appl. Environ. Microbiol*., **64**, 3042-3051.

Keller, J.; Yuan, Z.; Blackall, L. L. (2002) Integrating Process Engineering and Microbiology Tools to Advance Activated Sludge Wastewater Treatment Research and Development. *Environ. Sci. Biotechnol*., *1*, 83-97.

Kim, I. S.; Ivanov, V. N. (2000) Detection of Nitrifying Bacteria in Activated Sludge by Fluorescent in situ Hybridization and Fluorescence Spectrometry. *World J. Microbiol. Biotechnol*., **16**, 425-430.

Klappenbach, J. A.; Dunbar, J. M.; Schmidt, T. M. (2000) RRNA Operon Copy Number Reflects Ecological Strategies in Bacteria. *Appl. Environ. Microbiol*., **66**, 1328-1333.

Klappenbach, J. A.; Saxman, P. R.; Cole, J. R.; Schmidt, T. M. (2001) rrndb: the Ribosomal RNA Operon Copy Number Database. *Nucleic Acids Res*., **29**, 181-184.

Knowles, G.; Downing, A. L.; Barrett, M. J. (1965) Determination of Kinetic Constants for Nitrifying Bacteria in Mixed Culture with the Aid of an Electronic Computer. *Jour. General Microbiol*., **38**, 263-276.

Kowalchuk, G. A.; Naoumenko, Z. S.; Derikx, P. J. L.; Felske, A.; Stephen, J. R.; Arkhipchenko, I. A. (1999) Molecular Analysis of Ammonia-Oxidizing Bacteria of the β Subdivision of the Class Proteobacteria in Compost and Composted Materials. *Appl. Environ. Microbiol*., **65**, 396-403.

Laanbroek, H. J.; Bodelier, P. L. E.; Gerards, S. (1994) Oxygen Consumption Kinetics of *Nitrosomonas europaea* and *Nitrobacter hamburgensis* Grown in Mixed Continuous Cultures at Different Oxygen Concentrations. *Arch. of Microbiol*., **161**, 156-162.

Lane, D. J. (1991) 16S/23S rRNA Sequencing. In *Nucleic Acid Techniques in Bacterial Systematics*, Stackebrandt, E.; Goodfellow, M., Ed.; John Wiley & Sons: Chichester, England, 115-175.

Lawrence, A. W.; Brown, C. G. (1976) Design and Control of Nitrifying Activated Sludge Systems. *Jour. Water Poll. Control Fed.*, **48**, 1179-1802.

Lawrence, A.; McCarty, P. (1970) Unified Basis for Biological Treatment Design and Operation. *Journal of the Proceedings of the American Society of Civil Engineers* , **96**, 757-778.

Lau, A. O.; Strom, P. F.; Jenkins, D. (1984) Growth Kinetics of *Sphaerotilus natans* and a Floc Former in Pure and Dual Continuous Culture. *Jour. Water Poll. Control Fed.*, **56**, 41-51.

Lee, L. G.; Connell, C. R.; Bloch, W. (1993) Allelic Discrimination by Nick-Translation PCR with Fluorogenic Probes. *Nucleic Acids Res*., **21**, 3761-3766.

Lee, H. S.; Park, S. J.; Yoon, T. I. (2002) Wastewater Treatment in a Hybrid Biological Reactor Using Powdered Minerals: Effects of Organic Loading Rates on COD Removal and Nitrification. *Process Biochem*., **38**, 81-88.

Lie, Y.S.; Petropoulos, C.J. (1998) Advances in Quantitative PCR: Technology 5' Nuclease Assays. *Curr. Opin. Biotech*., **9**, 43-48.

Lishman, L. A.; Legge, R. L.: Farquhar, G. J. (2000) Temperature Effects on Wastewater Treatment Under Aerobic and Anoxic Conditions. *Water Res*., **34**, 2263-2276.

Livak, K. J.; Flood, S. J. A.; Marmaro, J.; Giusti, W.; Deetz, K. (1995a) Oligonucleotide with Fluorescent Dyes at Opposite Ends Provide a Quenched Probe System Useful for Detecting PCR Product and Nucleic Acid Hybridization. *PCR Methods Applications*, **4**, 357-362.

Livak, K. J.; Marmaro, J.; Todd, J. A. (1995b) Towards Fully Automated Genome-Wide Polymorphism Screening. *Nature Genet*., **9**, 341-342.

Madigan, M. T.; Martinko, J. M.; Parker, J. (1997) Brock Biology of Microorganisms. 8th ed. Prentice-Hall: New York, NY.

Marisili-Libelli, S.; Giovanni, F. (1997) On-line Estimation of the Nitrification Process. *Water Res*., **31**, 179-185.

McClintock, S. A.; Randall, C. W.; Pattarkine, V. M. (1993) Effects of Temperature and Mean Cell Residence Time on Biological Nutrient Removal. *Water Environ. Res.*, **65**, 110-118.

McTavish, H.; Fuchs, J. A.; Hooper, A. B. (1993) Sequence of the Gene Coding for Ammonia Monooxygenase in *Nitrosomonas europaea*. *J. Bacteriol*., **175**, 2436-2444.

Mendum, T. A.; Sockett, R. E.; Hirsch, P. R. (1999) Use of Molecular and Isotopic Techniques to Monitor the Response of Autotrophic Ammonia-Oxidizing Populations of the β Subdivision of the Class Proteobacteria in Arable Soils to Nitrogen Fertilizer. *Appl. Environ. Microbiol*., **65**, 4155-4162.

Metcalf and Eddy. (1991) *Wastewater Engineering: Treatment, Disposal, Reuse*; 3rd ed. McGraw-Hill: New York.

Mobarry, B. K.; Wagner, M.; Urbain, V.; Rittmann, B. E.; Stahl, D. (1996) Phylogenetic Probes for Analyzing Abundance and Spatial Organization of Nitrifying Bacteria. *Appl. Environ. Microbiol*., **62**, 2156-2162.

Muck, R. E. and C. P. L. Grady Jr., (1974) Temperature Effects on Microbial Growth in CSTRs. *J. Environ. Eng.,* **100**, 1147-1163.

Navarro, E.; Fernandez, M. P.; Grimont, F.; Clays-Josserand, A.; Bardini, R. (1992) Genomic Heterogeneity of the Genus Nitrobacter. *Int. J. Syst. Bacteriol*., **42**, 554-560.

Norusis, M. J. (2000) *SPSS 10.0 Guide to Data Analysis.* Prentice-Hall: Upper Saddle River New Jersey.

Norton, J. M.; Alzerreca, J. J.; Suwa, Y.; Klots, M. G. (2002) Diversity of Ammonia Monooxygenase Operon in Autotrophic Ammonia-Oxidizing Bacteria. *Arch. Microbiol*., **177**, 139-149.

Oerther, D.B.; de los Reyes, F.L.; Rankin, L. (1999) Interfacing Phylogenetic Oligonucleotide Probe Hybridizations with Representations of Microbial Populations and Specific Growth Rates in Mathematical Modelsof Activated Sludge Processes. *Wat. Sci. Technol.*, **39**, 1-20.

Okabe, S.; Oozawa, Y.; Hirata, K.; Watanabe, Y. (1996) Relationship Between Population Dynamics of Nitrifiers in Biofilms and Reactor Performance at Various C:N Ratios. *Water Res*., **30**, 1563-1572.

Okabe, S.; Satoh, H.; Watanabe, Y. (1999) In situ Analysis of Nitrifying Biofilms as Determined by in situ Hybridization and the Use of Microelectrodes. *Appl. Environ. Microbiol*., **65**, 3182-3191.

Parker, J. J. (2001) The Effects of Dissolved Oxygen Concentration and Biological Solids Retention Time on Activate Sludge Treatment Performance. M.S. Thesis, University of Tennessee at Knoxville.

Phillips, C. J.; Paul, E. A.; Prosser, J. I. (2000) Quantitative Analysis of Ammonia Oxidising Bacteria Using Competitive PCR. *FEMS Microbiol. Ecol*., **32**, 167-175.

Poduska, R. A.; Andrews, J. F. (1975) Dynamics of Nitrification in the Activated Slduge Process. *Jour. Water Poll. Control Fed.*, **47**, 2599-2619.

Prinčič, A.; Mahne, I.; Megušar, F; Paul, E. A.; Tiedje, J. M. (1998) Effect of pH and Oxygen and Ammonium Concentrations on the Community Structure of Nitrifying Bacteria from Wastewater. *Appl. Environ. Microbiol*., **64**, 3584-3590.

Prosser, J. I. (1989) Autotrophic Nitrification in Bacteria. *Adv. Microb. Physiol*., **30**, 897-925.

Purkhold, U.; Pommerening-Röser, A.; Juretschko, S.; Schmid, M. C.; Koops, H. P.; Wagner, M. (2000) Phylogeny of All Recognized Species of Ammonia Oxidation Based on Comparative 16S rRNA and *amo*A Sequence Analysis: Implications for Molecular Diversity Surveys. *Appl. Environ. Microbiol*., **66**, 5368-5382.

Randall, C. W.; Buth, D. (1984) Nitrite Build-Up in Activated Sludge Resulting from Temperature Effects. *Jour. Water Poll. Control Fed.*, **56**, 1039-1044.

Reynolds, T. D.; Richards, P. A. (1996) *Unit Operations and Processes in Environmental Engineering*, 2nd ed.; PWS Publishing: Boston.

Rittmann, B.E.; Laspidou, C. S.; Flax, J.; Stahl, D.A.; Urbain, V.; Harduin, H.; van der Waarde, J. J.; Geurkink, B.; Henssen, M. J. C.; Brouwer, H.; Klapwijk, A.; Wetterauw, M. (1999) Molecular and Modeling Analysis of the Structure and Function of Nitrifying Activated Sludge. *Wat. Sci. Technol.*, **39**, 51-59.

Rittmann, B. E.; McCarty P. L. (2001)*Environmental Biotechnology: Principles and Applications*; McGraw-Hill: New York.

Rittmann, B.E. (2002) The Role of Molecular Methods in Evaluating Biological Treatment Processes. *Water Environ. Res*., **74**, 421-427.

Rotthauwe, J.; Witzel, K.; Liesack, W. (1997) The Ammonia Monooxygenase Structural Gene *amo*A as a Functional Marker: Molecular Fine-Scale Analysis of Natural Ammonia-Oxidizing Populations. *Appl. Environ. Microbiol*., **63**, 4704-4712.

Saiki, R. K.; Scharf, S.; Faloona, F.; Mullis, K. B.; Horn, G. T.; Erlich, H. A.; Arnheim, N. (1985) Enzymatic Amplification of β-Globin Genomic Sequences and Restriction Site Analysis for Diagnosis of Sickle Cell Anemia. *Science*, **230**, 1350-1354.

Saiki, R. K.; Gelfand, D.H.; Stoffel, S.; Scharf, S. J.; Higuchi, R.; Horn, G.T.; Mullis, K. B.; Erlich, H. A. (1988) Primer-Directed Enzymatic Amplification of DNA with a Thermostable DNA Polymerase. *Science*, **239**, 487-491.

Sayigh, B. A.; Malina, J. F. (1978) Temperature Effects on the Activated Sludge Process. *Jour. Water Poll. Control Fed.*, **50**, 678-687.

Schramm, A.; Larsen, L. J.; Revsbech, N. P.; Ramsing, N. B.; Amann, R.; Schleifer, K.-H. (1996) Structure and Function of a Nitrifying Biofilm as Determined by in situ Hybridization and the Use of Microelectrodes. *Appl. Environ. Microbiol*., **62**, 4641.

Schramm, A.; de Beer, D.; Wagner, M.; Amann, R. (1998) Identification and Activities in situ of *Nitrosospira* and *Nitrospira* spp. as Dominant Populations in a Nitrifying Fluidized Bed Reactor. *Appl. Environ. Microbiol*, **64**, 3480-3485.

Schramm, A.; de Beer, D.; Van Den Heubel, J. C.; Ottengraf, S.; Amann, R. (1999) Microscale Distribution of Populations and Activities of *Nitrosospira* and *Nitrospira* spp. Along a Macroscale Gradient in a Nitrifying Bioreactor: Quantification by in situ Hybridization and the Use of Microsensors. *Appl. Environ. Microbiol*., **65**, 3690-3696.

Shammas, N. (1986) Interactions of Temperature, pH, and Biomass in the Nitrification Process. *Jour. Water Poll. Control Fed.*, **58**, 52-59.

Sinclair, C. G.; Ryder, D. N. (1975) Models for Continuous Culture of Microorganisms Under Both Oxygen and Carbon Limiting Conditions. *Biotechnol. Bioengineer*., **17**, 375-398.

Stenstrom, M. K.; Poduska, R. A. (1980) The Effect of Dissolved Oxygen Concentration on Nitrification. *Water Res*., **14**, 643-649.

Stephen, J. R.; Chang, Y.-J.; Macnaughton, S. J.; Kowalchuk, G. A.; Leung, K. T.; Flemming, C. A.; White, D. C. (1999) Effect of Toxic Metals on Indigenous p-Subgroup Proteobacterium Ammonia Oxidizer Community Structure and Protection Against Toxicity by Metal-Resistant Bacteria. *Appl. Environ. Microbiol*., **65**, 95-101.

Stover, E. L.; Kincannon, D. F. (1976) One- Versus Two- Stage Nitrification in the Activated Sludge Process. *Jour. Water Poll. Control Fed.*, **48**, 645-651.

Suzuki, M. T.; Taylor, L. T.; Delong, E. F. (2000) Quantitative Analysis of Small-Subunit rRNA Genes in Mixed Microbial Populations Via 5'-Nuclease Assays. *Appl. Environ. Microbiol*., **66**, 4605-4614.

Tennessee Department of Public Health (1999) *Rules of the Tennessee Department of Public Health Bureau of Environmental Health Services Division of Water Quality Control.* Chapter 1200-4-5 Effluent Limitations and Standards.

Theron, J.; Cloete, T. E. (2000) Molecular Techniques for Determining Microbial Diversity and Community Structure in Natural Environments. *Crit. Rev. Microbiol*., **26**, 37-57.

Tortora, G. J.; Funke, B. R.; Case, C. L. (1993) *Microbiology: An Introduction,* 3rd ed.; Benjamine/Cummings: Redwood City.

Urbain,V.; Mobarry, B.; de Silva, V.; Stahl, D. A.; Rittmann, B.E.; Manem, J. (1998) Integration of Performance, Molecular Biology and Modeling to Describe the Activated Sludge Process. *Wat. Sci. Technol.*, **37**, 223-229.

Wagner, M.; Amann, R.; Lemmer, H.; Schleifer, K.-H. (1993) Probing Activated Sludge with Oligonucleotides Specific for Proteobacteria – Inadequacy of Culture-Dependent Methods for Describing Microbial Community Structure. *Appl. Environ. Microbiol*., **59**, 1520-1525.

Wagner, M.; Rath, G.; Amann, R.; Koops, H.-P.; Schleifer K.-H. (1995) In situ Identification of Ammonia-Oxidizing Bacteria. *System. Appl. Microbiol*., **18**, 251-264.

Wagner, M.; Rath G.; Koops, H.-P.; Flood, J.; Amann, R. (1996) In situ Analysis of Nitrifying Bacteria in Sewage Treatment Plants. *Water Sci. Technol*., **34**, 237-244.

Wagner, M.; Noguera, D. R.; Juretschko, S.; Rath, G.; Koops, H.; Schleifer, K. (1998) Combining Fluorescent in situ Hybridization (FISH) with Cultivation and Mathematical Modeling to Study Population Structure and Function of Ammonia-Oxidizing Bacteria in Activated Sludge. *Wat. Sci. Technol.*, **37**, 441-449.

Wagner, M.; Loy, A.; Nogueira, R.; Purkhold, U.; Lee, N.; Daims, H. (2002) Microbial Community Composition and Function in Wastewater Treatment Plants. *Anton. Leeuwenhoek Int. J. Gen. M.*, **81**, 665-680.

Wild, H. E. Jr.; Sawyer, C. N.; McMahon, T. C. (1971) Factors Affecting Nitrification Kinetics. *Jour. Water Poll. Control Fed.*, **43**, 1845-1854.

Wilderer, P. A.; Bungartz, H. J.; Lemmer, H; Wagner M.; Keller J.; Wuertz S. (2002) Modern Scientific Methods and Their Potential in Wastewater Science and Technology. *Water Res*., **36**, 370-393.

Wood, B. The Effects of Dissolved Oxygen Concentration, Temperature, and Solids Retention Time on Activate Sludge Treatment Performance. M.S. Thesis, University of Tennessee at Knoxville. In preparation.

Wong-Chong, G.M.; Loehr, R. C. (1975) The Kinetics of Microbial Nitrification. *Water Res*., **9**, 1099-1106.

Ydstebo, L.; Bilstad, T.; Barnard, J. (2000) Experience with Biological Nutrient Removal at Low Temperatures. *Water Environ. Res.*, **72**, 444-454.

You, S. J.; Hsu, C. L.; Chuang, S. H.; Ouyang, C. F. (2003) Nitrification Efficiency and Nitrifying Bacteria Abundance in Combined AS-RBC and A20 Systems. *Water Res*., **37**, 2281-2290.

Yuan, Z.; Blackall, L. L. (2002) Sludge Population Optimisation: a New Dimension for the Control of Biological Wastewater Treatment Systems. *Water Res*., **36**, 482-490.

Appendices

Appendix A

Sample Calculations for Conversion of Real-time PCR Data to Units of Cells/L

Step 1. Convert C_T value into units of Gene Copies/PCR Reaction using the universal standard curve. For total eubacteria and *Nitrospira*, the standard curve was as follows.

$$\frac{\text{Gene Copies}}{\text{PCR Reaction}} = 10^{\left(-0.24C_T+10.7\right)}$$

Step 2. Convert Gene Copies/PCR Reaction to Gene Copies/Mixed Liquor volume by dividing by volume of DNA/PCR reaction and multiplying by volume of DNA extracted per volume of mixed liquor sample as follows.

$$\frac{\text{Gene Copies}}{\text{Volume Mixed Liquor}} = \frac{\text{Gene Copies}}{\text{PCR Reaction}} \times \frac{\text{PCR Reaction}}{\text{Volume DNA}} \times \frac{\text{Volume DNA Obtained}}{\text{Volume Mixed Liquor Sample}}$$

Step 3. Convert Gene Copies/Volume Mixed Liquor to Cells/Volume Mixed Liquor by dividing by assumed number of Gene Copies/Cell. For Total eubacteria the conversion factor was assumed to be 3.6 16S rDNA Gene Copies/Cell.

$$\frac{\text{Cells}}{\text{Volume Mixed Liquor}} = \frac{\text{GeneCopies}}{\text{Volume Mixed Liquor}} \times \frac{\text{Cell}}{\text{3.6 Gene Copies}}$$

Appendix B

Sample Calculation for Theoretical Values of %AOB and %NOB

Example: 20°C and θ_x = 20 days

Compute VSS production rates for all types of biomass.

$$\frac{\Delta X_v}{\Delta t} = Q\left(S^0 - S\right)Y\frac{1+\left(1-f_d\right)b\theta_x}{1+b\theta_x}$$

Assume f_d = 0.8 (Rittmann and McCarty, 2001)
Q = 27.4 L/day

For aerobic heterotrophs

$$\frac{\Delta X_v}{\Delta t} = \left(\frac{27.4\,\text{L}}{\text{day}}\right)\left(\frac{(102-13)\,\text{mg BOD}}{\text{L}}\right)\left(0.45\frac{\text{mg VSS}}{\text{mg BOD}}\right)\frac{1+\left[(1-0.8)(0.15/\text{day})(20\,\text{days})\right]}{1+(0.15/\text{day})(20\,\text{days})}$$

$$\frac{\Delta X_v}{\Delta t} = 441\frac{\text{mg VSS}}{\text{day}}$$

For ammonia oxidizers

It was first necessary to adjust S^0 to account for the ammonia-N assimilated into the aerobic heterotrophs and not available for nitrification. Assume biomass is comprised of 12.4% N (Rittmann and McCarty, 2001) and let N_1^0 equal the ammonia-N available for nitrification.

$$N_1^0 = \frac{19\,\text{mg ammonia} - \text{N}}{\text{L}} - \left(\frac{441\,\text{mg VSS}}{\text{day}}\times\frac{0.124\,\text{mg N}}{\text{mg VSS}}\times\frac{\text{day}}{27.4\,\text{L}}\right)$$

$$N_1^0 = \frac{17\,\text{mg ammonia} - \text{N}}{\text{L}}$$

Then,

$$\frac{\Delta X_v}{\Delta t} = \left(\frac{27.4\,\text{L}}{\text{day}}\right)\left(\frac{(17-0)\,\text{mg N}}{\text{L}}\right)\left(0.33\,\frac{\text{mg VSS}}{\text{mg N}}\right)\frac{1+[(1-0.8)(0.11/\text{day})(20\,\text{days})]}{1+(0.11/\text{day})(20\,\text{days})}$$

$$\frac{\Delta X_v}{\Delta t} = 69\,\frac{\text{mg VSS}}{\text{day}}$$

For nitrite oxdizers

It was necessary to calculate the amount of nitrite-N available for nitrite oxidation. This is determined by subtracting the ammonia-N assimilated into the aerobic heterotrophs and ammonia oxidizers and the steady-state ammonia concentration from the influent ammonia concentration. Let N_2^0 equal the nitrite-N available for nitrite oxidation.

$$N_2^0 = \frac{18.4\,\text{mg ammonia} - \text{N}}{\text{L}} - \frac{2.44\,\text{mg N}}{\text{L}}\left(\frac{64\,\text{mg VSS}}{\text{day}} \times \frac{0.124\,\text{mg N}}{\text{mgVSS}} \times \frac{\text{day}}{27.4\text{L}}\right)$$

$$N_2^0 = \frac{17\,\text{mg ammonia} - \text{N}}{\text{L}} - \left(\frac{69\,\text{mg VSS}}{\text{day}} \times \frac{0.124\,\text{mg N}}{\text{mg VSS}} \times \frac{\text{day}}{27.4\,\text{L}}\right)$$

$$N_2^0 = \frac{16.7\,\text{mg ammonia} - \text{N}}{\text{L}}$$

Then,

$$\frac{\Delta X_v}{\Delta t} = \left(\frac{27.4\,\text{L}}{\text{day}}\right)\left(\frac{(16.7-0)\,\text{mg N}}{\text{L}}\right)\left(0.083\,\frac{\text{mg VSS}}{\text{mg N}}\right)\frac{1+[(1-0.8)(0.11/\text{day})(20\,\text{days})]}{1+(0.11/\text{day})(20\,\text{days})}$$

$$\frac{\Delta X_v}{\Delta t} = 17\,\frac{\text{mg VSS}}{\text{day}}$$

Compute %AOB and % NOB from ratio of VSS production rates.

$$\%\text{AOB} = \frac{69\ \text{mg VSS/day}}{(441+69+17)\ \text{mg VSS/day}} \times 100\%$$

%AOB = 13.1%

$$\%\text{NOB} = \frac{17\ \text{mg VSS/day}}{(441+69+17)\ \text{mg VSS/day}} \times 100\%$$

%NOB = 3.2%

Vita

Janalyn Rae Brown was born in Cleveland, Ohio, on November 6, 1977. She was raised in Lowellville, Pennsylvania, until 1984, when she moved to Louisville, TN with her family. Janalyn went to elementary school at Middlesettlements Elementary School and was valedictorian of William Blount High School in Maryville, Tennessee, in 1996. She graduated Magna Cum Laude from the University of Tennessee, Knoxville, with a Bachelor of Science degree in Chemical Engineering and a minor in Environmental Engineering in 2001, and received a Master of Science degree in Environmental Engineering in 2003.